QuaesitUM

The Undergraduate Research Journal of The University of Memphis

Spring 2022

http://www.memphis.edu/quaesitum/

QuaesitUM is an annual publication that provides an academic forum where University of Memphis undergraduate students can showcase research from all disciplines.

ISSN 2375-5423

Editorial Board

Success is no accident. It is hard work, perseverance,
learning, studying, sacrifice and most of all,
love of what you are doing or learning to do.
– Pelé
Difficult roads often lead to beautiful destinations.
– Anonymous

To Our Readers

For the past two years, the theme of my message to Quaesitum readers has been perseverance. The COVID-19 pandemic has demanded that we persevere as it has tested our psychological limits. It has imposed distance and curtailed our ability to fertilize ideas through collaboration. It has brought a "fight-or-flight" response that has made us look for familiar, 'safe' options. In many ways, it has hampered our desire to seek the unfamiliar and innovate.

We have persevered. As a global community, we have risen to the challenge of facing a devastating threat. And while the difficulties of the pandemic have not gone away, we are learning to find a balance between maintaining what is safe and familiar and looking toward the possibilities ahead. Like a phoenix rising from the ashes, we have begun the journey toward renewal and regrowth.

In this age of new possibilities, the University of Memphis has celebrated clear victories. Perhaps most notable is the elevation of the University to Carnegie R1 status – a designation reserved only for top-tier research institutions. The communal effort involved in attaining this classification reveals a commitment to exploring new possibilities and ideas. The articles included in this volume reflect that commitment in their drive 'to seek and to know' (the Quaesitum motto). The authors represent research conducted in the disciplines of Psychology, History, English, Biomedical and Electrical Engineering, and Physics. They examined migration patterns, designed 3D hologram projectors, measured the effects of addiction and social isolation, assessed thematic language in literature, measured student success, and developed innovative approaches to biomedical processes. In each case, the authors embraced the opportunity to explore their passions – not relinquishing their perseverance, but using it to fuel their journey toward new possibilities.

As always, I am grateful to the many people who have helped bring this volume to fruition. First, thanks must go to Dr. Melinda Jones, the Director of the Honors College. Her partnership has proven invaluable as we have

continued to showcase our students' research year-by-year. Thanks also to Mr. Egemen Curuk, the Quaesitum technical editor, who has shown admirable energy in recruiting contributors and reviewers, guiding authors, and orchestrating the technical tasks so necessary for production of the journal.

The artwork of Gary Golightly has once again captured the spirit of Quaesitum in his cover design, a task he has undertaken since our inaugural issue. I am continually impressed with his ability to capture the essence of research in images that convey the fun and passion that bind good researchers to their projects. The financial support of the Honors College, under Dr. Jones' direction, deserves thanks as well, for the financial support of student authors through the best paper awards.

Dr. Jones, Mr. Curuk, and I are also grateful to the reviewers who contributed their time and expertise in ensuring the high-quality that Quaesitum readers have come to expect: Dr. Gustav Borstad, Dr. Dean Clement, Dr. Judith Cole, Dr. David H. Dye, Dr. Mohamed Laradji, Dr. Sanjay Mishra, Dr. Felio Perez, Dr. Caroline Peyton, Dr. Helen J.K. Sable, Dr. Aaryani Sajja, Dr. Charlie Santo, Ms. Amanda Lee Savage, Dr. Ali Shiri Sichani, Dr. Nicholas Simon and Mr. Halil Andaç Yiğit.

The faculty advisors who have guided their students in these projects obviously play an integral role in the success of the research reflected here: Dr. Joel Bumgardner, Dr. Ana Doblas, Dr. Thang Hoang, Dr. Mohamed Laradji, Dr. Deranda Lester, Dr. Susan O'Donovan, Dr. Chenhui Peng, Dr. Shawn Pollard, Dr. Don Rodrigues, Dr. Jaime Sabel and Dr. Xiao Shen.

Finally, however, the student authors deserve the most praise for their perseverance and willingness to explore the unknown. Publishing one's work requires extended commitment, and it is a process that can be daunting. These authors chose to meet that challenge to share their work with the wider intellectual community, and we are grateful to have been part of this effort.

With hope looking toward the future,

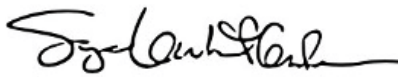

Dr. Sage L. Graham

Quaesitum Editor-in-Chief

Table of Contents

Social and Behavioral Sciences

1 The Effects of Chronic Cocaine Exposure and Withdrawal on Dopamine Functioning — Mackenzie L. Love, Rachel L. Pace, Patricia A. Nalan, Deranda B. Lester

18 Exploring Undergraduate Biology and Chemistry Students' Understanding of Enzymes — Em Micer

40 Age-Dependent Effects of Social Isolation on Behaviors Related to Anxiety and Addiction in Mice — Serena J. Addison, Sophia Lemus, Deranda B. Lester

Humanities

58 Germanic Emigrants in Memphis, 1865-1880 — Sophia Rouse

78 Cavendish's Queer Fancies, Scientific and Romantic, in The Blazing World and The Convent of Pleasure — Donald Young

Engineering

94 Analysis of in-vivo macrophage polarization in response to raspberry ketone-loaded chitosan membranes for guided bone regeneration — Samantha Hall, Melika Rad, Joel D. Bumgardner

110 Two-Way Pepper Ghost — Ethan Costello, Ana Doblas

Physical and Applied Sciences

124	Si2Te3 Dimer Orientation Structure	Justin Brutger
136	High-quality few-layered MoS2 thin films through plasma-enhanced CVD	Julian I Lopez
152	Remotely Controlled Curvature on Liquid Crystal Elastomer Networks Using Light	Andrew Johnson
164	Self-Induced Spatial Organization of Nanoparticles in a Polymer Brush: A Molecular Dynamics Study	Jacob Mims Mohamed Laradji
178	Utilizing Silver Nanocubes to Promote Förster Resonance Energy Transfer (FRET) Between Cadmium Selenide and Perovskite Quantum Dots Embedded in a Polymer Layer Upon Optical Excitation	Rohith Narra

Publication and Review Process

194 Faculty Reviewers Board

199 Submission Guidelines

Mackenzie Love is a junior Psychology major with a concentration in Behavioral Neuroscience and minors in Biology and American Sign Language. She has a passion for Behavioral Neuroscience, wanting to learn everything that she can. She is very focused on academics, as she continues to maximize her undergraduate experience and prepares to pursue a PhD program.

This paper received a QuaesitUM outstanding paper award.

Mackenzie L. Love, Rachel L. Pace
Patricia A. Nalan & Deranda B. Lester

The Effects of Chronic Cocaine Exposure and Withdrawal on Dopamine Functioning

Faculty Sponsor

Dr. Deranda B. Lester

Abstract

The mesolimbic dopamine pathway, often referred to as the reward pathway, consists of cell bodies in the ventral tegmental area (VTA) that project to limbic regions, particularly the nucleus accumbens (NAc). Cocaine increases dopamine activity by blocking dopamine transporters (DATs), consequently inhibiting dopamine reuptake. This study aimed to determine the effects of chronic cocaine exposure and withdrawal on dopamine functioning. Mice were divided into four groups: chronic cocaine exposure, chronic saline exposure, chronic cocaine exposure plus a withdrawal period, and chronic saline exposure plus a withdrawal period. In vivo fixed amperometry was used to measure VTA stimulation-evoked dopamine release and reuptake in the NAc of anesthetized mice before and after an in-test cocaine injection. Cocaine exposure and withdrawal seemed to have the greatest effect on variables related to DAT functioning rather than dopamine release. Studies such as these may be useful in improving treatments for substance use disorders.

Introduction

The 2019 National Survey on Drug Use and Health (NSDUH) reported that 5.5% of Americans between ages 18 and 25 used cocaine that year. The misuse of cocaine can lead to health conditions and even overdose causing death. According to the National Institute on Drug Abuse (NIDA, 2021), there were more drug-related overdose deaths in 2020 than in any other one-year period in history; this was an increase of 30 percent from the previous year. Surveys also report that relapse is common for those who attempt to quit cocaine, with drug addiction treatment resulting in a rate of relapse between 40% to 60% of the cases (Wagener & Thomas, 2021). There are different types of behavioral therapies that are offered to those who are wanting to stop using cocaine; however, there are currently no FDA-approved pharmaceuticals for stimulant use disorder. To work towards this pharmaceutical and improving treatment for stimulant use disorder, a better understanding of neural changes following chronic cocaine use is necessary.

Cocaine prolongs the activity of dopamine in the synapse by blocking the dopamine reuptake mechanism, dopamine transporters (Wise, 1984). The mesolimbic dopamine pathway, often referred to as the reward pathway, consists of dopamine cell bodies in the ventral tegmental area (VTA) that project to limbic regions, particularly the nucleus accumbens (NAc). When the NAc is stimulated by extracellular dopamine, the cells in the NAc further ignite neural circuits that produce reinforcing effects. Thus, cocaine's ability to greatly increase dopamine activity in the NAc drives the reinforcing properties of the drug and the continued use of the drug even while facing negative consequences (Nestler, 2005).

Previous research showed that repeated cocaine use alters the functioning of DAT, potentially altering the way brains respond to rewarding stimuli. For example, Mash et al. (2002) found that DAT function was severely elevated following chronic cocaine use in baboons compared to age-matched drug-free controls (Mash et al., 2002), and Daws et al. (2001) found that cocaine increases the cell surface distribution of DAT in rodents. Furthermore, abstinence from chronic cocaine use is known to induce withdrawal effects, such as cravings, anxiety, and anhedonia (Ball et al., 2018; Mendez & Salazar-Juarez, 2019; Stoker & Markou, 2011). Many of these withdrawal behaviors are thought to be driven by drug-induced dopaminergic changes. In a study by Cerruti et al. (1993), a 10 day withdrawal period from cocaine lead to a long-lasting decrease in DAT binding. In other words, the gene expression was altered many days after withdrawal from cocaine. Cerruti et al. (1993) concluded that this altered DAT could be a significant factor

underlying behavioral and biochemical changes during cocaine withdrawal. Altogether these studies suggest that chronic cocaine use increases the number of DAT, which is then decreased following a withdrawal period. DAT fluctuations greatly control the amount of extracellular dopamine available in the synapse.

Here, we are addressing the research question of how chronic cocaine plus withdrawal affects functional dopamine release. A better understanding of the neurochemical effects of cocaine use and abstinence may lead to improved treatments for cocaine use disorder. We used fixed potential amperometry in vivo to measure VTA stimulation-evoked dopamine release and reuptake in four groups mice: chronic cocaine exposure, chronic saline exposure (control), chronic cocaine exposure plus a withdrawal period, and chronic saline exposure plus a withdrawal period (control). Dopamine release was determined by measuring the magnitude of the stimulated response, and dopamine reuptake was quantified by measuring the synaptic half-life of dopamine. The synaptic half-life of dopamine is an indication of how quickly dopamine is being cleared from the synapse. The synaptic half-life of dopamine is dependent on DAT functioning, with a faster synaptic half-life indicating more efficient DAT functioning (Holloway, 2018).

To further test DAT functioning and the way the mesolimbic dopamine system response to a dopaminergic drug, all mice received an in-test cocaine challenge during dopamine recordings. Therefore, dopamine release and reuptake (synaptic half-life) were quantified before and after the in-test cocaine challenge. It was hypothesized that chronic cocaine would increase DAT functioning compared to saline, resulting in a shorter baseline dopamine half-life and a reduced dopaminergic response to the in-test cocaine challenge. It was also hypothesized that chronic cocaine plus a withdrawal period would decrease DAT functioning compared to saline, resulting in a longer baseline dopamine half-life and an increased dopaminergic response to cocaine. The findings of the current study will further the understanding of neural changes following chronic cocaine administration and potentially further the research in addiction treatments.

Methods

The proposed experiment was approved by the Institutional Animal Care and Use Committee (IACUC) at the University of Memphis and were also aligned with those outlined in The Public Health and Service Policy on Humane Care and Use of Laboratory Animals (National Institutes of Health 2012) and the Guidelines for the Care and Use of Mammals in Neuroscience and Behavioral Research (National Research Council 2015).

Subjects

Twenty-seven male C57BL/6J mice were acquired from Jackson Laboratory (Bar Harbor, ME, USA) at 3 weeks of age. Upon arrival, mice were immediately and randomly separated into separate cages with 2 to 4 mice per cage. Cages were kept in a temperature-controlled room (21 ± 1° C) with a 12-hour circadian cycle. Food and water were available ad libitum. Mice remained in the animal colony until time of experiments. Mice were adults at the time of experiments (3-5 months old).

Procedures

Drug pretreatments consisted of the mice being intraperitoneally (ip) injected with cocaine (20 mg/kg) or saline every day for seven days. Some of the mice (n = 16, 8 cocaine-exposed and 8 saline-exposed) were tested on the eighth day, which is 24 hours after the last injection. The other mice were exposed to a one week withdrawal period (n = 11, 5 cocaine-exposed and 6 saline-exposed), meaning that the testing occurred on day 15. See Table 1 for a list of experimental groups and Figure 1 for a depiction of the experimental timeline. On the day of dopamine measurements, the mice were permanently anesthetized using two urethane injections (totaling 1.5 g/kg, ip). Foot and tail pinch and eye blink induced reflexes fifteen minutes after second injection guaranteed proper anesthetization. They were then mounted in a stereotaxic frame, while maintaining a body temperature of approximately 37°C. Stereotaxic carriers were used to guide all electrodes.

A stimulating electrode was placed into the left VTA (coordinates: AP -3.3 mm from bregma, ML +0.3 mm from midline, and DV -4.0 mm from dura; Paxinos & Franklin, 2001). A reference and auxiliary electrode combination was placed in contact with cortical tissue contralateral to the stimulating electrode (-3.0 mm from bregma). Lastly, a carbon fiber recording electrode was implanted into the left NAc (AP +1.5 mm from bregma, ML +1.0 mm from midline, and DV -4.0 mm from dura). See Figure 2 for a depiction of the surgical setup. A fixed current of +0.8 V was applied, with dopamine oxidation currents being continuously monitored (10K samples/sec) by an electrometer (ED401 e-corder 401 and EA162 Picostat, eDAQ Inc). Stimulation parameters consisted of 20 pulses at 50 Hz every 30 sec. Baseline measurements were recorded for 5 minutes, then mice received a cocaine challenge (20 mg/kg, ip). The same stimulation parameters continued, and dopamine recordings continued 1-hour post-cocaine injection. Immediately following data collection, direct anodic current of 100 mAmps was applied for 10 seconds to mark the electrode positions. Mice were then euthanized by intracardiac injection of an overdose of urethane (0.345 g/mL)

Data Analysis

There were two independent variables for this project: chronic drug exposure (cocaine or saline) and withdrawal period (no withdrawal period or plus withdrawal period). There were four dependent variables: (1) baseline dopamine release (nAmp), (2) baseline dopamine half-life (sec), (3) dopamine release following cocaine administration (% change from baseline, with baseline set at 100%), and (4) dopamine half-life following cocaine administration (% change from baseline, with baseline set at 100%). Dopamine release and half-life measurements were compared at the peak effect time of cocaine (which was 20 min following the in-test cocaine challenge). Two-way between-subject ANOVAs were used to determine the effect of drug exposure and withdrawal on each of the 4 dependent variables. When appropriate, one-way ANOVAs with Tukey HSD post hoc analyses were used to determine specific group differences.

Table 1. Experimental Groups

Drug Exposure	Withdrawal	*N*
Cocaine	None	8
	Withdrawal	5
Saline	None	8
	Withdrawal	6
	TOTAL	**27**

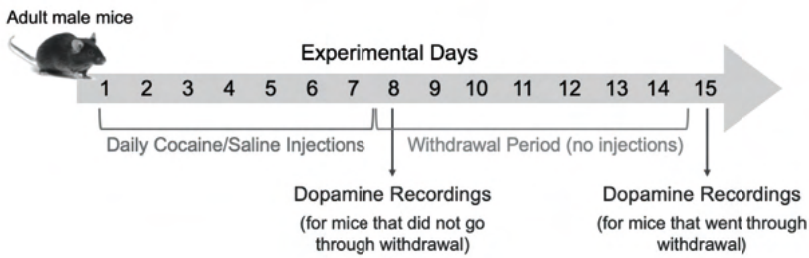

Figure 1. Experimental Timeline

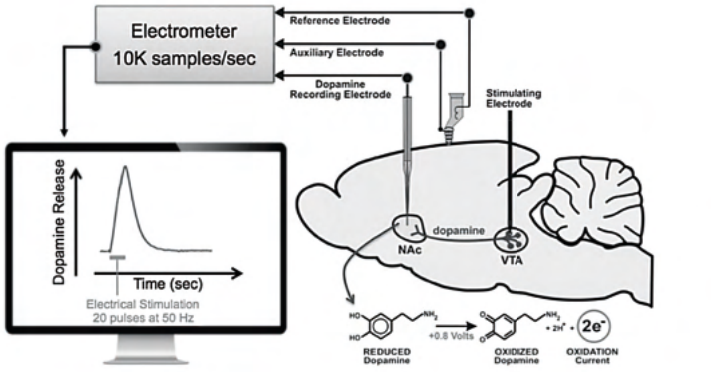

Figure 2. Surgical Set-up for Amperometric Recordings. In vivo fixed amperometry with carbon fiber recording electrodes quantified nucleus accumbens (NAc) dopamine release and half-life evoked by stimulation of dopamine cell bodies within the ventral tegmental area (VTA).

Results

Baseline Dopamine Functioning

Regarding the baseline dopamine release, a two-way between subjects ANOVA was used to compare mean dopamine release before the in-test cocaine administration. There was not a significant main effect of drug (chronic cocaine or saline) or withdrawal on baseline dopamine release, [drug: $F(1,1) = 2.2$, $p = 0.152$; withdrawal: $F(1,1) = 0.481$, $p = 0.495$], and no significant interaction was observed between the effects of drug and withdrawal on baseline dopamine release, [$F(1,1) = 0.007$, $p = 0.936$] (Figure 1).

Regarding the baseline dopamine half life, a two-way between-subjects ANOVA was used to compare the mean synaptic half-life of dopamine before the in-test cocaine administration. Similarly to that observed in baseline dopamine release, there was not a significant main effect of drug or withdrawal on baseline dopamine half-life, [drug: $F(1,1) = 0.193$, $p = 0.664$; withdrawal: $F(1,1) = 0.057$, $p = 0.814$]. However, there was a statistically significant interaction between drug and withdrawal on baseline dopamine half-life, [$F(1,1) = 8.618$, $p = 0.007$] (Figure 2), indicating that the synaptic half-life of dopamine was affected by the withdrawal period differently depending on drug exposure (cocaine or saline). A follow up one-way ANOVA was used to compare group differences in baseline dopamine half-life. The ANOVA neared significance, but did not reach significance, [$F(3,23) = 2.880$, $p = 0.058$]; therefore, post hoc analyses were not conducted.

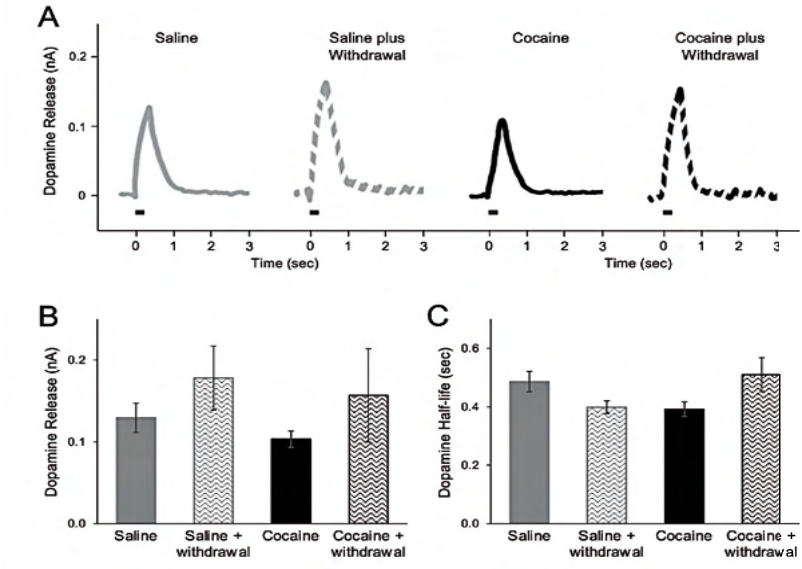

Figure 3. Baseline Dopamine Responses. Profiles indicate representative responses from each group (A). No significant effects were observed in mean (± SEM) dopamine release between chronic drug or withdrawal groups (B). There was a significant interaction between drug and with-drawal on baseline dopamine half-life, but no significant differences were observed between groups (C).

Dopamine Functioning Following the Cocaine Challenge

Regarding the dopamine release following the cocaine challenge, a two-way ANOVA was used to compare percent change in dopamine release following the in-test cocaine administration. There was not a significant main effect of drug or withdrawal on cocaine-induced changes in dopamine release, [drug: $F(1,1) = 0.354$, $p = 0.558$; withdrawal: $F(1,1) = 1.408$, $p = 0.248$], and no significant interaction was observed between drug and withdrawal on percent change in dopamine release following cocaine, [$F(1,1) = 0.334$, $p = 0.569$] (Figure 3).

Regarding the dopamine half-life following the cocaine challenge, a two-way ANOVA was used to compare mean dopamine half-life after cocaine administration. There was a near significant main effect of drug on dopamine half-life, [$F(1,1) = 3.412$, $p = 0.078$], but no follow-up analyses were conducted. There was a statistically significant main effect of withdrawal on dopamine half-life, [$F(1,1) = 5.603$, $p = 0.034$]. A follow up independent samples t-test showed that there was a statistically significant difference in dopamine half-life post cocaine when comparing the no-withdrawal group to the withdrawal group, $t(25) = 2.213$, $p = 0.036$. These results indi-

cate that the mice that experienced a withdrawal period (1 week without injections) displayed an increased percent change in dopamine half-life following cocaine. No significant interaction was observed between drug and withdrawal on dopamine half-life post cocaine challenge, [$F(1,1) = 0.346$, $p = 0.592$] (Figure 4)

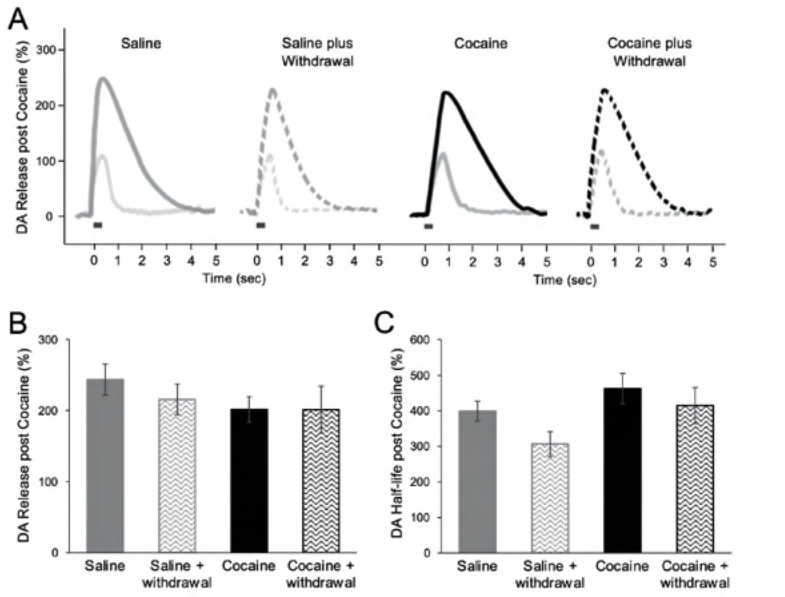

Figure 4. Dopamine Responses post Cocaine Administration. Profiles indicate representative responses from each group at 20 min post injection (A). No significant effects were observed in mean (± SEM) percent change in dopamine release following cocaine (B). There was a near significant main effect of drug and a significant main effect of withdrawal on percent change in dopamine half-life follow-ing cocaine, but no interactive effect between drug and withdrawal (C).

Discussion

The purpose of the current study was to examine the effects of cocaine exposure and withdrawal on NAc dopamine functioning. This study used four groups depending on the changes of the two variables, which are drug exposure and withdrawal, resulting in 4 experimental groups: chronic cocaine exposure, chronic saline exposure (control), chronic cocaine exposure plus a withdrawal period, and chronic saline exposure plus a withdrawal period (control). We used fixed potential amperometry to measure dopamine

release before and after the cocaine challenge. The dependent variables were baseline dopamine release, baseline dopamine half-life, dopamine release post cocaine challenge, and dopamine half-life post cocaine challenge. Overall, cocaine exposure and withdrawal seemed to have the greatest effect on variables related to dopamine transporter (DAT) functioning rather than dopamine release.

Effects of Chronic Cocaine

All mice in this project were chronically exposed with daily injections to either cocaine or saline. Regarding baseline dopamine functioning, which was before the in-test cocaine challenge, no main effect of cocaine exposure was observed on either dopamine release or synaptic half-life. Given that cocaine does not directly alter dopamine release mechanisms, it was expected that cocaine exposure would not alter baseline dopamine release. These results fit with a previous study (Pattison et al., 2012). However, unexpected results showed that cocaine exposure did not alter baseline dopamine half-life. Given that DAT are responsible for clearing dopamine from the synapse, dopamine half-life is a measurement of DAT function. Daws et al. (2001) found that cocaine exposure increases the cell surface redistribution and expression of dopamine transporters, which should lead to faster synaptic clearance. A direct visual comparison of the cocaine-exposed mice and the saline-exposed mice, without including the withdrawal groups, does indicate a reduced dopamine half-life, which means faster clearance following cocaine exposure, but these direct comparisons were not statistically analyzed given the initial plan of the project.

Regarding the dopaminergic response to the in-test cocaine challenge, cocaine increased both dopamine release and half-life in all mice, as expected. Chronic cocaine exposure did not alter the percent change in dopamine release following the cocaine challenge. However, there was a near significant main effect of drug exposure on percent change in dopamine half-life following the cocaine challenge. Although not to a significant extent, the time dopamine remained in the synapse was increased by cocaine to a greater degree in cocaine-exposed mice compared to saline-exposed mice. These differences may have been driven by the surprisingly low responses observed in the saline-withdrawal group, which is discussed below. We expected a decreased dopaminergic response to the cocaine challenge following chronic cocaine exposure, as observed in previous studies (Francis et al., 2019; Lopez-Arnau et al., 2019). Our results may be related to drug exposure periods; however, we chose this dosing regimen as others have shown it to alter dopamine-related cellular functioning and behaviors (Feng et al., 2014; Hiroi et al., 1997)

Effects of Chronic Cocaine Plus Withdrawal

Roughly half of the mice in this project were subjected to a 7-day withdrawal period with no injections before dopamine recordings. Some of the mice were going through withdrawal following chronic cocaine exposure and some following chronic saline exposure. It was important to have a saline withdrawal group to serve as a control for the cocaine withdrawal group in order to determine whether the 7-day absence of the injection protocol made a difference. It has been shown that animals can experience injection stress with any kind of injection (Baik, 2020), and stress has been shown to affect dopamine levels and neuronal activity in the mesolimbic dopamine system (Baik, 2020). Thus, removal of daily injections may have altered dopamine functioning, regardless of the drug. Withdrawal, without taking the cocaine/saline exposure into consideration, did not alter baseline dopamine release or half-life, but it did alter the dopaminergic response to the in-test cocaine challenge.

Specifically, a main effect of withdrawal was observed on the percent change in dopamine half-life following cocaine. Mice that went through withdrawal displayed a decreased dopaminergic response to cocaine. Mice in an active state of stress have been shown to have increased dopaminergic responses to psychostimulants (Baik, 2020). Thus, animals that did not go through the withdrawal period (7 days of no injections) may have been in an active state of stress, especially if they were receiving saline injections). Future studies could monitor stress levels, such as through hormone measurements or behavioral assays, to answer these questions. Future studies could also use a different route of drug administration, such as consumption through food or drink, in order to subject the animals to less stress. Future studies could also lengthen the withdrawal period to better understand the development and timing of withdrawal-related effects.

Examining the interactions between the drug exposure and withdrawal is the important component in determining whether cocaine withdrawal resulted in differences in dopamine functioning relative to saline withdrawal. There was no interaction observed between drug exposure and withdrawal on baseline dopamine release. There was, however, a significant interaction observed in baseline dopamine half-life. It looked as though withdrawal following cocaine exposure lead to an increased dopamine half-life compared to the cocaine exposed mice, indicating that some DAT compensation occurred during the cocaine withdrawal, as the dopamine half-life of the cocaine withdrawal mice more closely resembled that of the saline exposed controls.

Saline withdrawal, however, seemed to result in a reduced dopamine half-life (increased DAT function) relative to the saline exposed. The follow-up one way ANOVA analysis was not significant ($p = .058$). Adding a few mice per group may reduce the observed error and clarify these results. No significant interaction was observed between drug and withdrawal on the dopaminergic response to cocaine (in either percent change-in-release or half-life).

Conclusion

The present study indicates that cocaine exposure and withdrawal alter dopamine functioning, specifically dopamine transmission related to DAT function. These findings are not surprising given that cocaine's mechanism of action is to inhibit DAT and have shown DAT expression to fluctuate based on cocaine administration. DAT functioning seems to be restored to some degree by the withdrawal period, but more research is needed given that the withdrawal period also altered dopamine functioning in the saline-exposed mice. These findings are limited by a few aspects of the experimental design.

Sex has been shown to affect dopamine release and responses to psychostimulants (Perez et al., 2018), and the current study was only conducted on males. Future studies should include females to determine whether these findings are generalizable to females. Also, as mentioned above, altering the dosing regimen and length of the withdrawal period could provide useful information about the timing of compensatory mechanisms. Furthermore, some limitations could be due to the age of the mice.

Future studies could include a wider variety of age in subjects to examine the differences in adolescent metabolism versus adult metabolism. This would be a further investigation into dopaminergic response, as there may be a cocaine dopamine sensitization difference across ages. Overall, the current study further adds to the understanding of neural changes following chronic cocaine administration and withdrawal. Such studies are needed to improve treatments for substance use disorders.

References

Baik, J. (2020). Stress and the dopaminergic reward system. Experimental and Molecular Medicine, 52, 1879-1890.

Ball, K. T., Stone, E., Best, O., Collins, T., Edson, H., Hagan, E., Nardini, S., Neuciler, P., Smo-linsky, M., Tosh, L., & Woodlen, K. (2018). Chronic restraint stress during withdrawal increases vulnerability to drug priming-induced cocaine seeking via a dopamine d1-like recep-tor-mediated mechanism. Drug and Alcohol Dependence, 187, 327–334. https://doi.org/10.1016/j.drugalcdep.2018.03.024

Cerruti, C., Pilotte, N., Uhl, G., & Kuhar, M. J. (1993). Reduction in dopamine transporter mRNA after cessation of repeated cocaine administration. Molecular Brain Research, 22, 132-138.

Daws, L. C., Callaghan, P. D., Moron, J. A., Kahlig, K. M., Shippenberg, T. S., Javitch, J. A., & Galli, A. (2001). Cocaine increases dopamine uptake and cell surface expression of dopamine transporters. Biochemical and Biophysical Research Communications, 290(5), 1545-1550.

Francis, T. C., Gantz, S. C., Moussawi, K., & Bonci, A. (2019). Synaptic and intrinsic plasticity in the ventral tegmental area after chronic cocaine. Current Opinion in Neurobiology, 54, 66–72.

Feng, J., Wilkinson, M., Liu, X., Purushothaman, I., Ferguson, D., Vialou,V., ... & Shen, L. (2014). Chronic cocaine-regulated epigenomic changes in mouse nucleus accumbens. Genome Biology, 15(4), 1-18.

Hiroi, N., Brown, J. R., Haile, C. N., Ye, H., Greenberg, M. E., & Nestler, E. J. (1997). FosB mutant mice: Loss of chronic cocaine induction of Fos-related proteins and heightened sensitivity to cocaine's psychomotor and rewarding effects. Proceedings of the National Academy of Sciences, 94(19), 10397-10402.

Holloway, Z.R. (2018). Examining cerebellar modulation of mesolimbic dopamine transmission using fixed potential amperometry. ProQuest Dissertations Publishing.

Lopez-Arnau, R., Duart-Castells, L., Aster, B., Camarasa, J., Escubedo, E., & Pubill, D. (2019). Effects of MDPV on dopamine transporter regulation in male rats comparison with cocaine. Psychopharmacology,

236, 925-938.

Mash, D. C., Pablo, J., Ouyang, Q., Hearn, W. L., Izenwasser, S. (2002). Dopamine transport function is elevated in cocaine users. Journal of Neurochemistry, 82(2), 292-300.

Mendez, S. B. & Salazar-Juarez, A. (2019). Mirtazapine attenuates anxiety- and depression-like behaviors in rats during cocaine withdrawal. Journal of Psychopharmacology, 33(5), 543-547.

National Institute of Health (NIH) Office of Laboratory Animal Welfare (OLAW), (2015). PHS Policy on Humane Care and Use of Laboratory Animals. https://olaw.nih.gov/policies-laws/phs-policy.htm

National Research Council. 2011. Guide for the Care and Use of Laboratory Animals: Eighth Edition. Washington, DC: The National Academies Press. https://doi.org/10.17226/12910.

Nestler, E. J. (2005). The Neurobiology of Cocaine Addiction. Science Practice Perspectives, 3(1), 4–10. https://doi.org/10.1151/spp05314.

NIDA. (2021). Drug overdose deaths in 2020 were horrifying. Radical change is needed to address the drug crisis. Retrieved from https://www.drugabuse.gov/about-nida/noras-blog/2021/08/drug-overdose-deaths-in-2020-were-horrifying-radical-change-needed-to-address-drug-crisis on 2021, September 17.

Pattison, L. P., McIntosh, S., Budygin, E.A., & Hemby, S.E. (2012). Differential regulation of accumbal dopamine transmission in rats following cocaine, heroin, and speedball self-administration. National Institute of Health, 111, 223-230.

Paxinos, G., & Franklin, K. B. J. (2001). The Mouse Brain in Stereotaxic Coordinates (2nd ed.). San Diego, CA: Academic Press.

Perez, P. D., Hall, G., Zubcevic, J., & Febo, M. (2018). Cocaine differentially affects synaptic activity in memory and midbrain areas of female and male rats: an in vivo MEMRI study. Brain Imaging and Behavior, 12(1), 201-216.

Substance Abuse and Mental Health Services Administration. (2019). Key substance use and mental health indicators in the United States: Results from the 2018 National Survey on Drug Use and Health (HHS Publication No. PEP19-5068, NSDUH Series H-54).

Rockville, MD: Center for Behavioral Health Statistics and Quality, Substance Abuse and Mental Health Services Administration. Retrieved from https://www.samhsa.gov/data/

Stoker, A. K., & Markou, A. (2011). Withdrawal from chronic cocaine administration induces deficits in brain reward function in C57BL/6J mice. Behavioural Brain Research, 223(1), 176–181. https://doi-org.ezproxy.memphis.edu/10.1016/j.bbr.2011.04.042.

Wagener, D., & Thomas, S. (2021). Dealing with cocaine addiction relapse: Relapse triggers. Recovery.org. Retrieved September 17, 2021, from https://www.recovery.org/cocaines/relapse/.

Wise R. A. (1984). Neural mechanisms of the reinforcing action of cocaine. NIDA research monograph, 50, 15–33.

Em Micer graduated from the University of Memphis in 2021 with a double major in Chemistry and Biology. In 2020, they were awarded the Honors Summer Research Fellowship from the University of Memphis, which led to their continued research, the completion of their honors thesis, and, eventually, this publication. Throughout this research journey, they have presented at multiple conferences, even winning 1st place for 2 of these presentations. Since graduating, Em has begun working in a laboratory while in preparation to take the MCAT and apply to medical school. Outside of education, they enjoy gaming, cross-stitching and volunteering for organizations such as the Ronald McDonald House Charity and the Red Cross.

Em Micer

Exploring Undergraduate Biology and Chemistry Students' Understanding of Enzymes

Faculty Sponsor

Dr. Jaime Sabel

Abstract

When undergraduate students in introductory biology and chemistry courses learn about enzymes, their understanding tends to be superficial, and students tend to struggle with thinking about the functionality of enzymes in a visually representative way. In this study, we created and tested an activity based on Dr. Nathan DeYonker's NSF CAREER grant-funded website, RINRUS, that is intended to increase students' long-term retention and understanding of enzymes. We first ran a pilot study in a class of graduate students to determine assignment accessibility. We then surveyed and interviewed students in introductory biology and chemistry courses to determine what information about enzymes students learn and retain. Results from this study will help to develop student understanding about enzymes and provide ideas and strategies for instructors to support their students in understanding enzyme structure and function.

Introduction

For early biology and chemistry students, typically freshmen and sophomores, developing an intricate network of long-term memory that is parallel to accepted scientific thought is a key to learning the sciences (Gabel, 1999). Students may often have a difficult time understanding scientific concepts, particularly chemistry concepts, because they are unable to relate these concepts to real life (Gabel, 1999). However, undergraduate students are sometimes able to correctly solve problems that graduate students are unable to due to the undergraduate student's ability to think about a problem on a deeper level, without as many restrictions based on prior understanding of a concept (Rickey and Stacy, 2000). Although undergraduate students may be more open to new ideas, teaching science to undergraduate college level students can prove to be difficult for a myriad of reasons. Some of these reasons include, but are not limited to, changing fields, a professor's resistance to change, student fear of new types of instruction, and scarcity of resources in a changing institution (Sunal et al., 2001). Finding new ways to teach scientific concepts that are accessible and beneficial to college students is essential.

According to Stains et al. (2018), a majority of students are being taught chemistry through didactic measures alone, while instructors spend very little time adapting their teaching method to student-centered learning. This occurs in many STEM courses; however, Oludipe and Awokoy (2010) show that this occurs in chemistry courses frequently. Teaching students in this manner often leads to asking questions within the classroom by calling on individual students, which will cause students anxiety (Oludipe and Awokoy, 2010). Oludipe and Awokoy (2010) also suggest that students who have experienced this type of anxiety are more likely to limit their participation when learning. Based on the results found by Oludipe and Awokoy (2010), group assignments can cause stress to individuals if effort is not put in by all parties, but they have also been proven to be useful in fostering ideas and relieving anxiety. Chemistry courses tend to be high stress for many students, since they involve a wealth of new, complex material. The introduction of more group activities involving student-centered learning can increase confidence and success in chemistry courses.

Metacognition is the understanding of one's own cognitive processes (Sabel, Dauer, and Forbes, 2017; Schraw, Crippen, and Hartley, 2006). Rickey and Stacy (2000) state that "whether students' knowledge is coherent or fragmented and context-bound, a keen awareness of their own conceptions should allow students to recognize when their ideas are not productive. One effort made to increase understanding of chemistry concepts is the addition

of concept maps, which allow students to construct visual diagrams that show how concepts are related. Another method of chemistry learning is the Predict-Observe-Explain (POE) task, which is often used in beginner chemistry courses when students are just learning concepts. While POE tasks can be useful by allowing students the opportunity to observe actual outcomes and compare them to their initial predictions, Tien, Rickey and Stacy (1999) elaborated on this and created the Model-Observe-Reflect-Explain (MORE) Thinking Frame which "is used to help students think about the inquiry process and their own process of learning about science concepts" (p. 318). By allowing students to interact with material and observe what happens, they are able to challenge their own misconceptions to determine the true answers. Overall, students are often able to best learn about chemistry concepts when they are given the opportunity to evaluate their own understanding.

Oftentimes when undergraduate students begin progressing into upper-level biology and chemistry courses, they have difficulties piecing together information from earlier classes. One topic that students find particularly difficult is specific information regarding enzymes. To combat this gap in enzyme understanding in undergraduate biology students, an assignment was created by adopting portions of the Residue Interaction Network-based ResidUe Selector (RINRUS). RINRUS was created by Dr. Nathan DeYonker. RINRUS was created by Dr. Nathan DeYonker and his research group (see Summers et al. 2019 for another project using this program). It is a computational biochemistry research software package with a user-friendly web interface. RINRUS functions to create models of enzyme-substrate complexes at different levels of specificity that are able to be visualized through software such as the Molecular Operating Environment (MOE) or online through several web-based viewers.

The Multiple Intelligence Theory shows that humans all have 8 different types of intelligence, and each of these types of intelligences interact in a different way within the world (Gardner, 2011). Gardner (2011) lists the intelligences as the following: linguistic, logical-mathematical, musical, spatial, bodily-kinesthetic, interpersonal, intrapersonal, and naturalistic. In one study by Yalmanci and Gözüm (2013), students were taught about enzymes using eight different activities that aligned with each type of intelligence. Results from this study showed that students retained enzyme information to a greater extent than students in a control group (Yalmanci and Gözüm, 2013). Although the visual-spatial mode of intelligence is often thought to be of use in architects and others who work with their hands, the basis behind it is the ability to perceive information and create visual images from this information (Gardner, 2011). In the study completed by Yalmanci

and Gözüm (2013), the visual-spatial category of intelligence was placed into an activity by use of visual presentations such as PowerPoint. However, we propose that by extending the visual-spatial area of intelligence to allow students to create three-dimensional models of enzyme-ligand complexes, students will have the ability to understand these complexes to a greater degree. Construction and manipulation of protein models will help students develop a more concrete understanding of what happens in these complexes, rather than simply being taught this concept through a PowerPoint lecture.

To begin with, we created an assignment based on the RINRUS website previously mentioned. To understand the effectiveness and accessibility of the RINRUS assignment, we ran a pilot study in a class of chemistry graduate students. To better understand the current level of content that introductory undergraduate students were taught and the extent of their enzyme knowledge, we evaluated class materials that focused on enzymes and asked students to complete surveys and interviews within General Biology I, General Chemistry I, and General Chemistry II courses. Our overarching goal was to enrich General Biology I student understanding of enzymes, as this is a required course for all students in the Biology and Chemistry majors. Students in General Biology I also have course material already dedicated to learning about enzymes. The purpose of this study was to explore the results of the following research questions:

1. How do graduate chemistry students perceive the RINRUS assignment as it pertains to understanding enzymes?
2. What information about enzymes are beginner undergraduate biology and chemistry students obtaining and retaining from their courses?

Methods

Participants and Context

To create the RINRUS assignment, we viewed class materials and typical textbooks that are used in General Biology I to see what students are usually taught regarding enzymes through this course. Once we evaluated and compiled all lecture material, we began creating the RINRUS assignment. At the beginning of the assignment, we provided an overview of enzymes, including a review of what students are taught during class. Additionally, we added some more specific information that would be necessary to the assignment, including topics such as chemical mechanisms and arrow pushing, which is a way to show the movement of electrons and the formation and breaking of bonds within a mechanism. In addition, we included information about x-ray crystallography and why computational chemistry is important. Following

this background material, we tasked students with finding a peer-reviewed article about a specific enzyme in the Protein Data Bank (PDB) repository. The function of requiring an article was to bridge any gaps that might not be clear with visualization of the enzyme alone. Students then viewed the enzyme through the PDB Ligand Interaction viewer, allowing them to visualize the connections between the enzyme and ligand. Students were then tasked with inserting PDB information into the RINRUS website, and from the website students would receive a zip file. Finally, students would open this zip file using the program MOE, which would allow the students to visualize the enzyme-ligand complexes in a variety of ways. We obtained IRB approval from the University of Memphis (protocol #PRO-FY2021-241) before we began testing the assignment with students.

All 11 students from a graduate level chemistry class, CHEM 8711: Approximate Chemical Modeling Methods, were recruited to participate in the pilot run of the RINRUS assignment over 2 class meetings during the Fall 2019 semester. All students were graduate students in the Department of Chemistry. This class consisted of three 50-minute meetings per week, and students learned about classical and quantum mechanical techniques for modeling chemical systems and molecular mechanics. Eight of these students participated in interviews lasting approximately 25 minutes long to understand what alterations to the RINRUS assignment might be needed for introduce it to beginner chemistry and biology students. Each student who participated in an interview was given a $10 gift card.

At the University of Memphis, students following biology and chemistry degree paths are required to enroll in and pass General Chemistry I before they are able to take General Biology I. This often leads to students being enrolled in General Biology I and General Chemistry II simultaneously, however students do not always follow this exact path. Following interviews with the graduate-level class, students enrolled in General Biology I and General Chemistry I were asked to complete surveys and interviews following the Spring 2020 semester to determine the difference in understanding between these courses, with General Chemistry I acting as a baseline. Students enrolled in General Biology I learned about cell structure and function, heredity, and evolution, and the class consisted of two 85-minute meetings per week. Of the 158 students enrolled in General Biology I, 12 students participated in the survey during the summer, and 3 students participated in interviews. Students enrolled in different sections of General Chemistry I were taught about the following: laws of chemistry, atomic theory and bonding, molecular geometry, states of matter, the periodic table and chemical periodicity, and many other topics. Of the 352 students enrolled

in General Chemistry I in the spring semester, 17 students participated in the survey during the summer, and four students participated in the interviews. The surveys consisted of 20 questions and lasted approximately 25-30 minutes, and the interviews lasted 20-25 minutes. Each student who participated in the surveys was placed into a drawing for a $50 gift card, and all students who participated in the interviews were given $10 gift cards for their time. Participation in these surveys was quite low due to quarantine and online schooling brought on by COVID-19.

During the Fall 2020 semester, students enrolled in General Biology I and General Chemistry II were recruited to complete pre and post surveys as well as interviews detailing their understanding of enzymes. General Biology I was structured similarly to the class during the Spring 2020 semester, albeit entirely online. Of the 164 students enrolled in General Biology I, 24 students participated in the pre-survey, six participated in the post-survey, and five participated in an interview. Students enrolled in General Chemistry II were taught of the physical properties of solutions, chemical kinetics and equilibrium, thermodynamics, electrochemistry, and acid-base reactions. This course consisted of two 85-minute meetings per week. Of the 91 students enrolled in this section of General Chemistry II, 12 students participated in the pre-survey, five participated in the post-survey, and two participated in an interview. Each student who participated in the pre-survey was entered into a drawing for a $50 gift card, and a separate drawing was done for each student who completed the post-survey for a $50 gift card. In addition to this, each student who participated in an interview was given a $10 gift card for their time.

Data Collection

A total of 57 students engaged in either interviews or a survey, as described in Table 1. Eleven students from the graduate class completed the RINRUS assignment over the course of two days. Throughout these two class periods, we observed the students, providing guidance as needed throughout the assignment. Any issues students had were noted, whether they be technical or general confusion on the subject matter. In the two weeks after the assignment, 8 graduate students participated in semi-structured interviews, and were asked several questions about their experience with the assignment. The interview questions can be found in Appendix A.

Students in General Biology I and General Chemistry I in the 2020 Spring semester and General Biology I and General Chemistry II in the 2020 Fall semester were given surveys to determine multiple aspects of their learning throughout the semesters. Students who participated in these surveys

that were enrolled in the Spring 2020 semester were asked extra questions about how the shift to online/remote schooling had affected them. Students enrolled in these classes in the Fall of 2020 were given pre- and post-surveys, with the only variations between questions being a tense change, questions about their overall experience, and the insertion of reflection questions. The full list of survey questions regarding enzymes can be found in Appendix B.

Each of the 14 students who participated in semi-structured interviews from this group were asked 15 questions about their demographics, study methods, and enzyme knowledge. The interview question list can be viewed in Appendix C. Each of these interviews were audio-recorded and transcribed to assist with analysis. Students were given randomly generated numbers to serve as IDs to protect their privacy. All data were saved with these numbers rather than names.

	Undergraduate Students	Graduate Students
Fall 2019	0	8
Spring 2020	30	0
Fall 2020	29	0

Table 1. Graduate and Undergraduate Student Participation by Semester. This table shows the number of undergraduate and graduate students who participated in surveys and interviews during each semester.

Data Analysis

For each group of students, graduate and undergraduate, the data obtained from the interviews and surveys were qualitatively analyzed. The graduate student interviews were analyzed to determine the changes that would need to be made to the RINRUS assignment to make it most accessible for undergraduate students. To analyze these interviews, we searched through the responses to see the most common ideas expressed to determine what most graduate students thought would benefit the assignment. For example, every answer to *"What revisions would you suggest to make this assignment more accessible to beginning undergraduate students?"* was categorized based on the response. The categories fell under "literature search revision," "modeling revisions (MOE or another modeling software)," "RINRUS revisions," and "other" for any other categories not previously mentioned.

From each undergraduate student, every answer to *"Explain what an enzyme is?"* was qualitatively analyzed by determining the frequency of certain phrases to determine what students most frequently could recall about enzymes. We searched for key phrases in these answers, such as "catalysts", "lowering activation energy", "lock and key mechanism", and "speed up/

accelerate/induce a reaction" as these are some of the phrases commonly used when describing enzymes in these courses. Evaluating the frequency of these phrases helps determine how much information these students are retain.

Additionally, those students enrolled in the Fall 2020 semester who participated in both pre and post surveys were categorized based on the difference in knowledge from the beginning to the end of the semester. Since so few individuals completed both the pre and post survey interviews, we read through and compared the first and second responses to see if each student had any more specific information to provide about enzymes, including searching for the presence or absence of key words listed above.

Results

Graduate Student Pilot Study

In our graduate student interviews, we focused on determining the accessibility of the RINRUS assignment as well as any changes that needed to be made for undergraduate student success. To begin with, graduate students were worried about undergraduate students' ability to read through the enzyme literature. One of these students suggested including the reading assignment as a pre-lab activity; and another suggested that we only make the students read through the abstract. In addition to this, some of the graduate students experienced some confusion with what information they were supposed to use from the literature which could lead to undergraduate students experiencing confusion as well.

The next issue for graduate students was the ligand viewer. Two students suggested switching to Chem3D rather than the PDB online viewer. In addition to this, some students were concerned with the lack of specificity in the definition of the seed of the complex, and issues with enzymes that have multiple ligands or crystallization cofactors. During insertion of the ligand chains into RINRUS, graduate students suggested providing more specificity in what chains are supposed to be inserted, especially multiples. Finally, in visualizing the complexes through MOE, graduate students were concerned about accessibility for undergraduate students. As many do not use MOE until much later in their degree path, 1 student suggested inserting pictures into the procedure to show what to click on for each question, and 3 students suggested providing a step-by-step video to either work alongside or watch before the assignment began. These interviews showed that some changes were essential before presenting the RINRUS assignment to undergraduate students.

General Chemistry I and General Biology I (Summer 2020)

Of the 18 students who participated in the survey in General Chemistry I, many understood the basic function of enzymes. In response to the question asking students to explain their understanding of enzymes, 10 mentioned that an enzyme is, or acts as, a catalyst, and 8 explained that enzymes accelerate the rate of a reaction. For example, 1 student wrote:

> "An enzyme is a substance that could partially act as a catalyst to induce a specific reaction because it is produced by a living organism."

Many students noted that enzymes are proteins. 1 student stated:

> "Enzymes are molecules that act like catalysts. I have only taken CHEM 1110 so that is about all I know right now."

Although many students were aware of what enzymes are, 2 students mentioned that they were unsure of what an enzyme was and what its functions were.

While most of the students understood the very basic functions of an enzyme, there was no evidence of a higher level of understanding of their mechanisms of action. Of the 4 General Chemistry I students who participated in the interview, most did not provide answers that showed any understanding of enzymes. All 4 students mentioned that their professor did not go over enzymes during the semester, and 1 student mentioned that they were unsure of what an enzyme was during the interview. Overall, their understanding of enzymes was essentially that they were biological catalysts, with only one student mentioning that they accelerate the rate of reaction. It is important to note that students do not learn about kinetics or reaction rates until General Chemistry II, so this prior knowledge likely came from high school instruction. From the interviews, we also confirmed that students at this level have had minimal experience in reading scientific literature.

Twelve students in General Biology I participated in the survey, and 7 of these students specifically stated that enzymes act as catalysts. Five students mentioned that enzymes speed up a reaction, and 3 students specified that enzymes work to lower the required activation energy of a reaction. Several of these students noted that enzymes are a type of protein. These students did show a more advanced understanding than students from General Chemistry I; 1 student specified:

> "An enzyme is a biological catalyst that speeds up chemical reactions by lowering the activation energy of a reaction. The enzyme has an area where a specific substrate can attach, and the enzyme can break that substrate down. The enzyme itself does not break down and can be used again."

Four students in the class noted that enzymes are very specific about what

they break down, and 3 students said that enzymes are not used up in a reaction. Only 3 students in General Biology I participated in interviews. Each of the three students noted that they went over enzymes in class. One student said:

> "What they do is lower the activation energy of chemical processes, making it occur faster than they would if they were not there. They are not changed or lost during the process."

This student followed by listing the 4 levels of structure for proteins. One of the other students explained that enzymes interact with inhibitors that affect how the enzyme works. These students shared a greater understanding of enzyme concepts. Similarly to General Chemistry I students, however, these students also had little experience with reading scientific papers.

General Chemistry II and General Biology I (Fall 2020)

Students in General Chemistry II were asked to participate in pre- and post-surveys as well as interviews. Twelve students participated in the pre-survey, and several of these students had a basic understanding that enzymes act as catalysts to accelerate the rate of a reaction. Of these 12 students, 4 were simultaneously taking General Biology I. Over half the students also mentioned that enzymes are proteins. However, most students could not provide more specific answers. One student who was also enrolled in General Biology I noted:

> "Enzymes are proteins within a living organism. They help speed up processes and chemical reactions. They do so by lowering the activation energy."

Of the 12 responses to the survey, this was the only response that specifically mentioned that enzymes lower the activation energy required for a reaction. Three students mentioned that enzymes have an active site and are very specific in what molecules are able to bind. The post-survey showed similar results on a smaller scale. Four students participated in the post-survey, only 2 of whom had also participated in the pre-survey. Of the two students who completed both surveys, both seemed to have a greater amount of knowledge about enzymes at the end of the semester, but specifics were not used. For example, 1 student wrote in the pre-survey:"*I believe enzymes break down other molecules*." This is not a completely correct statement as some enzymes repair and construct proteins, DNA, etc. In the post-survey, however, this student specified:

> "An enzyme can be used to speed up a reaction by cutting down the activation energy."

Of the 4 responses received, 3 students mentioned that enzymes accelerate the rate of a reaction, and 3 mentioned that enzymes are proteins. Two of the students who were taking this section of General Chemistry II participated in interviews. Both students mentioned that they were unsure if their professor taught them about enzymes throughout the semester, and neither student was simultaneously taking General Biology I. One student said,

> "The last time I remember talking about enzymes was in high school anatomy."

This student also said that enzymes are used to break substances down, and that we have enzymes in our saliva and digestive system. The other student mentioned that enzymes act to speed up bodily processes and mentioned they would know more once they took a biology course. Through analysis of interviews, it was clear that these students did not have a good understanding of what an enzyme is, how it works, or how it interacts with substrates. When asked about their comfortability and experience in reading scientific literature, both students mentioned sometimes reading psychology journals. One of the 2 mentioned:

> "I'll just Google random stuff that I'm interested in and then I know to skim the abstract…I don't really go too much into the statistics because that stuff is over my head right now."

These students reinforced that, while they did not always understand every piece of a work of scientific literature, they could determine the important aspects when necessary. In a comparison of class content to knowledge, we determined that students in General Chemistry II did not obtain much of the information given to them regarding enzymes in that class alone. Students were taught about solid state materials, including proteins, and the properties of these materials. In addition to this, they were also given a laboratory exercise to navigate through the PDB website.

This exercise focused on viewing the main protease of the SARS-CoV2 virus. In this assignment, students were informed of the different levels of structure of a protein and the difference between superfamily, family, and species. These students were also asked questions such as "*Does this drug have a dipole moment? Hydrogen bonding?*" and "*What keeps these ligands associated with the protein?*". While this course focused on the structure of proteins and, in turn, enzymes, students generally did not seem to correlate one with the other when asked for all information on enzymes.

Twenty-five students in General Biology I participated in the pre-survey. Eighteen of these students mentioned that enzymes are catalysts for a reaction, and 17 students showed that enzymes are proteins or biological

molecules. Fourteen students mentioned that enzymes speed up the rate of a reaction, and 8 specified that enzymes are very specific in the ligands they will accept, noting the lock and key and induced fit models. One student said that enzymes can be affected by an influence in their environment, such as temperature and pH levels, and 1 other student mentioned the 4 levels of structure of proteins. Few students mentioned that enzymes are not used up in a reaction. One student, for example, wrote

> "An enzyme, usually proteins, are used to speed up a reaction that takes place in cells. They are a part of an enzyme-substrate complex that allows the reaction to catalyze, and enzymes can be used multiple times."

Five students participated in the post-survey, 2 of whom also completed the pre-survey. The 2 students that completed both, had a similar level of understanding of enzymes. One of these students specified that enzymes are useful "in processes such as the DNA-to-protein path and immunological defenses", showing that over the course of the semester, they learned more about functions of enzymes as they relate to health. Of the other 3 responses to the post-survey, 1 mentioned circumstances in which enzymes are necessary within the body, and all 5 students mentioned that enzymes catalyze reactions within the body.

Five students in General Biology I participated in an interview. These interviews allowed students to explain much more of their understanding of enzymes. Four of the 5 students mentioned that enzymes work by lowering the activation energy necessary for a reaction to occur. One student referred to enzymes as a "*Support system for reactions to take place.*" One of the students related enzymes to processes that happen within the body, such as the electron transport chain. Two students mentioned the way in which enzymes bond to ligands, and most of the 5 students mentioned the specificity of the binding of enzymes to ligands. One student even noted that there are specific receptors that the enzymes look for, and they must be in the proper orientation for binding of enzymes to ligands to occur. This student also mentioned that enzyme changes are dependent on their environment, including pH, temperature, and concentration levels.

Overall, all 5 students that participated in an interview showed that they understood the functions of enzymes quite well, but only 2 mentioned the specific interactions with ligands. These students, however, seemed to absorb and understand most information provided to them through lecture. When asked about their experience and comfortability in reading scientific literature, most students interviewed said they had a very base-line comprehension level, with 1 student mentioning:

> "It's written very dense, and it's a lot of material to work through. But as long as I set that time aside, you can certainly understand the purpose of the experiment."

Most of the students interviewed showed that they had little experience, but that they were capable of evaluating a paper to determine the main ideas. In General Biology I, students learn many specifics about enzyme interactions and functions. Throughout the first unit of General Biology I, students learn about cells and the molecules of life. One section of this unit is devoted to teaching students about enzymes. In this section, students learn how enzymes lower activation energy, how they bind to their substrates, which molecules can act as enzymes, and how pH and temperature affect enzyme-catalyzed reactions.

The 2nd unit of this class is entirely focused on enzymes, energy, and communication, and focuses on the specific functions of enzymes, including how enzymes are used in transport methods, glycolysis, photosynthesis, and metabolism. Comparing this information to the students' answers in the surveys and interviews indicated that students were much more aware of some of the basic concepts of enzymes than some of the more intricate details about enzymes. Overall, retention about enzymes seemed to be decent when concerned with basic enzyme function, few students retained more intricate enzyme binding details.

Summary of Results

Overall, General Biology I students had better understanding of enzymes and enzyme function. Most of these students were able to explain what enzymes are and what function they provide within the body. Several of these students were also able to elaborate on some key features, such as the structure of proteins (therefore enzymes), and a basic description of how enzymes bind to ligands. Most students enrolled in General Chemistry I could give no more information than that an enzyme can be a protein, and enzymes speed up chemical reactions. Students in General Chemistry II did not seem to have much more of an understanding of enzymes than those enrolled in General Chemistry I.

A majority of students who completed the pre and post surveys for General Chemistry II were not concurrently taking General Biology I, which likely accounts for a lack of increase in knowledge for the two classes, as General Chemistry II does not elaborate on enzyme specifics heavily. However, General Chemistry II does define and introduce them in the context of catalysis, transition states, and kinetics.

Discussion and Conclusion

Currently limited work has shown different methods for teaching students about enzymes, such as using the visual-spatial aspect of the Multiple Intelligence Theory by incorporating PowerPoints into lecture (Yalmanci and Gözüm, 2013). By providing students with the opportunity to not only visualize, but also manipulate, a 3-D enzyme-ligand complex within the RINRUS assignment, we expect students will retain more of the key concepts regarding enzyme-ligand binding and will have an experience that they will remember and take on to further classes.

In the 1st research question, we asked, "How do graduate chemistry students perceive the RINRUS assignment as it pertains to understanding enzymes?". Interviews with graduate students reaffirmed that the RINRUS assignment will be useful in teaching undergraduate students about enzymes to prepare them for courses in both the biology and chemistry majors. Importantly, this pilot and the interviews gave us critical feedback on the issues that undergraduate students might have. We have been able to substantially improve the assignment based on this feedback.

In the second research question, we asked, "What information about enzymes are beginner undergraduate biology and chemistry students obtaining and retaining from their courses?". We found that students in introductory courses at the University of Memphis are retain very little about enzymes. The primary piece of information they are obtain is about proteins. Although most enzymes are proteins, not all proteins are enzymes, and many students do not accurately relate the two concepts.

From student responses in interviews, it is clear that General Biology I students learn much about enzyme function, however, they frequently have trouble understanding enzyme structure and function in regard to enzyme-ligand binding. Many students in General Biology I have the potential to understand and excel when it comes to enzyme specifics; however, they need to be specifically taught these concepts. The RINRUS assignment can be useful in helping these students understand the enzyme specifics that they will need for more advanced courses in both biology and chemistry majors. The assignment is also a way to introduce students to reading scientific literature in their first few years of college to provide a basis for the increased reliance on primary literature in upper division courses. Students will revisit proteins again in Organic Chemistry and Bioorganic Chemistry (both required for biology and chemistry majors) and in the Biochemistry course.

Within this research study, few students completed interviews and surveys. This can, in part, be a result of the COVID-19 pandemic. However, a common theme found is that students in introductory undergraduate chemistry courses are retain very little about enzymes although they retain understanding of proteins more generally. While students are taught about proteins, they often have trouble relating to enzymes. While General Biology I students learn about enzyme function, they still do not retain knowledge about enzyme structure and function and how that relates to enzyme-ligand binding. The PowerPoint lectures we reviewed did not tend to teach students specific information about enzyme-ligand interactions. Including an intervention in this course could increase long-term enzyme understanding.

In this study, we have shown that the current methods for teaching undergraduate biology and chemistry students about enzymes can be improved to enhance student understanding and retention. We have shown that existing PowerPoint lectures do not adequately teach students specific information about enzyme-ligand interactions, and providing a hands-on, small group activity is more likely to help students better understand this information. For example, as Oludipe and Awokoy (2010) showed, having peers to deliberate with is very useful in not only relieving anxiety but also allows for the sharing of ideas and information that may be pertinent to the exercise. Separately, the characterization of what students currently retain from their courses may be useful to professors, as it could help professors understand what topics need to be prioritized when teaching students about enzymes.

Our future directions are to continue development of the RINRUS assignment and test it with General Biology I students to determine its effect on their understanding of enzyme structure and function.

References

Gabel, D. (1999). Improving teaching and learning through chemistry education research: A look to the future. Journal of Chemical Education, 76(4), 548-554.

Gardner, H. (2011). Frames of mind: The theory of multiple intelligences (3rd ed., pp.45-75). Basic Books.

Yalmanci, S.G., & Gözüm, A.İ.C. (2013). The effects of Multiple Intelligence Theory based teaching on students' achievement and retention of knowledge (example of the enzymes subject). International Journal on New Trends in Education and Their Implications, 4(3), 27-36.

Oludipe, D., & Awokoy, J. (2010). Effect of cooperative learning teaching strategy on the reduction of students' anxiety for learning chemistry. Journal of Turkish Science Education, 7(1), 30-36.

Rickey, D., & Stacy, A. (2000). The role of metacognition in learning chemistry. Journal of Chemical Education, 77(7), 915-920.

Sabel, J., Dauer, J., & Forbes, C. (2017). Introductory biology students' use of enhanced answer keys and reflection questions to engage in metacognition and enhance understanding. CBE—Life Sciences Education, 16(3), 1-12.

Schraw, G., Crippen, K. J., & Hartley, K. (2006). Promoting self-regulation in science education: Metacognition as part of a broader perspective on learning. Research in Science Education, 36, 111-139.

Stains, M., Harshman, J., Barker, M.K., Chasteen, S.V., Cole, R., DeChenne-Peters, E., Eagan Jr., M.K., Esson, J.M., Knight, J.K., Laski, F.A., Levis-Fitzgerald, M., Lee, C.J., Lo, S.M., McDonnell, L.M., McKay, T.A., Michelotti, N., Musgrove, A., Palmer, M.S., Plank, K.M., ... & Young, A.M. (2018). Anatomy of STEM teaching in North American universities. Science, 359(6383), 1468-1470.

Summers, T., Daniel, B., Cheng, Q., and DeYonker, N. (2019). Quantifying inter-residue contacts through interaction energies. Journal of Chemical Information and Modeling, 59(12), 5034-5044.

Sunal, D. W., Hodges, J., Sunal, C. S., Whitaker, K. W., Freeman, L. M., Edwards, L., Johnston, R. A., & Odell, M. (2001). Teaching science in higher education: Faculty professional development and barriers to

change. School Science and Mathematics, 101(5), 1-13.

Tien, L., Rickey, D., & Stacy, A. (1999). The MORE thinking frame: Guiding students' thinking in the laboratory. Journal of College Science Teaching, 28(5), 318-324.

Appendix A - Graduate Student Interview Questions

Biographical information – focus of study, career goals, background education.

Think aloud activity: students instructed to go through the assignment and talk through their process for completing the activity and answering the questions. Students asked to note specific areas they were confused or did not understand the assignment or what was expected of them.

1. What was your overall experience with this assignment?

2. Were there any parts you found difficult?

5. How did this assignment influence your thinking about enzyme modeling?

3. How did this assignment influence your thinking about biochemical research?

4. Did you have any issues with the Protein Data Base when transferring enzyme models into the software?

5. Do you have any feedback on how to make the Protein Data Base website easier to navigate?

6. Did you have any trouble downloading or using files from the Protein Data Base?

7. Did you have trouble with the instructions in the RINRUS software?

8. Did peer discussion threads on eCourseware/Desire2Learn enrich the exercise?

9. Do you think this task would be appropriate for beginning undergraduate students? Why or why not?

10. What revisions would you suggest to make this assignment more accessible in general?

11. What revisions would you suggest to make this assignment more accessible to beginning undergraduate students?

12. Did this assignment improve your understanding of enzymes and ligand-binding?

13. Do you have any additional comments or suggestions on how to improve this assignment?

Appendix B - CHEM 1110, CHEM 1120, and BIOL 1110 Survey Questions

1. What is your major?

2. What year are you in school?

3. How did you study for this class?

4. How would you determine if you understood a topic or if you needed to study it further?

5. (BIOL 1110 only) In what ways were the practice tests prior to exams helpful for you?

6. Explain what an enzyme is and how it works. Include any information you know about the structure of enzymes and their interactions with other molecules.

7. Are you planning on taking classes in the Biological Sciences department? If so, which do you plan to take?

8. (For BIOL 1110 and CHEM 1120, respectively) Are you currently enrolled in General Chemistry II/General Biology I?

Appendix C – Undergraduate CHEM 1110, CHEM 1120, and BIOL 1110 Interview Quesitions

Enzyme Questions

1. Throughout CHEM 1110/CHEM 1120/BIOL 1110, what did you learn about enzymes?

    a. Explain your current understanding of enzymes.

    b. From what you have learned so far about enzymes, are there any concepts you had a hard time understanding? If so, what are those concepts?

    c. What new information did you learn about enzymes in BIOL 1110 compared to CHEM 1110? (BIOL 1110 students only)

2. If any, what is your experience and comfortability with reading scientific papers thus far?

Serena (Jones) Addison grew up in Central Arkansas before moving to Memphis, Tennessee in 2018 in order to attend the University of Memphis. She graduated from the University of Memphis in 2020 with a Bachelors in Psychology/Behavioral Neuroscience, and while being a full time student she also worked full time in healthcare as a surgical technologist amid the start of the COVID19 pandemic and in the neuroscience research lab with Dr. Deranda Lester. Currently, she serves in the United States Army Reserves and is working towards gaining her Masters in Healthcare Administration before applying to medical school.

This paper received a QuaesitUM outstanding paper award.

Serena J. Addison, Sophia Lemus,
& Deranda B. Lester

Age-Dependent Effects of Social Isolation on Behaviors Related to Anxiety and Addiction in Mice

Faculty Sponsor

Dr. Deranda B. Lester

Abstract

Reduced social interaction is associated with an increased occurrence of anxiety and substance use disorder. Using open field testing in mice, this study addressed two questions: 1) Can the behavioral effects of adolescent isolation be reversed through social interaction in adulthood? 2) Does social isolation during adulthood have a similar detrimental effect as adolescent isolation? The study included 4 groups: mice that remained in enriched housing from adolescence to adulthood (environmental enrichment: EE), mice that were group housed during adolescence then isolated as adults (EE-ISO), mice that remained isolated from adolescence to adulthood (ISO), and mice that were isolated during adolescence then group housed as adults (ISO-EE). ISO-EE and EE-ISO mice responded more similarly to EE than ISO mice, indicating that the behavioral effects of adolescent isolation were reversed through social interaction in adulthood and that isolation during adulthood does not have the same impacts as adolescent isolation.

Introduction

Almost 1 in 5 adults in the United States live with a mental illness (Substance Abuse and Mental Health Services Administration Report, 2019). Of these mental illnesses, anxiety and substance use disorder are 2 of the most common. In the US, 18% of the adult population has reported annual anxiety symptoms, with 22% of those suffering from severe symptoms (Shirneshan et al., 2013). Anxiety is often defined as "a psychological, physiological, and behavioral state induced in animals and humans by a threat to well-being or survival, either actual or potential" (Steimer, 2011, p. 496). Anxiety is an excessive, medically unexplained, worry that occurs more days than not, over at least a period of 6 months and causes impairments in other aspects of functioning (American Psychiatric Association, 2017). Symptoms of anxiety can be nervousness, tenseness, restlessness, or having feelings of impending danger, panic, or doom. In more severe cases anxiety can lead to panic attacks, concentration issues, and even gastrointestinal problems. 7.2% of adults in the United States have been diagnosed with substance use disorder, and nearly 75% of those fell under alcohol use disorder. Substance abuse disorder is a pattern of maladaptive, repeated drug or alcohol use that often interferes with health, work, or social relationships with an inability to control their use of the drug (American Psychiatric Association, 2017). Research identifying risk factors associated with these disorders can be valuable for both prevention and treatment.

Animal studies are particularly useful for identifying risk factors given that researchers can control and manipulate sensitive variables (Stevens & Vaccarino, 2015). Animal studies allow us to understand neural substrates and disorders associated with adolescent experiences via the manipulation of many variables (Jaworska & MacQueen, 2015). Mice in particular are widely used in scientific research due to them being compact, cost-effective, easily available and conserve ~99% of human genes and physiologically resemble humans (Dutta & Sengupta, 2016). The lifespans of mice and humans differ significantly with mice average lifespan of 24 months while humans average 80 years (~24 months and ~80 years, respectively); however, similar molecular mechanisms of aging and patterns of disease pathogenesis are observed in mice and humans. Faster aging patterns in mice enables research on various life stages in a shorter time period. Mice are weaned at 3 weeks and reach the onset of puberty at 4 weeks and sexual maturity at 8-12 week (10 weeks average); therefore, adolescence in mice is often defined as the age of 3-10 weeks (Dutta & Sengupta, 2016). Adolescence in particular is an important developmental period for both physiological and neurobiological changes. In humans, stress during childhood and adolescence is 1 environmental factor

that has been associated with both anxiety and substance use disorder in adulthood (Watt et al., 2017). In rodents, social isolation during adolescence has been shown to increase release of the stress hormone corticosterone and induce behaviors related to anxiety (Lopez & Laber, 2015; Lukkes, et al., 2009) and increased drug-seeking (Alexander et al., 1978; Walker et al., 2019).

Open field testing is a common way of assessing behaviors associated with anxiety and substance use disorder. During open field chamber testing, time spent in the center of the chamber and exploratory behaviors are recorded. In mice, decreased time spent in the center is associated with increased levels of anxiety, as mice prefer to stick to the edges of the chambers (Sáenz, Villagra & Trías, 2006). Exploratory behavior is measured with locomotor activity (total distance traveled within the chamber) and rearing (number of times mice stand on their back legs). Increased exploratory behaviors has been correlated with an increased likelihood of drug self-administration, a well-established measure related to substance abuse disorders (Mitchell, Gao, Hallett, & Voon, 2016). Preliminary studies in our lab have shown that mice that have been isolated during adolescence, which ranges from 3 weeks old to 12 weeks old, spent less time in the center which is an indication of increased anxiety and displayed increased locomotor activity and rearing which both indicate an increased vulnerability to drug abuse. These findings are similar to results from other labs (Pietropaolo, Feldon & Yee 2008; Seibenhener & Wooten, 2015). This leads us to ask two questions related to impact of social isolation on these behaviors:

1) Can the behavioral effects of adolescent social isolation be reversed through social interaction in adulthood?

2) Does social isolation during adulthood have the same detrimental effect as social isolation during adolescence?

Both of these questions aim to understand the importance of developmental stage on the effects of an environmental stressor. Neural plasticity has been shown to be more dynamic during adolescence compared to adulthood (Watt et al., 2017). Therefore, regarding the first question, the neural changes induced by adolescent isolation may not be reversible with adulthood interventions. For example, Pietropaolo, Feldon & Yee (2008) found that social isolation during early post weaning phase (3-7 weeks) induces behavioral changes, such as startle reactivity, isolation-induced hyperactivity, and enhanced locomotor response that cannot be reversed via subsequent resocialization. Also, early environmental stress has been shown to cause a biological response of altering DNA methylation, which in turn affects transcriptional activity of DNA and can have long-term impacts (Walters & Kosten, 2019). However, Solinas et al. (2008) found that after 30

days of environmental enrichment behavioral sensitization preference for cocaine was eliminated in previously isolated mice, supporting the idea that environmental stimulation and social interaction can eliminate an already-formed drug propensity due to isolation.

The second research question addresses whether social isolation during adulthood has the same detrimental effect as isolation during adolescence. Adolescence is a key developmental window during which stressful experiences may result in long-term alterations of brain structure and functioning (Burke et al., 2017). However, moving mice from environmentally enriched to non-enriched conditions increased the rewarding effect of cocaine and increased neural functioning associated with anxiety and emotional distress (Nader et al., 2012). Smith et al. (2017) found that enrichment removal in rats, who during adolescence had an enriched environment, presented features of depression that otherwise are only rarely observed in animal models. This same study also found that these symptoms of stress, hyperphagia and weight gain, were unique to enrichment removal as the removal of other rewards did not produce the same symptoms (Smith et al., 2017). These findings indicate that positive life conditions during early life stages, if not maintained during adulthood, may have negative emotional consequences and associations with anxiety and substance use disorder (Nader et al., 2012).

The current study aims to expand on previous results and address the above-mentioned research questions. We hypothesized that the mice raised in isolation and transferred to an enriched environment would have reduced behavioral phenotypes related to anxiety and substance use disorder compared to mice raised in isolation. In other words, we expect that enrichment during adulthood could reverse the measured behavioral effects of adolescent isolation. We also hypothesize that the mice raised in an enriched environment and transferred to isolation would have increased behavioral phenotypes related to anxiety and substance use disorder compared to mice left in enrichment. Thus, we expect that adult isolation will induce similar behavioral changes as seen with adolescent isolation. Currently, gaps exist between our understanding of adolescent brain development and the clinical research involving adolescents with emerging, or later established, psychiatric disorders (Jaworska & MacQueen, 2015). The findings from this study will elucidate the importance of developmental stage in mediating anxiety, and addiction related behavioral effects of social isolation. This information can be beneficial to programs aiming to prevent or treat anxiety and/or substance use disorder.

Methods

This experiment was approved by the University of Memphis Institutional Animal Care and Use Committee (IACUC) and was conducted in accordance with the guidelines set by the Public Health Service (PHS).

Subjects and Housing Conditions

Sixty-four female C57 mice were obtained from Jackson Laboratory (Bar Harbor, ME) at 3 weeks old and were randomly divided into 4 housing condition groups. Female mice were exclusively used in the present study due to male mice co-habitation following isolation often resulting in fighting, injury, and/or death of the subjects (Kappel, Hawkins & Mendl 2017). Given that adolescence in mice is defined as between the ages of 3-10 weeks (Dutta & Sengupta, 2016), the housing conditions were designed to persist from the beginning of adolescence to adulthood. Socially enriched environments (EE) included 4-5 mice per cage. Twenty-five mice remained in EE, from 3 to 15 weeks old, throughout the study. Isolated environments (ISO) consisted of 1 mouse per cage. Twenty-one mice remained in ISO throughout the study, again from 3 to 15 weeks old. Nine mice were isolated during adolescence, 3 to 12 weeks, then moved to EE for 6 weeks. The mice in this group will be referred to as ISO-EE (isolated to enriched housing). Nine mice were housed in EE during adolescence, 3 to 12 weeks, then moved to ISO for 6 weeks. The mice in this group will be referred to as EE-ISO (enriched to isolated housing). See Table 1 for a breakdown of the experimental groups. All housing conditions were in a temperature-controlled room (21±1° C) with food and water available ad libitum, on a 12 hr light/dark cycle (lights on at 0600). Cages were cleaned and bedding refreshed consistently twice per week.

Experimental Groups

Adolescent Housing Condition	Adult Housing Condition	N
EE	EE	25
EE	ISO	9
ISO	ISO	21
ISO	EE	9
	Total	**64**

Table 1. Housing conditions. EE: environmentally enriched; ISO: isolated.

Procedure

On the day following the end of the allotted housing condition period, open field testing was conducted once on each mouse. On the day of testing, mice were individually caged in the testing room in a dark, soundproof cabinet

45 minutes before being placed in the open field chamber. This habituation period was to prevent exposure to aversive stimuli and to get the mice used to the testing environment. Open field testing occurred consistently in the morning, between the hours of 0800 and 1100. Four open field chambers were available for simultaneous testing of individual mice. The mice were placed in the front center of the open field, and the infrared recording button started at the same moment of placement. The mice were allowed to freely roam in the chamber for 20 minutes while locomotor behavior was quantified by infrared beam breaks and distance traveled within the chamber. HamiltonKinder SmartFrame™ (Hamilton Kinder, Poway, CA), with a 4 x 8 photo beam strip and a 4 x 8 photo beam rearing attachment, was used for open field testing in junction with MotorMonitor version 4.14 (HamiltonKinder, Poway, CA) recording the locomotor behavior. The walls of the open field chamber were clear Plexiglass, and lighting included a 15-W bulb. The center area of the open field chamber was set in the software to measure 12.05 cm x 22.86 cm. This central area was located 6.03 cm from the left and right walls and 11.43 cm from the front and back walls. After each 20 min. recording session, the mice were returned to their home cages. The open field chambers were cleaned with 10% isopropyl alcohol and allowed to dry before a new mouse as introduced to the chamber.

Data analysis

Three dependent variables were measured using open field testing: time in center of chamber, overall locomotor activity, and number of rears. For each dependent variable, a one-way between-subjects ANOVA with Tukey HSD post hoc test was used to determine differences between the 4 housing conditions (EE, EE-ISO, ISO, and ISO-EE).

Results

Time in Center

A one-way between-subjects ANOVA was conducted to compare the total time (in sec) spent in the center of the chamber between housing condition groups. Housing conditions significantly affected the time spent in the center [$F(3,60) = 7.850$, $p < .001$] (Figure 1). A post-hoc Tukey HSD test indicated a near significant difference between ISO and EE mice ($p = .069$), with ISO mice spending less time in the center compared to EE mice, indicating increased anxiety in ISO mice, as expected. No statistical difference was observed between EE and EE-ISO mice ($p = .803$), indicating that moving mice to isolation during adulthood did not alter anxiety-related behavior. Interestingly, the ISO-EE mice spent a significantly increased amount of

time in the center compared to both the EE mice (p = .031) and ISO mice (p = .000), indicating decreased occurrence of anxiety-related behavior in the ISO-EE mice.

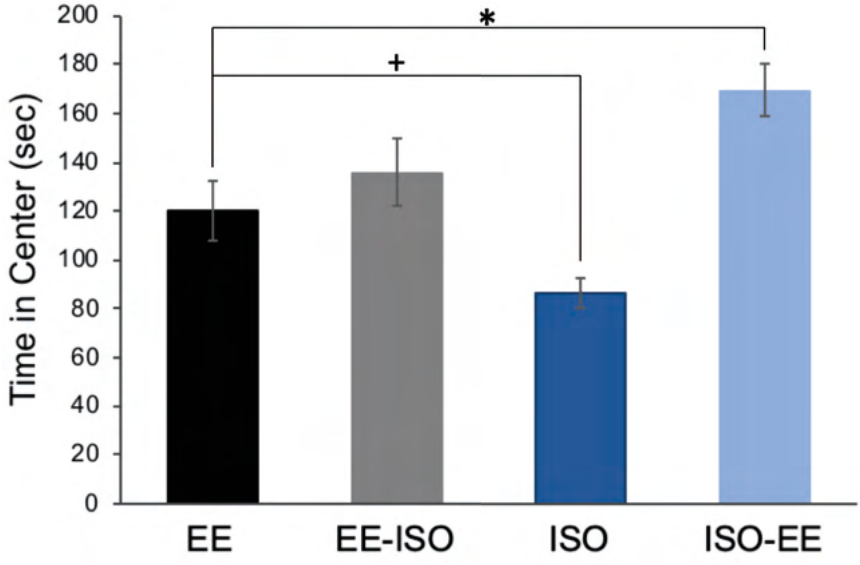

Figure 1. Time in Center

Increased time in the center is an indication of reduced anxiety. No differences were observed between EE and EE-ISO mice. A trend in the data suggested that ISO mice were more anxious than EE mice (+ p = .069 compared to EE). ISO-SH mice were less anxious than EE mice (* p < .05 compared to EE). EE: environmentally enriched housing during both adolescence and adulthood; EE-ISO: environmentally enriched housing during adolescence and isolation in adulthood; ISO: isolation during both adolescence and adulthood; ISO-EE: isolation during adolescence and environmentally enriched in adulthood.

Locomotor Activity

A one-way between-subjects ANOVA was conducted to compare the effect of housing conditions on the locomotor activity (distance travelled in cm). Housing conditions significantly affected locomotor activity [F (3,60) = 5.898, p = .001] (Figure 2). Specifically, ISO mice displayed significantly increased locomotor activity relative to EE mice (p = .001), as expected. However, neither EE-ISO nor ISO-EE significantly differed from EE mice in regards to locomotor activity (p = .692 and .622, respectively).

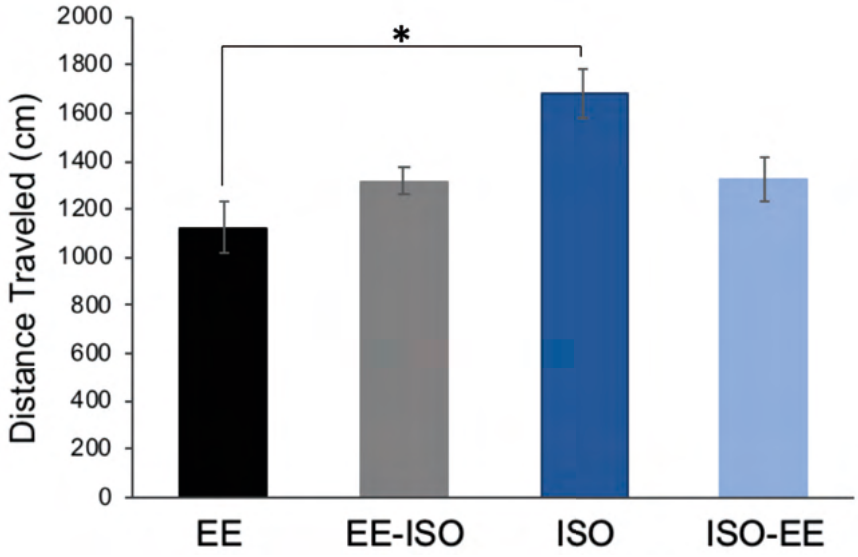

Figure 2. Locomotor Activity

Increased locomotor activity indicates increased exploratory behavior. No differences were observed between EE, EE-ISO, and ISO-EE mice. ISO mice exhibited increased locomotor activity compared to EE mice (* $p < .05$ compared to EE). EE: environmentally enriched housing during both adolescence and adulthood; EE-ISO: environmentally enriched housing during adolescence and isolation in adulthood; ISO: isolation during both adolescence and adulthood; ISO-EE: isolation during adolescence and environmentally enriched in adulthood.

Number of Rears

A one-way between-subjects ANOVA was conducted to compare the effect of housing conditions on the number of rears. Housing conditions significantly affected the number of rears [$F(3,60) = 8.951$, $p < .001$] (Figure 3). As expected, ISO mice had a significantly increased number of rears compared to EE mice ($p = .003$). EE-ISO also showed an increase in their number of rears relative to EE mice ($p < .001$). However, no rearing differences were observed between ISO-EE and EE mice ($p = .693$).

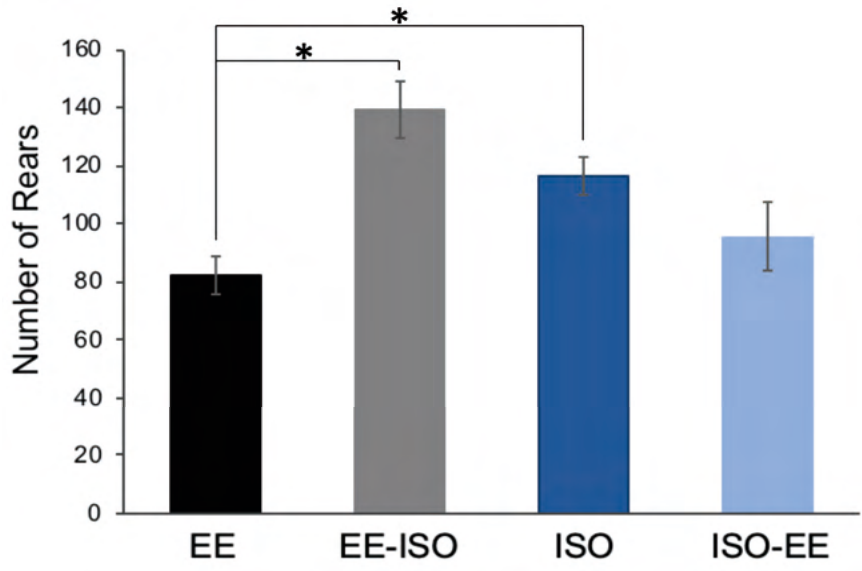

Figure 3. Number of Rears

Increased rearing indicates increased exploratory behavior. No differences were observed between EE and ISO-EE mice. EE-ISO and ISO mice exhibited increased rearing activity compared to EE mice (* $p < .05$). EE: environmentally enriched housing during both adolescence and adulthood; EE-ISO: environmentally enriched housing during adolescence and isolation in adulthood; ISO: isolation during both adolescence and adulthood; ISO-EE: isolation during adolescence and environmentally enriched in adulthood.t

Discussion

For mice, isolation during adolescence is known to induce behaviors associated with anxiety and substance use disorder. The purpose of this project was to determine if the behavioral effects of adolescent social isolation can be reversed through social interaction in adulthood; and if social isolation during adulthood has the same detrimental effect as social isolation during adolescence. It was hypothesized the mice raised in isolation and transferred to an enriched environment (ISO-EE) would have reduced behavioral phenotypes related to anxiety and substance use disorder compared to mice that remain in isolation (ISO). In regards to the second question, we expected that the mice raised in an enriched environment and transferred to isolation (EE-ISO) would have increased behavioral phenotypes related to anxiety and substance use disorder compared to mice left in enrichment (EE). Regarding behavioral phenotypes, the anxiety-related behavior measured

in the current study was time spent in the center of the open field chamber. Decreased time spent in the center is associated with increased occurrence of anxiety-related behavior (Sáenz, Villagra, & Trías, 2006). Exploratory behavior (as measured with locomotor activity and rearing in the open field chamber) was used as an indication of propensity for drug abuse. Increased exploratory behaviors correlates with hyperdopamineric functioning and increased drug-seeking behaviors (Beninger, 1983).

As expected, ISO mice spent less time in the center and displayed increased exploratory behaviors compared to EE mice. These findings support many previous studies in which adolescent isolation in rodents induced increased occurrence of behaviors related to anxiety and increased drug-seeking and drug responses (Pietropaolo, Feldon & Yee, 2008; Rodríguez-Ortega, & Cubero, 2018; Seibenhener & Wooten, 2015). Regarding the first research question of whether EE during adulthood can reverse the behavioral effects of adolescent isolation, we found that ISO-EE mice behaved more similarly to the EE mice than the ISO mice. ISO-EE mice actually spent more time in the center compared EE mice (indicating reduced anxiety), and ISO-EE mice displayed similar exploratory behaviors as EE mice. These findings indicate that moving isolated mice to EE housing did reverse the observed isolation-induced behavioral deficits; and support the findings of Rodríguez-Ortega and Cubero (2018) in which adulthood access to EE blunted isolation-induced operant responses in the cue-related reinstatement of heroin seeking in rats. Studies such as these are important for clinicians treating disorders centering around stressful events and/or negative social interactions during adolescence.

Regarding the second research question of whether social isolation during adulthood has the same detrimental effect as social isolation during adolescence, our results showed that EE-ISO mice did not significantly differ in their time spent in the center of the chamber nor in their locomotor activity compared to EE mice. As mentioned previously, locomotor activity in the novel open field often signals mesolimbic dopamine functioning, similar to that of drugs of abuse, and can be used as a correlation link between addiction related behaviors in mice (Beninger, 1983).

Thus, our findings indicate that adulthood isolation does not have the same effect as adolescent isolation, given that the time in center and locomotor activity of the EE-ISO group more closely resembled that of the EE mice rather than the ISO mice. Reduced neural plasticity in adulthood may prevent environmental stressors from impacting behavior to the same extent as is possible during adolescence, a time in which neural changes are more rampant (Watt et al., 2017). However, we did find that the EE-ISO mice exhibited an increased number of rears compared to EE mice. Previous

studies have shown that moving mice from EE to non-enriched conditions increased the rewarding effects of cocaine, increased neural functioning associated with emotional distress, and increased occurrence of behaviors associated with depression (Nader et al., 2012; Smith et al., 2017). It is possible that the isolation paradigm of the current study was not stress-inducing enough to alter the behaviors of the adult mice. The mice were isolated, in a cage by themselves, but still able to see, hear, and smell mice from other cages. Future studies could use total isolation and/or measure corticosterone levels to determine whether the isolation induced a stress response.

Conclusion

In conclusion, the findings of the current study indicate that adolescent isolation was associated with increased behavioral phenotypes of anxiety and substance use disorder in female mice, but these behavioral changes seem to be reversible and age dependent.

The data supported the hypothesis that the mice raised in isolation and transferred to an enriched environment (ISO-EE) would have reduced behavioral phenotypes related to anxiety and substance use disorder compared to mice that remained in isolation, but the data did not support the hypothesis that the mice raised in an enriched environment and transferred to isolation (EE-ISO) would have increased behavioral phenotypes related to anxiety and substance use disorder compared to mice left in enrichment. Instead, adult isolation did not seem to have a major impact on the measured behaviors.

It should be noted again that the current study was only conducted in females. Male and female mice have been shown to react differently to altered social interactions during both adolescence and adulthood (see Walker et al., 2019), but repeating these experiments with a focus on the physical stimuli rather than the social stimuli may be useful in males. Nonetheless, the present findings highlight the importance of EE during adolescence and the potential use of EE in adulthood to rescue isolation-induced behavioral phenotypes. The present findings also support the use of social and environmental stimuli in therapeutic programs for disorders related to anxiety and substance abuse.

References

Alexander, B. K., Coambs, R. B., & Hadaway, P. F. (1978). The effect of housing and gender on morphine self-administration in rats. Psychopharmacology, 58(2), 175–179. https://doi.org/10.1007/bf00426903

American Psychiatric Association. (2017). Diagnostic and statistical manual of mental disorders: Dsm-5. Arlington, VA.

Burke, A. R., Mccormick, C. M., Pellis, S. M., & Lukkes, J. L. (2017). Impact of adolescent social experiences on behavior and neural circuits implicated in mental illnesses. Neuroscience & Biobehavioral Reviews, 76, 280–300. https://doi.org/10.1016/j.neubiorev.2017.01.018

Beninger, R.J. (1983). The role of dopamine in locomotor acivity and learning. Brain Research Reviews, 287, 173-196.

Dutta, S., & Sengupta, P. (2016). Men and mice: Relating their ages. Life Sciences, 152, 244-248. doi:10.1016/j.lfs.2015.10.025

Jaworska, N., & MacQueen, G. (2015). Adolescence as a unique developmental period. Journal of Psychiatry & Neuroscience, 40(6), 291-293. https://doi.org/10.1503/jpn.150268

Kappel, S., Hawkins, P., & Mendl, M. T. (2017). To group or not to group? Good practice for housing male laboratory mice. Animals: An Open Access Journal from MDPI, 7(12), 88. Lopez, M. F., & Laber, K. (2015). Impact of social isolation and enriched environment during adolescence on voluntary ethanol intake and anxiety in C57BL/6J mice. Physiology & Behavior, 148, 151–156. https://doi.org/10.1016/j.physbeh.2014.11.012

Lukkes, J. L., Mokin, M. V., Scholl, J. L., & Forster, G. L. (2009). Adult rats exposed to early-life social isolation exhibit increased anxiety and conditioned fear behavior, and altered hormonal stress responses. Hormones and Behavior, 55(1), 248–256. https://doi.org/10.1016/j.yhbeh.2008.10.014

Mitchell, S., Gao, J. & Hallett, M. & Voon, V. (2016). The role of social novelty in risk seeking and exploratory behavior: Implications for addictions. PLOS ONE. 11. e0158947. 10.1371/journal.pone.0158947.

Nader, J., Claudia, C., Rawas, R. E., Favot, L., Jaber, M., Thiriet, N., & Solinas, M. (2012). Loss of Environmental Enrichment Increases Vulnerability to Cocaine Addiction. Neuropsychopharmacology, 37(7), 1579–1587. https://doi.org/10.1038/npp.2012.2

Pietropaolo, S., Feldon, J., & Yee, B. K. (2008). Nonphysical contact between cagemates alleviates the social isolation syndrome in C57BL/6 male mice. Behavioral Neuroscience, 122(3), 505–515. https://doi.org/10.1037/0735-7044.122.3.505

Rodríguez-Ortega, E., & Cubero, I. (2018). Environmental enrichment modulates drug addiction and binge-like consumption of highly rewarding substances: A role for anxiety and compulsivity brain systems? Frontiers in behavioral neuroscience, 12, 295. https://doi.org/10.3389/fnbeh.2018.00295

Sáenz, J. C. B., Villagra, O. R., & Trías, J. F. (2006). Factor analysis of forced swimming test, sucrose preference test and open field test on enriched, social and isolated reared rats. Behavioural brain research, 169(1), 57-65.

Seibenhener, M. L., & Wooten, M. C. (2015). Use of the open field maze to measure locomotor and anxiety-like behavior in mice. Journal of Visualized Experiments, 96, 524-534 https://doi.org/10.3791/52434

Shirneshan, E., Bailey, J., Relyea, G., Franklin, B. E., Solomon, D. K., & Brown, L. M. (2013). Incremental direct medical expenditures associated with anxiety disorders for the U.S. adult population: Evidence from the medical expenditure panel survey. Journal of Anxiety Disorders, 27(7), 720–727. https://doi.org/10.1016/j.janxdis.2013.09.009

Smith, B. L., Lyons, C. E., Correa, F. G., Benoit, S. C., Myers, B., Solomon, M. B., & Herman, J. P. (2017). Behavioral and physiological consequences of enrichment loss in rats. Psychoneuroendocrinology, 77, 37–46. https://doi.org/10.1016/j.psyneuen.2016.11.040

Solinas, M., Chauvet, C., Thiriet, N., Rawas, R. E., & Jaber, M. (2008). Reversal of cocaine addiction by environmental enrichment. Proceedings of the National Academy of Sciences, 105(44), 17145–17150. https://doi.org/10.1073/pnas.0806889105

Steimer T. (2011). Animal models of anxiety disorders in rats and mice: some conceptual issues. Dialogues in clinical neuroscience, 13(4), 495–506.

Stevens, H. E., & Vaccarino, F. M. (2015). How animal models inform child and adolescent psychiatry. Journal of the American Academy of Child & Adolescent Psychiatry, 54(5), 352–359. https://doi.org/10.1016/j.jaac.2015.01.019

Substance Abuse and Mental Health Services Administration. (2019). Key substance use and mental healthindicators in the United States: Results from the 2018 National Survey on Drug Use and Health (HHS PublicationNo. PEP19-5068, NSDUH Series H-54). Rockville, MD: Center for Behavioral Health Statistics and Quality,

Substance Abuse and Mental Health Services Administration. Retrieved from https://www.samhsa.gov/data/

U.S. Department of Health and Human Services, Substance Abuse and Mental Health Services Administration, Center for Behavioral Health Statistics and Quality. (2018). National Survey on Drug Use and Health 2016 (NSDUH-2016-DS0001). Retrieved from https://datafiles.samhsa.gov/

Walker, D. M., Cunningham, A. M., Gregory, J. K., & Nestler, E. J. (2019). Long-Term Behavioral Effects of Post-weaning Social Isolation in Males and Females. Frontiers in Behavioral Neuroscience, 13. doi: 10.3389/fnbeh.2019.00066

Walters, H., & Kosten, T. A. (2019). Early life stress and the propensity to develop addictive behaviors. International Journal of Developmental Neuroscience, 78, 156–169. https://doi.org/10.1016/j.ijdevneu.2019.06.004

Watt, M. J., Weber, M. A., Davies, S. R., & Forster, G. L. (2017). Impact of juvenile chronic stress on adult cortico-accumbal function: Implications for cognition and addiction. Progress in Neuro-Psychopharmacology and Biological Psychiatry, 79, 136–154. https://doi.org/10.1016/j.pnpbp.2017.06.015

Sophia Rouse earned a Bachelor of Arts in History and German in May 2022. Her immediate plans post-graduation are to attend Texas A&M University in the fall to work towards her graduate degree in history. She wants to continue studying German American immigration history in the southeastern United States and hopes to be able to understand how the formation of Germany and the Reconstruction era in the United States, both in the late-nineteenth-century, influenced German political involvement. While at Memphis, Sophia has been active on campus as a member of Alpha Delta Pi, Helen Hardin Honors College, and the Student History Society.

Sophia Rouse

Germanic Emigrants of Memphis, 1865 - 1880

Faculty Sponsor

Dr. Susan E. O'Donovan

Abstract

During the nineteenth century, Germanic people from modern-day Germany and surrounding countries including Austria, Belgium, the Netherlands, Poland, Sweden, and Switzerland integrated into Memphis. By 1865, Germanic emigrants had begun to transform Memphis as their new home. Despite being outnumbered by Irish emigrants, between 1865-1880 through educational involvement, Germanic emigrants enriched Memphis to further establish the city. After the Civil War, Memphis transformed their public school system as education-related legislation developed across Tennessee. Germanic Memphians aided in the establishment of public schools and public education in Memphis during the formational years of the Shelby County Board of Education. Moreover, the expansion of public schools included the creation of black schools and developing segregation in the south. Understanding what role Germanic emigrants had in this development as Germanic teachers taught at both black and white schools, provides more understanding into the creation of this system. While integrating into the City of Memphis, Germanic Memphians founded churches that created communities within the larger city. Although some German churches had parochial schools, Germanic Memphians still served on the Board of Education and as teachers to help advance the school system in their new home. Germanic influence helped to establish Memphis during the late 19th century and expand the city after the Civil War. By studying Germanic emigration in a city where Irish emigration is the main focus, more insight to Memphis' educational and political histories is offered.

Introduction

Between 1865-1880, almost 2,000 Germanic emigrants resided in Memphis. Much of the historical scholarship on nineteenth-century Memphis describes a city dominated by black and white Southerners. While that is true, it was also a multi-national, multi-ethnic place that included a sizeable population of European immigrants, including around 1,946 of Germanic origin.[i] Germanic emigrants embedded themselves in the Bluff City, especially through their growing involvement in politics and public education. Political engagement, in their new home and their former home, was common among Germanic emigrants. In post-Civil War Memphis, Germanic immigrants participated freely in the city's politics, unlike the formerly enslaved African Americans. Through their involvement in the city government—the Board of Aldermen, the Board of Education, and the Common Council—Germanic Memphians enriched their city and became active in the proceedings of their new home.

As the City of Memphis grew in the early 19th century, the growth aligned with the prioritization of public education by the state. In Memphis, the lack of a well-funded school drew distinct attention from the state legislature. According to the Tennessee state government in Memphis and in Tennessee, while private and religious schools existed, there was still the need for well-funded public schools. Although the Irish founded some of the first public schools in Memphis in 1848, Germanic emigrants helped expand the Memphis public school system directly through teaching and serving on the Board of Education during the school system's formational years after the emigration waves of the mid-nineteenth century. [ii]

Methodology

Most historians of Memphis history and historians of German Americans in the Reconstruction era have focused primarily on the shifting relationships between black and white southerners. Beverly Bond and Janann Sherman's *Memphis in Black and White* (2003) examines the changing social and economic relationships between black and white Memphians during the late nineteenth century. Beverly Bond and Susan O'Donovan's *Remembering the Memphis Massacre* (2020) and Beverly Bond's chapter, "Educating the Common Man," in John M. Amis and Paul M. Wright's *Race, Economics, and the Politics of Educational Change: The Dynamics of School District Consolidation in Shelby County, Tennessee* (2018) concentrate on specific events and legislation that highlight the changing relationships between black and white Memphians in their narratives.[iii]

The abundant scholarship on Germanic immigration to the United States has focused primarily on Germanic immigration to the northern United States and the Midwest due to their larger communities. Walter Kamphoefner's *Germans in America, A Concise History* (2021), focuses on Germanic immigrants in the Midwest. Although Kamphoefner touches on some southern states, he limits his attention to Texas. David Blackbourn's *The Long Nineteenth Century, A History of Germany, 1780-1918 and Matin Kitchen's A History of Modern Germany*, 1800 to Present discuss Germanic immigration to the United States during the mid-nineteenth century, but both books specify northern or midwestern cities as destinations. In more recent years, scholarship has begun to investigate Germanic immigration to the southern United States. Kathleen Condray's *Das Arkansas Echo* (2020) and Ellen C. Merrill's *Germans of Louisiana* (2005) focus on southern states.[iv] Yet few historians have investigated the almost 2,000 Germanic emigrants who settled in Memphis during the mid-nineteenth century as Memphis' second largest immigrant group.[v]

Understanding the Origins of Germanic Memphians

Understanding the Germany that Germanic Memphians emigrated from provides insight about their involvement in the Shelby County Board of Education. The 1840s saw a change among the German states as the identities and priorities of residents changed. The revolutions brought by the differing ideas of a German Confederation forced some Germanic emigrants to leave Germany for religious reasons, but most left in the wake of failed political revolutions. Germanic emigrants who grew up during the formation of the German Confederation experienced the differences between the Germanic states rather than a unified Germany. After the Congress of Vienna, there was a call for reform among the Germanic states and regions. The idea of what reform would look like varied among the different states. However, the French Revolution and the Napoleonic regime helped to create a temporary sense of German nationalism among the states. Prussia and southern Germanic states had disparities with their different constitutions, governments, and economies.[vi]

In 1848, the Frankfurt Parliament attempted to piece together and form a singular "Germany." However, cultural, linguistic, geographical, and historical aspects limited the expansion and concise formation of the German Confederation. The variations among the states and populations created a mosaic region and further complicated the "German" identity. Moreover, the Frankfurt Parliament attempted to piece together a Germany that excluded states within the modern borders of Germany, such as Holstein

and Schleswig. The individual wars with these states in order to incorporate them into the German Confederation further individualized the Germanic identity. Moreover, the Frankfurt Parliament pushed to expand the German Confederation to also include Bohemia and Poland. By the latter part of the 1840s, widespread poverty and a lack of political representation among multiple economic classes began to spark revolutions in the Germanic regions. Violence began occurring throughout the Germanic states and regions. While Prussia and Austria experienced the most violence, areas like Frankfurt, Munich, and Baden also faced upheavals. [vii]

Germanic emigrants came from these individual provinces rather than a distinct unified country. Although the modern borders of Germany include the states of Baden, Baden-Württemberg, Bavaria, Hessen, and Saxony, Germanic emigrants came from these individual provinces rather than from a distinct unified country. The surrounding countries of Austria, Belgium, Denmark, the Netherlands, Poland, and Prussia also contained "Germans." 86,000 Germanic inhabitants lived in the neighboring countries of Belgium and the Netherlands; both were considered "Little" Germany. The thirty-eight states that formed the German Confederation in the mid-nineteenth century each had their own government. Most were monarchies, though they also participated in the Bundestag. Each state responded to the 1848 revolutions differently, thus furthering their individuality. [viii]

The 1860 federal manuscript census illuminates the complexity of "German" identity prior to the formation of Germany (see Figures 1 and Table 1).[ix] According to the census taker, while 895 Germanic Memphians identified "Germany" as their home, nearly as many (638) associated "home" with specific areas such as Baden, Prussia, Sachsen, Saxony, and Württemberg. Germanic emigrants were one of the only groups, aside from two distinct families from the United Kingdom, to list specific cities such as Bremen, Hannover, and Heidelberg, thus implying a different connection to their homeland's identity and potential reasons for leaving.[x]

Homeland	People from Each Region *N*
"Germany"	805
Prussia	151
Switzerland	101
Baden	102
Bavaria	56
Northern Germany (Hannover, Bremen, Hamburg)	53
Württemberg	42
Hessen	39
Sachsen	31
Denmark	18
Holland	13
Austria	10
Miscellaneous Cities	8
Poland	8
The Netherlands	2
Total	**1439**

Table 1. Germanic Memphians Places of Birth, 1860 - by Number

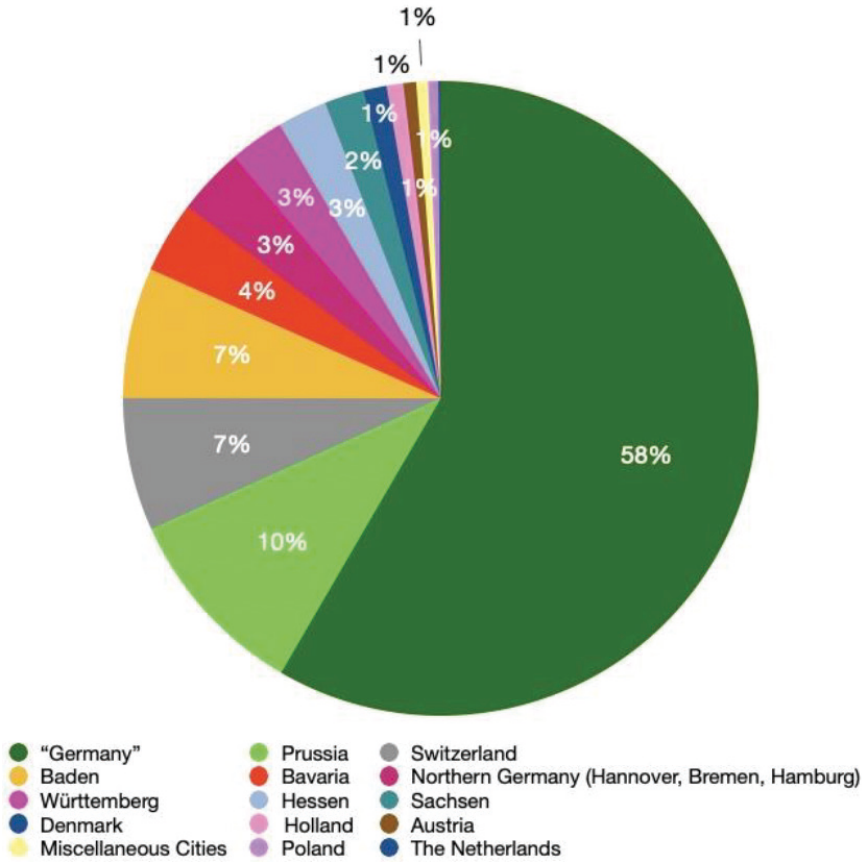

Figure 1. Germanic Memphians' Place of Birth, 1860 - in percentages

These ties to specific homelands did not erode very quickly. Indeed, according to the data collected for the 1870 federal census, the connection to the German identity as Germanic emigration to Memphis increased.[xi] The 1870 census shows a more diverse group of Germanic Memphians. The Germanic population expanded from 1,533 to 1,856 during the second major wave of Germanic emigration (see Figure 2. and Table 2.).[xii]

Homeland	People from Each Region *N*
"Germany"	580
Prussia	532
Bavaria	217
Switzerland	135
Baden	110
Northern Germany (Hannover, Bremen, Hamburg)	57
Württemberg	50
Poland	38
Hessen	35
Sachsen	35
Holland	24
Miscellaneous Cities	20
Austria	12
Denmark	7
The Netherlands	2
Westphalia	2
Total	**1856**

Table 2. Germanic Memphians Places of Birth, 1870 - by number

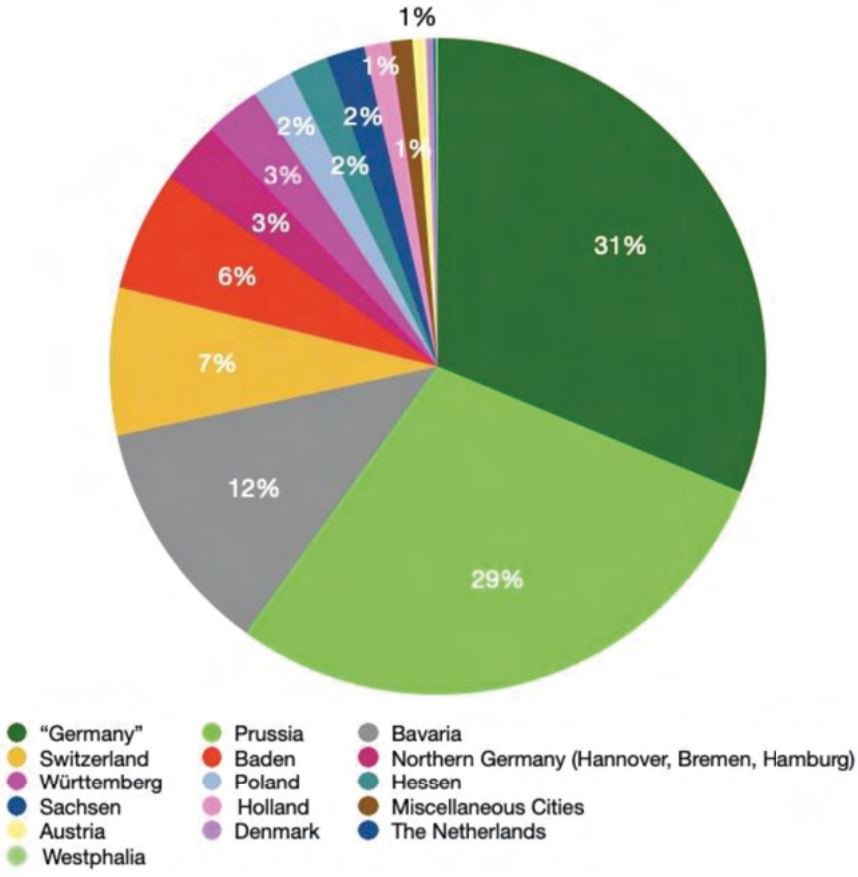

Figure 2. Germanic Memphians Place of Birth, 1870 - by percentage

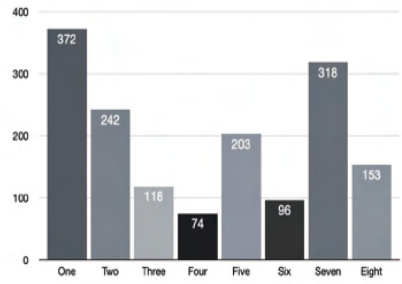

Number of Germanic Emigrants per Ward 1860

Wards	Germanic Emigrants
One	372
Two	242
Three	118
Four	74
Five	203
Six	96
Seven	318
Eight	153

Figure 3. Germanic Distribution in Memphis 1860

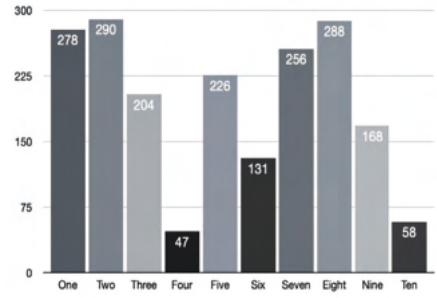

Number of Germanic Emigrants per Ward 1870

Wards	Germanic Emigrants
One	278
Two	290
Three	204
Four	47
Five	226
Six	131
Seven	256
Eight	288
Nine	168
Ten	58

Figure 4. Germanic Distribution in Memphis 1870

The census was voluntary, so it can be assumed that some "Germans" were not included. The number of Memphians who identified "Germany" as their place of birth decreased to 580, with Prussia now at 532.[xiii]The Germanic emigrants in Memphis coincided with patterns of emigration from the German confederation in the mid-nineteenth century. Prussia's Rhine Valley and northern areas like Saxony, Mecklenburg, Württemberg, and eastern Prussia experienced heavy waves of emigration to the United States.[xiv] While "Germany" remained the primary place of birth for most emigrants, Prussian-born emigrants consistently represented a quarter of the Germanic emigrants in each ward in 1870. Moreover, the Germanic varied as only 31% claimed "Germany" as their place of birth in 1870, whereas the rest of Germanic emigrants claimed specific provinces and cities.[xv] Germanic emigrants lived throughout the city and concentrated within different wards (see Figure 3). A majority of the shops were located near the Germanic churches and Germanic culture clubs in the first through fifth wards (see Figure 4)[xvi]. These businesses kept Germanic Memphians in Memphis and aided in their desire to participate in politics.[xvii] Moreover, the grouped-together locations of these businesses and German-language institutions furthered the Germanic identity in Memphis.

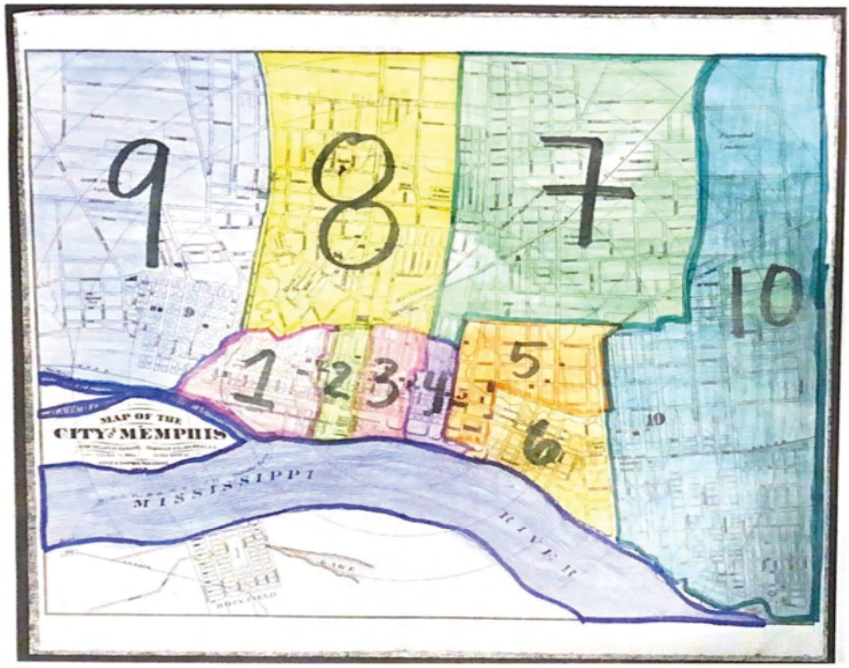

Figure 5. Map of Memphis Wards, 1872

Figure 6. Map of Germanic Memphis.

Germanic emigrants were in but not necessarily of their new home. Although embedded into the city's social and economic structures, they nonetheless retained connections to their European roots. The census records reveal clear distinctions among the different identities of Germanic emigrants. While they unified to form German-language organizations and religious institutions, the newcomers also maintained ties to their specific homelands, creating something of a mosaic pattern that kept Germans visible even as they contributed to the city's well-being more generally through education.

Germanic Involvement in Memphis Board of Education

Many German-language immigrants voted and were active in school board politics. [xviii] In the 1860s, as the number of Germanic immigrants increased, Germanic leaders supported the addition of German language instruction in public schools throughout the United States. [xix] Their interests in the Board of Education shows their integration into Memphis. In 1865, after the Civil War, German-language emigrants not only ran for positions on the Board of Education, but also actively voted and supported it.

The government of the City of Memphis changed after the Civil War, mainly due to education and an increase in population. Germanic immigrants were involved in each aspect. Until 1868-1869, the Board of Aldermen included an education standing committee. In 1869, the state of Tennessee officially founded the Board of Education for the City of Memphis. Prior to this, the board of school visitors had allowed for one elected citizen from each ward to be involved in the discussions about public education, while the Board of Aldermen still had the primary jurisdiction about public education. But after 1869, the Board of Education became a separate, distinct entity of the City of Memphis that included two elected members from each ward.[xx] Aldermen functioned as members of the education subcommittee until the establishment of the Board of Education. [xxi] The late 1860s saw the prioritization of education in Memphis. There was a desire, among many but not all, to create schools for African Americans and to get more children to attend school in Memphis. [xxii] Germanic immigrants participated in politics as teachers, voters, and members of the Board of Education.

The most significant contribution of Germanic emigrants was the expansion of the Board of Education. According to Dr. Walter Kamphoefner, Germanic immigrants valued education. The focus on education was a common trend among Germanic immigrants throughout the United States as Germany also concentrated on the accessibility of education. Religion and politics influenced the Germanic involvement in education. Freethinkers

and German-speaking Jews supported public education, whereas Germanic Catholics and Lutherans supported private education. However, all preferred schools included the German language. [xxiii] In Memphis, Trinity Lutheran School and the school at St. Mary's German Catholic Church with German Jews on the Board of Education reflects this pattern.

Many Germanic immigrants immersed themselves in public education. During the 1865 Board of Education elections, Germans voted for reform to expand public education. While some newspapers such as the *Memphis Daily Appeal* speculated that there were underlying attempts to add German and Dutch lessons to schools, no evidence was ever produced.[xxiv] However, a push to add the German language instruction to public schools would not have been misplaced considering the involvement of Germanic immigrants in public education. The Board of Education purchased supplies for schools from local Germanic merchants such as F. Katzenbach and Charles Damman. While Damman served on the Board of Education with the School House and Furniture committee, Katzenbach was a music professor as well. [xxv]

German-language voters voted for Germanic candidates—"Germanic candidates" included German-language speakers, candidates from Germany, or people supported by a cohort of Germanic citizens. According to Germanic voters in 1865, in order to have reform in public schools, Richard Hines, the superintendent, needed to be replaced. While voting allowed many Germanic male emigrants to participate in their community, many also ran to enact reform in schools.[xxvi] Joseph Gronauer, Dr. Laski, John Hollywood, John Fuerst, Hans Lemon and Dr. Jacob Peres were among the candidates Germanics voted for to replace Richard Hines.[xxvii] While those candidates opposed Hines, Germanic candidates ran in other wards and occasionally against each other. Dr. Jacob Peres and T.W. Buttinghaus were among the Germanic candidates that won.[xxviii] During the 1860s most Germanics lived in Ward One and Ward Six.[xxix] The election results printed in the Memphis Daily Bulletin show the influence of Germans as both candidates and voters. Of the twenty-one candidates, ten were either German or Dutch or had support from Germanic voters thus reinforcing both the integration of Germans in Memphis and their position as the second largest immigrant in Memphis during the nineteenth-century. [xxx]

In 1867, Germanic emigrants occupied positions on the school visitors board as funding for schools became a debated topic. Moreover, two of the aldermen who served on the school subcommittee, J.C. Holst and E.W. Wickersham, were of Germanic descent. [xxxi] Both Holst and Wickersham favored giving money from the city government to the public schools, implying a dedication to education. While several aldermen debated funding the

schools, the German-language aldermen favored the improvement of the public schools.[xxxii]

For every election year between 1865 and 1880, Germans held positions in the school system, whether on the school board, school board visitors, or as teachers. The exception was 1868, when no Germanic Memphians held positions as school board members and no Germanic aldermen served on the school committee.[xxxiii] In 1869, Germanics had one person to represent them on the board.[xxxiv] The following year saw four Germanics as members of the Board of Education.[xxxv] While Germanic emigrants occupied positions on the Board of Education, they were not longstanding members. Many held positions for a year with the exception of a few who remained on the board for two years; others held positions consecutively for two terms.[xxxvi]

Irish immigrants constantly outnumbered Germanic immigrants. The Irish population was double that of the Germanic population between 1865-1880. While on the board of education, Germanics held positions within the board itself, such as board secretary, finance committee, and building committee. Each member typically held one to two committee positions.[xxxviii] The number of Germanic immigrants on the board of education never exceeded four at a time while the twenty positions were available.

Education provided the gateway for female Germanic immigrants to contribute significantly to their community. Teaching allowed for some female Germanic immigrants to shape Memphis. As Germanic men expanded and rejoined the board of education, Germanic teachers taught at schools for both white and black students.[xxxviii] Through teaching, Germanics expanded education in Memphis. Annie Reudelhuber migrated to Memphis after being born in New Orleans to German emigrants. Reudelhuber taught at the Market School near Third street. The school welcomed students primarily of foreign birth.[xxxix]

Women such as Reudelhuber and her sister, Pauline, established leadership roles as principals of schools. [xl] The Shelby County Board of Education prioritized principals to energize schools and provide results.[xli] In 1874, Annie Reudelhuber transitioned from teacher to principal. [xlii] The job of principal was originally reserved for men. Therefore, female teachers, including the German teachers, worked to expand their leadership role over the schools during the Board of Education's first years.[xliii]

Germanic Parochial Schools in Memphis

Nationally, Germanic emigrants funded German-language parochial schools.[xliv] Although the number of schools increased in Memphis during

the late 19th century and Germanics were active in public schools, they also funded the parochial school at Trinity Lutheran Church, the "German Church." [xliv] In the Midwest, Lutheran Germanic emigrants funded schools that catered to their group. [xlvi] The school at Trinity Lutheran was no different. Trinity Lutheran school promoted both the Lutheran religion and Germanic culture.[xlvii]

The church organized the school in 1855, upon the establishment of the church. While the school was open to the public—the public that could pay—the school catered to German-language emigrants, displaying an inclusive exclusivity. Moreover, the city directories did not advertise the school at Trinity Lutheran Church, and they did not always advertise the church. In O.F. Vedder's *A History of Memphis, Tennessee Vol. II*, Trinity Lutheran does not list a school.

The school functioned as a Germanic school that welcomed all children from the neighborhood located in the Third Ward. Classes were taught in English, but the church required teachers to be fluent in both English and German. While the church welcomed members and school children, primarily of German descent, the school board prioritized having a German Lutheran teacher. By prioritizing who taught the children and enforcing a German-Lutheran school teacher, the church imposed a level of exclusivity in order to maintain a specific identity.[xlviii] By having specific religious and language requirements, the church school committee could ensure the influence of a certain identity. However, the church did not require a teacher's ethnicity to be German. Trinity Lutheran was founded and formed primarily by German-language Lutheran emigrants who were also involved in the City of Memphis.

Conclusion

Germanic Memphians contributed to the overall expansion of education in the City of Memphis. While they founded parochial schools in order to maintain their Germanic identity, they integrated into the City of Memphis by being elected to the board of education and city government. As government officials, they involved themselves in the greater fabric of Memphis. Although in Memphis, Germanic emigrants continued their political involvement in their homeland through education.

References

Primary Sources

A. E. Sholes, Boyle & *Chapman's Memphis City Directory*, 1872-1873, Boyle & Chapman Publishing, 1876.

Annual Report of School Visitors and Board of Education, 1868-1869 (Champaign: University of Illinois, 1966)

Boyle & Chapman's Memphis City Directory, 1872-1873, Boyle & Chapman Publishing, 1872.

Boyle & Chapman's Memphis City Directory, 1872-1873, Boyle & Chapman Publishing, 1874.

C. W. Norwood, *Shole's Directory of the City of Memphis,* 1877, Southern Baptist Publication Society, 1877.

C. W. Norwood, *Shole's Directory of the City of Memphis,* 1878, Southern Baptist Publication Society, 1878.

C. W. Norwood, *Shole's Directory of the City of Memphis*, 1879, S. C. Too and Company Pres., 1879.

C. W. Norwood, *Shole's Directory of the City of Memphis,* 1880, S. C. Too and Company Pres., 1880.

Keating, John M., the *Memphis Daily Appeal,* Memphis, Tennessee, 1865-1880.

Long, A. C., *Long's Memphis Directory* 1865-1866, Blelock & Co. 1865-1866.

Matthew Gallaway, *Memphis Daily Avalanche,* Memphis, Tennessee, 1866-1880.

Memphis Daily Bulletin, Memphis, Tennessee, 1868.

Ray Holt Memphis School Article Collection, Shelby County Register's Office/Archives, vol. 1-9.

Sieck, Henry, *Yellow Fever Quarantine in Memphis,* TN, August 14th-October 30th, 1878, Trinity Lutheran Church, 2005.

T. M. Halpin, *Edward's Annual Directory,* Edwards & Co Publishers, 1869.

T. M. Halpin, *Edward's Annual Directory,* Edwards & Co Publishers, 1870

T. M. Halpin, *Edward's Annual Directory,* Southern Publishing Company, 1871.

T. M. Halpin, *Edward's Annual Directory,* Southern Publishing Company,

1872.

T. M. Halpin, *Halpin's City Directory*, Bingham, Williams, & Co., 1866.

T. M. Halpin, *Halpin's City Directory,* Bulletin Publishing Company, 1867.

Trinity Lutheran Church Meeting Minutes,1855-1882, vol. 1, Trinity Church.

Whitmore Brothers, Memphis Public Ledger, Memphis, Tennessee, 1865-1880.

U.S. Census Bureau. Federal Census, 1860. Prepared by Ancestry.com. (accessed 29 October 2021).

U.S. Census Bureau. Federal Census, 1870. Prepared by Ancestry.com. (accessed 29 October 2021).

Secondary Sources

Amis, John M. and Paul M. Wright, *Race, Economics, and the Politics of Educational Change: The Dynamics of School District Consolidation in Shelby County, Tennessee,* University of Tennessee Press, 2018.

Blackbourn, David, *The Long Nineteenth Century: a History of Germany, 1780-1918,* Oxford University Press, 1997.

Berkeley, Kathleen, *Like a Plague of Locusts: Social Change and Immigration in Memphis, TN,* 1850-1880, University of California Press, 1980.

Bond, Beverly and Janann Sherman, *Memphis in Black and White,* Arcadia Publishing, 2003.

"History of Trinity Lutheran Church,"https://trinitymemphis.org/about-us-2/history-of-trinity

Kamphoefner, Walter D., *Germans in America, A Concise History*, Rowman & Littlefield, 2021.

Kitchen, Martin, *A History of Modern Germany, 1800-Present*, Wiley-Blackwell, 2012

Endnotes

[i] U.S. Census Bureau. Federal Census, 1870. Prepared by Ancestry.com. (Accessed 29 October 2021).
[ii] Beverly Bond. "Educating the Common Man" in *Race, Economics, and the Politics of Education Change: the Dynamics of Schools District Consolidation in Shelby County, Tennessee*. John M. Amis and Paul M. Wright, (Knoxville: University of Tennessee Press), 2018, 26.
[iii] Beverly Bond and Janann Sherman, *Memphis in Black and White*, (Charleston: Arcadia Publishing, 2003), Gerald M. Capers Jr, *Biography of a River town, Memphis: Its Heroic Age* (New Orleans, Tulane University Press, 1966), Jeannette Keith, Fever Season, (London: Bloomsbury, 2012), John E. Harkins, *Metropolis of the American Nile* (Oxford: The Guild Bindergy Press, 1982), John M. Amis and Paul M. Wright, R*ace, Economics, and the Politics of Educational Change: The Dynamics of School District Consolidation in Shelby County, Tennessee* (Knoxville: University of Tennessee Press, 2018), Molly Crosby Caldwell, *The American Plague: the Untold Story of Yellow Fever, the Epidemic that Shaped Our History*, (New York: Berkley Publishing, 2007), O. F. Vedder, *History of Memphis, Tennessee*, vol. II (Syracuse: D. Mason & Co. Publishers, 1888).
[iv] David Blackbourn, *the Long Nineteenth Century, A History of Germany*, 1780-1918, (New York: Oxford University, 1998), Ellen C. Merrill, *Germans of Louisiana*, (Gretna: Pelican Publishing, 2003), Kathleen Condray, *Das Arkansas Echo* (Fayetteville: University of Arkansas Press, 2020), Martin Kitchen, *A History of Modern Germany, 1800 to Present*, (Hoboken: Wiley-Blackwell, 2012), Walter Kamphoefner, *Germans in America, A Concise History*, (Lanham: Rowman & Littlefield, 2021).
[v] Kathleen Berkeley, L*ike a Plague of Locusts: Immigration and Social Change in Memphis, Tennessee, 1850-1880*, (Los Angeles: University of California, 1980), 7. Robert Rauchle. "*Prominent Germans in Memphis.*" Tennessee Historical Quarterly 22 (1968), 73-85.
[vi] Kitchen, A *History of Modern Germany*, 23, 54, 55, 68-9, 73-4.
[vii] Ibd, 23, 54, 55, 68-9, 73-4.
[viii] Blackbourn, *the Long Nineteenth Century*, 194.
[ix] Ibid, 96.
[x] U.S. Census Bureau. Federal Census, 1860.
[xi] Ibid, U.S. Census Bureau. Federal Census, 1870.
[xii]Ibid, 192.
[xiii] U.S. Census Bureau. Federal Census, 1860., U.S. Census Bureau. Federal Census, 1870.
[xiv] Blackbourn, t*he Long Nineteenth Century*, 192-3.
[xv]U.S. Census Bureau. Federal Census, 1870.
[xvi] Memphis Wards, 1872[map]. 5.57 in and 5.03 in. Hand-drawn. Memphis: Sophia Rouse, 17 November 2021. Using: manual. *Germanic Memphis*, 1872[map]. 5.57 in and 5.03 in. Hand-drawn. Memphis: Sophia Rouse, 17 November 2021. Using: manual.
[xvii] A. E. Sholes, *Boyle & Chapman's Memphis City Directory, 1872-1873*, Boyle & Chapman Publishing, 1876, *Annual Report of School Visitors and Board of Education, 1868-1869* (Champaign: University of Illinois, 1966). Beverly Bond. "Educating the Common Man" in *Race, Economics, and the Politics of Education Change: the Dynamics of Schools District Consolidation in Shelby County, Tennessee.* John M. Amis and Paul M. Wright, (Knoxville: University of Tennessee Press), 2018. *Boyle & Chapman's Memphis City Directory, 1872-1873*, Boyle & Chapman Publishing, 1872, *Boyle & Chapman's Memphis City Directory, 1872-1873*, Boyle & Chapman Publishing, 1874, C. W. Norwood, *Shole's Directory of the City of Memphis, 1877*, Southern Baptist Publication Society, 1877, C. W. Norwood, S*hole's Directory of the City of Memphis, 1878*, Southern Baptist Publication Society, 1878, C. W. Norwood, *Shole's Directory of the City of Memphis, 1879*, S. C. Too and Company Pres., 1879, C. W. Norwood, S*hole's Directory of the City of Memphis, 1880*, S. C. Too and Company Pres., 1880, Long, A. C., *Long's Memphis Directory 1865-1866*, Blelock & Co. 1865-1866, *Ray Holt Memphis School Article Collection*, Shelby County Register's Office/Archives, vol. 1-9, T. M. Halpin, Edward's Annual Directory, Edwards & Co Publishers, 1869, T. M. Halpin, *Edward's Annual Directory,* Edwards & Co Publishers, 1870, T.

M. Halpin, Edward's Annual Directory, Southern Publishing Company, 1871, T. M. Halpin, *Edward's Annual Directory*, Southern Publishing Company, 1872, T. M. Halpin, *Halpin's City Directory*, Bingham, Williams, & Co., 1866, T. M. Halpin, Halpin's City Directory, Bulletin Publishing Company, 1867.

[xviii] Ray Holt *Memphis School Article Collection*, Shelby County Register's Office/Archives (hereafter RHMSAC), vol. 1-9.

[xix] Kamphoefner, *Germans in America*, 90.

[xx] O.F. Vedder, *History of Memphis, Tennessee*, vol. II (Syracuse: D Mason & Co. Publishers, 1888), 145-7.

[xxi] T. M. Halpin, *Halpin's City Directory*, Bingham, Williams, & Co., 1866, 1.

[xxii] "Report of the President," *Annual Report of School Visitors and Board of Education*, 1866-1867 (Champaign: University of Illinois, 1966), 11-2.

[xxiii] Walter Kamphoefner, *Germans in America, A Concise History*, (Lanham: Rowman & Littlefield, 2021), 90.

[xxiv] John Keating, "The Election Yesterday," *Memphis Daily Bulletin*, June 3rd, 1865, RHMSAC, vol. 2, 200.

[xxv] Halpin, *Halpin's City Directory.* Tim Sharp, *Memphis Before the Blues*, (Charleston: Arcadia Publishing Company, 2007),

[xxvi] John Keating, "The Election Yesterday," *Memphis Daily Bulletin*, 3 June 1865, RHMSAC, vol. 2, 200.

[xxvii] Ibd.

[xxviii] Halpin, *Halpin's City Directory*, 280.

[xxix] U.S. Census Bureau. Federal Census, 1860.

[xxx] John Keating, "The Election Yesterday," *Memphis Daily Bulletin*, June 3rd, 1865, RHMSAC, vol. 2, 200.

[xxxi] T. M. Halpin, *Halpin's City Directory*, Bulletin Publishing Company, 1867, 318.

[xxxii] "The City Fathers Yesterday," *Memphis Public Ledger*, August 9th, 1867, RHMSAC, vol. 3, 28-9.

[xxxiii] T. M. Halpin, *Edward's Annual Directory*, Edwards & Co Publishers, 1868, 1, 26-7.

[xxxiv] "Official Proceedings of the Board of Education Visitors," *Memphis Daily Avalanche*, March 3rd, 1869, RHMSAC, vol. 3, 341.

[xxxv] "Board of Education Visitors," *Memphis Daily Avalanche*, April 12th, 1870, RHMSAC, vol. 3, 563.

[xxxvi] "Official Proceedings of the Board of Education Visitors," *Memphis Daily Avalanche,* March 3rd, 1869, RHMSAC, vol. 3, 341

[xxxvii] *Boyle & Chapman's Memphis City Directory*, 1872-1873, 67.

[xxxviii] "Popular Education, Condition of the Public Schools—the Teachers," *Memphis Daily Avalanche* September 14th, 1870, RHMSAC, vol. 3, 582-3.

[xxxix] *Annie Reudelhuber Obituary*. Commercial Appeal, 1920, 1.

[xl] Ibd.

[xli] *Annual Report of School Visitors and Board of Education, 1868-1869* (Champaign: University of Illinois, 1966), 68.

[xlii] *Annual Report of School Visitors and Board of Education, 1873-1874* (Champaign: University of Illinois, 1966), 31.

[xliii] Ibd, 81.

[xliv] Kamphoefner, *Germans in America, A Concise History*, 89.

[xlv] "History of Trinity Lutheran Church,"https://trinitymemphis.org/about-us-2/history-of-trinity/.

[xlvi] Kamphoefner, 89.

[xlvii] "History of Trinity Lutheran Church,"https://trinitymemphis.org/about-us-2/history-of-trinity/.

[xlviii] Trinity Lutheran Church Meeting Minutes, 61, Special Meeting August 23rd, 1870

Donald Young is an undergraduate senior at the University of Memphis. He is a double major in Philosophy and English with a concentration in Literature. His interests are in gothic fiction, early modern literature, queer theory, and 20th century French philosophy. He has won first place in both the Joseph and June Riley Essay Contest and the Seshat Prize Essay Contest. He intends to pursue a graduate education after obtaining his undergraduate degree.

Donald Young

Cavendish's Queer Fancies, Scientific and Romantic, in *The Blazing World* and *The Convent of Pleasure*

Faculty Sponsor

Dr. Don Rodrigues

Abstract

In *The Blazing World*, Margaret Cavendish presents a concept of fancy, whereby an individual creates their own fictional world to realize those ambitions which cannot be realized in the real world. This concept is similar to the queer futurity of José Esteban Muñoz as presented in his book, *Cruising Utopia: The Then and There of Queer Futurity*, but Cavendish distinguishes herself from Muñoz in fancy's lack of concern with the real world. This article analyzes how Cavendish uses this concept to imagine scientific, social, and sexual realities unavailable to her in The Blazing World and The Convent of Pleasure. In imagining social, sexual and romantic possibilities in The Convent of Pleasure, Cavendish exposes the limits of her concept of fancy: its inability to bring about tangible change in the real world.

Introduction

In "The Defense of Poesy," Sir Philip Sidney defends poetry against various charges brought against it by his contemporaries. Poetry's detractors claim that it is useless fancy that breeds idleness at best and is morally and spiritually corrosive at worst. Sidney's response to this attack is to assert poetry's utility as a tool to instill virtue. "For if it be as I affirm, that no learning is so good as that which teacheth and moveth to virtue; and that none can both teach and move thereto so much as poetry: then is the conclusion manifest that ink and paper cannot be to a more profitable purpose employed" (Sidney 570). The value of poetry—and literature as a whole—then comes from its capacity to provide social utility. The fanciful nature of literature justifies itself by its ability to have a positive utilitarian effect on the real world.

A very different approach to the fantastical is found in Margaret Cavendish's *The Blazing World*. This idiosyncratic work, published alongside one of Cavendish's philosophical texts, is considered by many to be the first work of science fiction. *The Blazing World* shows the creation and domination of another world, ruled by women who eagerly inquire into scientific and philosophical mysteries. In this text, one finds a radically different approach to fancy, one that is ostensibly queer, where fancy exists in spite of the real world, rather than for the sake of it, while in her later play, *The Convent of Pleasure*, she portrays what fancy cannot accomplish: meaningful transformation of structures of oppression in the real world. In these fancies she creates, Cavendish imagines worlds of female agency, women's inclusion in the scientific community, and same-sex romance.

This paper seeks to analyze the specific conception of fancy which Cavendish develops in *The Blazing World*, enumerating the different ends to which Cavendish applies fancy and how these fancies contrast with the historical reality of her lifetime. Following this, the events of her play *The Convent of Pleasure* will be read as an application of Cavendish's concept of fancy to realize female social and homosexual desires. In this instance though, its application serves to reveal the concept's own limits.

Cavendish begins *The Blazing World* with a section titled "To the Reader," where she declares: "[…] although I have neither power, time nor occasion to conquer the world as Alexander and Caesar did; yet rather than not be mistress of one, since Fortune and the Fates would give me none, I have made a world of my own: for which no body, I hope, will blame me, since it is in every one's power to do the like" (124). In this excerpt, Cavendish elucidates her reason for creating this work of fancy, that being to realize her desire to have a world of her own. Unlike Sidney's concept of fancy, Cavendish's fancy is not justified by any social utility external to the one who

fancies. Fancy needs no justification, rather "fancy creates of its own accord whatsoever it pleases, and delights in its own work" (*The Blazing World* 123).

Tessie Prakas has previously discussed fancy in *The Blazing World*, concluding that the fancy as introduced in the section titled, "To the Reader," is undermined by the narrative of the work. The author of this essay contends that the actions of the Duchess of Newcastle in *The Blazing World* reinforce this concept, rather than undermining it. Cavendish's concept of fancy is in many ways similar to José Esteban Muñoz's concept of queer futurity, presented in his book *Cruising Utopia: The Then and There of Queer Futurity* (Muñoz 18). In this text, Muñoz defines queerness as "a structuring and educated mode of desiring that allows us to see and feel beyond the quagmire of the present" (1). For Cavendish, fancy fulfils a similar role. She is cognizant that her ambitions are doomed to be unrealized, but the fanciful world she creates offers her a way to get beyond the disappointing present. Furthermore, Cavendish's creation of a world of fancy is a mode of desiring. In imagining this idealized world, she is actively desiring the alternate reality she has created, while the projection of herself into this fantasy (which she does quite literally) serves simultaneously as a fulfillment of that desire (*The Blazing World* 182).

In Cavendish's concept of fancy, I contend, fancy is a potentiality. Muñoz defines potentiality as "a certain mode of nonbeing that is eminent, a thing that is present but not actually existing in the present tense" (9). Without fancy existing in the present, the potential of its existence is present in the imagining, and that presence exists as a queer, invigorating force that allows its creator to survive a disappointing reality. Take the Duchess of Newcastle's simultaneous existence within her real world and *the Blazing World*. *The Blazing World* being a fancy, her simultaneous existence in these two worlds is analogous to the experience of one having a fancy. The presence of *the Blazing World* offers the Duchess reprieve from her native world, with its "so many several nations, governments, laws, religions, opinions, etc." that "all yet so generally agree in being ambitious, proud, self-conceited, vain, prodigal, deceitful, envious, malicious, unjust, revengeful, irreligious, factious, etc." (*The Blazing World* 190).

What differentiates Cavendish's fancy from Muñoz's queer futurity is its relationship with time. Whereas queer futurity is expressly concerned with the future, fancy is not. Fancy, rather, emphasizes the relationship to the present. Queer futurity involves a hope that the potentiality will become actuality. Cavendish's fancy has no such hope. Fancy offers an individual the opportunity to encounter a potentiality which is extremely unlikely to become actuality anytime soon. Fancy is the imagining of a world which is

not and will not be actual but exists as a potentiality which can be felt out by the individual.

A result of this distinction is that fancy does not share the external character of queer futurity. Queer futurity is attached to the possibility of change in the real world, and it is this hope that serves as a positive force. Cavendish's fancy, in contrast, is an internal project, one that serves as a survival mechanism for an individual more so than a positive political force. One imagines what could be but will not be, and this imagining allows the individual to take pleasure in these fictitious worlds. It is very similar to escapism. The individualism of fancy is even reflected in Cavendish's writing, take these lines from the epilogue of *The Convent of Pleasure*: "...she is careless, and is void of fear; / If you dislike her play she doth not care" (54). There is a disregard for those desires, such as virtue or social utility, that are not for the self.

The Blazing World Analysis

Moving on to the narrative of *The Blazing World*, it begins significantly: "a young Lady" (*The Blazing World* 125) is kidnapped by a foreign merchant who intends to sexually assault her. However, before this heinous act can be committed, a storm causes the young Lady's captors to lose control of the vessel. It drifts on to the North Pole where the merchant and his men freeze to death. That *The Blazing World* begins with an act of sexual violence directed towards a woman is important. This establishes the grim condition of women which Cavendish is going beyond in creating her fancy. *The Blazing World* exists as a world in which this patriarchal structure of power is reversed. Consider the young Lady's elevation to the Empress. When she is brought before the Emperor, rather than seizing her by force as the merchant did, he "conceived her to be some goddess, and offered to worship her" (*The Blazing World* 132). After their subsequent marriage, the Emperor "gave her an absolute power to rule and govern all that world as she pleased" (*The Blazing World* 132). Here, the Emperor gives up his absolute monarchial power to the Empress, who thus realizes Cavendish's ambition to rule her own world.

The Blazing World is also a homosocial space for women, where they can socialize free from the restrictive effects of patriarchy. The friendship between the Empress and the Duchess is so intimate that they are called "platonic lovers' (*The Blazing World* 183). In stark contrast to the isolated situation of the Empress at the beginning of the play, and very similar to Cavendish's later play, *The Convent of Pleasure*, *the Blazing World* is a distinctively female space, where women can coexist and engage in activities which bring them pleasure.

Within the text, the Empress and the Duchess engage in the same fancy-creation that Cavendish herself is engaged in. The Duchess suffers from a melancholy which "proceeds from an extreme ambition" (*The Blazing World* 183). The fictional Cavendish desires to be the ruler of her own world. Finding no terrestrial world uninhabited, and deigning not to conquer an inhabited one, the Duchess takes the advice of some friendly spirits and decides to create a celestial world for herself. Hearing of this possibility from the spirits, the Empress asks, "[C]an any mortal be a creator?" (*The Blazing World* 185). To which the spirits respond: "Yes … for every human creature can create an immaterial world fully inhabited by immaterial creatures, and populous of immaterial subjects, such as we are, and all this within the compass of the head or scull … And since it is in your power to create such a world, what need you to venture life, reputation and tranquility, to conquer a gross material world?" (*The Blazing World* 185-186).

The creation of worlds of fancy serves as an alternative to the real world. When one finds one's ambitions too great for the scope of the real world, or the conditions of the real world too harsh, a fanciful world is where one can go to escape uncompromising reality. The purpose of creating these worlds is not to cultivate virtue in the real world, but for the creator to "enjoy as much pleasure and delight as a world can afford [them]" (*The Blazing World* 186). There is something undeniably queer in this turn away from utilitarian justifications for fancy. One of the goals of queer theory broadly is the recontextualization and subsequent reevaluation of normative positions, such as the claim that art ought to have a social utility (Berlant and Warner 345), making this text's challenge to this claim decidedly queer. In its place, Cavendish offers fancy for fancy's sake, fancy that exists because it is pleasurable and precisely because what it depicts is not real.

Returning to the world the Duchess constructs, she attempts to create this world in accordance with the doctrines of various philosophers—Thales, Pythagoras, Plato, Epicurus, Descartes, and Hobbes—but none of them prove adequate. Thus, she "resolves to make a world of her own invention" (*The Blazing World* 188), using her own philosophical thought as the basis for the fantasy world she creates. The inability of the thought of canonical philosophers to capture the world the Duchess desires displays the failure of traditional Western thought to articulate the "queer" desires of those not found within the philosophical canon, such as women. Cavendish directly speaks of the prejudice against women in philosophy in *Observations upon Experimental Philosophy*:

> I might set up a sect or school for myself, without any prejudice to them [ancient philosophers]: But I, being a woman, do fear they would soon cast me out of their schools; for, though the muses, graces and sciences are all of the female gender, yet they were more esteemed in former ages, than they are now; nay, could it be done handsomely, they would now turn them all from females into males: So great is grown the self-conceit of the masculine, and the disregard of the female sex. (249)

Cavendish's fancy of a feminine scientific utopia in *The Blazing World* is a reaction to the distinctly masculine and misogynistic character of the early modern scientific project. Consider the scientific utopia imagined by Francis Bacon in *New Atlantis*. In *New Atlantis*, Bacon imagines the island of Bensalem, whose utopian conditions are owed to the work of Salomon's House, a mysterious scientific organization. Bacon's utopia, despite its lofty dreams of progress, offers little place for women within it. Women are only discussed in relation to the family structure and marriage—two patriarchal institutions. Bensalem's Feast of the Family, "a most natural, pious, and reverend custom" (Bacon 169), honors the supreme patriarch of the family, while Bensalem's marital traditions celebrate chastity and the naturalness of "the faithful nuptial union of man and wife" (Bacon 173). It is not only in family and marriage practices that Bacon's utopia is masculine and patriarchal, but also in the structure of Salomon's House. The leaders of Salomon's House are called "the Fathers of Salomon's House" (Bacon 175), a title evocative of the role of the father within the family structure of patriarchal societies. Bacon's utopia offers a decidedly masculine scientific utopia, serving as an indication of the general attitude of the period, to which Cavendish's feminine scientific utopia can be contrasted.

Turning now to Cavendish's *The Blazing World*, there is a section near the beginning of text where the Empress engages in a lengthy dialogue with the various species of animal-men of *the Blazing World*, whom each practice a particular profession within natural philosophy, mathematics, logic, or rhetoric. The Empress impresses these animal-men scholars with her knowledge and insight, as they did not know "that her Majesty had such great and able judgement in natural philosophy" (*The Blazing World* 155).

This peculiar section of *The Blazing World* shows Cavendish creating a fancy of a scientific community that allows women a place within it. This fancy starkly contrasts with reality, as there was no place for Cavendish in the scientific community at her time because she was a woman. Cavendish could not join the premier natural philosophical society of her day, the Royal Society, because she was a woman. Furthermore, Marcy Lascano notes that "very few philosophers engaged with Cavendish" (30). "Cavendish points to

misogyny and the barring of women from universities as key factors in this exclusion" (Lascano 36). Due solely to her gender, Cavendish hit a wall which she could not get beyond. Her wealth and privilege afforded her far more freedom than other women of her day, but she was still unable to have the same opportunities as a man. Her world of fancy allowed her to get past this insurmountable barrier through creating a fictitious world where a woman can be welcomed into the scientific community. A world of fancy exists then as a space where those not represented within traditional thought can develop their own way of being-in-the-world distinct from what is deemed acceptable within patriarchal scientific conventions.

Moving on to the content of Cavendish's philosophical thought, Cavendish was very critical of experimental natural philosophy, which believed that systematic observations and experiments would provide insight into the causes of phenomena in the natural world. Her opposition to this methodology likely contributed to her exclusion from the Royal Society as well. The stated goal of many experimental natural philosophers was the understanding of Nature. Cavendish scoffed at this. Unlike many natural philosophers, she understood people as part of Nature. Since people are part of nature and "no part of nature is able to understand the whole" (Lascano 33), people cannot hope to understand Nature. The relationship between most natural philosophers and Nature becomes more complicated when the gendering of Nature as a woman, by both them and Cavendish, is considered. These masculine natural philosophers (Cavendish directly responds to Robert Hooke) place themselves outside of and opposing feminine Nature, rather than within it.

The scientific community in *The Blazing World*, in contrast, through embracing the ideas of the Empress which are themselves the ideas of Cavendish, reconcile the opposition to the feminine found in natural philosophy. Cavendish even more directly says this in the passage already quoted from *Observation Upon Experimental Philosophy,* where she claims that "science [is of] the female gender" (249), but men would rather make it masculine, thus emphasizing that gendered conflict. By accepting the unity of themselves with feminine nature, the gendered tension of science is reconciled, and it is achieved by the inclusion of a woman in the scientific community. In this way, Cavendish's fancy imagines the flaws of science which could be overcome if her and other women would be included.

The gendered opposition of science is further criticized by Cavendish in her discussion of "art," by which she means tools such as microscopes and telescopes. Ventriloquizing Cavendish, the Empress says, "[N]ature has made your sense and reason more regular than art has your glasses, for they

are mere deluders, and will never lead you to the knowledge of truth" (*The Blazing World* 141-142). To attempt to use tools to understand Nature, like the experimental natural philosophers, is folly. Nature has already provided you with everything you need to understand causes, that being your unaided senses and your reason; the use of technology will only serve to make your understanding less clear. The internal turn that this emphasis on reason versus experimentation proposes is reminiscent of Cavendish's concept of fancy. There is this implication that the potential for what you need is already inside of you, and any attempt to find a solution outside of yourself is a mistake.

In *The Blazing World* then, Cavendish offers a specific notion of fancy, one which she uses to create a utopia of female agency and scientific engagement which could not be realized in the real world. In her play released two years later, *The Convent of Pleasure*, Cavendish continues to utilize the concept of fancy, this time to again create a female utopia, but also to imagine female same-sex relationships and even the limits of her own individualist concept of fancy.

The Convent of Pleasure Analysis

In *The Convent of Pleasure*, Cavendish imagines a convent of only women who have chosen to escape men entirely so they may pursue pleasure and avoid pain. These women, led by Lady Happy, enter the convent explicitly to avoid the sufferings of heterosexual marriage, which are clearly depicted in the play within the play that occurs in Act III, showing the pain of childbirth and adulterous, deadbeat husbands. Though it is impossible to know whether *the Convent of Pleasure* was a fancy for Margaret Cavendish, the opulence of the convent and its celebration of pleasure, found also within *The Blazing World*'s idea of fancy, makes this a likely possibility.

Over the course of the play, Lady Happy falls in love with a princess who has joined *the Convent of Pleasure*, but these feelings which Lady Happy experiences put her in a melancholic state. In Act IV, Scene 1, there are two fantastical sequences where the Princess and Lady Happy, occupying masculine and feminine roles respectively, play characters in a heterosexual romantic pairing with one another. These sequences are fancies in the same sense as in *The Blazing World*. Lady Happy imagines these sequences to experience the homosexual desire she feels but is unable to reconcile. Lady Happy says, at the beginning of Act IV, Scene 1,

> "But why may not I love a woman with the same affection I could a man? / No, no, Nature is Nature, and still will be / The same she was from all eternity" (*The Convent of Pleasure* 33).

The difficulty that Lady Happy has encountered is that she has devoted herself to Nature and to pleasure, but she considers homosexual desire unnatural. Considering the unity of Nature and pleasure asserted by Lady Happy in Act 1, Scene 2, then same-sex desire must be natural as it is pleasurable. The imitations of heterosexual romance found in these sequences, rather than championing the naturalness of heterosexuality, exhibit Lady Happy's inability to get beyond the heteronormative assumptions which inform her concept of what is natural and unnatural. That the Princess and Lady Happy must occupy separate masculine/feminine roles within their relationship is the result of a discourse of romance that could only be understood through a heterosexual lens.

In Act V, Scene 1 of the play, it is revealed that the Princess is actually a prince in disguise. Despite this event, the Princess and the Prince can be read as two distinct characters. Contrasting the disguised gender plot found within *The Convent of Pleasure* with the one found in Ben Jonson's *Epicoene or the Silent Woman* clarifies this point. First, in *Epicoene*, there are clues that Epicoene is not in fact a woman, so the inevitable reveal at the end of the play can be anticipated. The most obvious clue is Epicoene's name, which comes from the word "epicene" defined by *Oxford English Dictionary* as "a person having characteristics of both sexes, or of neither; a person of indeterminate sex; a hermaphrodite, transsexual, or transvestite." Meanwhile, the clues as to the Princess's identity as the Prince are sparse and vague. One such clue is a statement by the Princess that embraces of Lady Happy "though of a female kind, / May be as fervent as a masculine mind" (*The Convent of Pleasure* 34).

Similarly, consider Shakespeare's *Twelfth Night*, where the bulk of the play's comedy comes from the audience's knowledge that Cesario is not a man, but rather the woman, Viola, disguised as one. Secondly, *Epicoene* was a play written to be performed, while *The Convent of Pleasure* is a closet drama. When a theatergoer would see a performance of Epiocene in the early modern period, they would know that the character of Epicoene was being played by a male. The revelation that Epicoene was a man pretending to be a woman would then be a confirmation of what they already knew, but within the context of the play rather than outside of it. In contrast, being a closet drama and hence not to be performed, the Princess in *The Convent of Pleasure* does not have this peculiar relationship to gender. The absence of this means that the revelation that the Princess is really a prince functions as a transformation rather than a reveal of something that was in front of the audience's eyes the whole time. While Epicoene is always to some degree a man in women's clothes, the Princess goes from a woman in women's clothes to a woman in man's clothes, before transforming into a man in man's clothes

in an instant. These discrepancies between *The Convent of Pleasure* and other plays with similar plot elements lend themselves to a reading of *The Convent of Pleasure* where the Princess and the Prince are two separate characters. In response to this, one could argue that because of narrative conventions of the time, the Princess's transformation into the Prince could be anticipated, but just because narrative conventions could lead one to anticipate this does not mean the distinguishing characteristics of *The Convent of Pleasure* should be discredited. Cavendish's play is one which feigns operation within narrative conventions, but surreptitiously subverts them.

The existence of *the Convent of Pleasure* and the relationship between Lady Happy and the Princess are both underscored by the knowledge that this is not a state which the play itself can allow to continue uninterrupted. The state of things found in Acts II, III, and IV of *The Convent of Pleasure* is one which cannot continue. It is a convention of early modern comedies that their conclusions involve a restoration of the heteronormative order which is subverted throughout the other parts of the play.

Consider Shakespeare's *Twelfth Night*, where the play concludes with the queer romance between Viola and Olivia being reconciled by their marriages to Orsino and Sebastian respectively. Olivia and Sebastian's heterosexual marriage also reconciles the romantic desire of Antonio for Sebastian. Although many early modern plays may meander within the queer over the course of their narrative, there is seemingly an inability for them to finish within the queer. The conclusion must bring with it the reinforcement of heteronormative values and the reintegration of any ostensibly queer characters into the acceptable, heteronormative social order. Although one may wish to imagine a version of *The Convent of Pleasure* where the convent continues to exist and Lady Happy and the Princess live happily forever after, it is evident that this could not be so, at least at the time of Cavendish's writing. Despite this, reading *The Convent of Pleasure*, one can feel Cavendish straining against the restriction of convention.

In Act III, as mentioned briefly before, the women of the convent put on a play in which they enumerate the sufferings of women in heterosexual marriage. These many snapshots of marital life showcase adulterous, drunken, gambling husbands, and even one husband fittingly named Mr. Negligent. Also seen is both the pain of losing a child and of giving birth to one. This fictitious play eventually reaches this conclusion:

> *Marriage is a curse we find,*
> *Especially to womenkind:*
> *From the cobbler's wife, we see,*
> *To ladies—they unhappy be.* (*The Convent of Pleasure* 31)

Having finished the play, one may conclude that it reaffirms the value and necessity of heterosexual marriage over any non-normative desires, such as desire for a solely female space or romantic desire for another woman, through the marriage of Lady Happy to the Prince and the dismantling of *the Convent of Pleasure*, but the queerness of *The Convent of Pleasure* seems to reach beyond its conventional heteronormative finale.

What Act III and much of the play prior to the final act shows is a queerness that eludes the attempted reintegration of the conclusion. The reasons for the creation of the convent and the refusal of heterosexual marriage are clearly provided. Lady Happy provides a philosophical argument as to why the convent should exist in Act I, Scene II and the play within a play further justifies this by exhibiting the sufferings of heterosexual marriage for women in Act III. The play does not provide a rebuttal to the outlook of Lady Happy and the convent posit. To conclude, because the play ends with a heterosexual marriage and the disintegration of the convent, Cavendish is asserting the value of heteronormativity, is a mistake. The failure of heteronormative society to answer the criticisms of it brought forward by Lady Happy and the women of *the Convent of Pleasure* exposes the play's conclusion as empty; it is the failure to silence the queer and reintegrate them into heterosexual norms.

Reading *The Convent of Pleasure* an important question may arise: what is the conflict? The interpretation of the central conflict in this play is the basis for any further interpretation. A traditional interpretation of *The Convent of Pleasure* would likely conclude that the withdrawal of the women is the central conflict. The problem is then that this denial of heteronormative and patriarchal conventions will result in the destruction of society if something is not done. The anxiety experienced by the side characters Facile, Adviser, Courtly, Take-Pleasure, and Dick shows the mayhem caused by the convent. They need wives to be able to reproduce and continue the status quo, so they come up with the plan to "put [themselves] in women's apparel, and so by that means get into the Convent" (*The Convent of Pleasure* 21). What the reader wants to happen is for the convent to be dissolved so order may be restored.

If the central conflict is interpreted as the attempts to destroy *the Convent of Pleasure* though, then the play's interpretation takes a different course. While narrative convention may lead one to prefer the traditional interpretation of the conflict, the content of the play does lend itself to this queer alternative. This queer reading of the conflict does require a queering of form, as the structure of the play favors the traditional interpretation, with the play beginning with the convent's creation and ending with its dissolution. As has already been noted, there are the justifications for the convent in Acts I, II and III which are oddly sympathetic if *the Convent of Pleasure* is meant

to be read as the problem and again, these justifications are never rebutted.

What also must be considered is the framing of the previously mentioned male side characters. Facile, Adviser, Courtly, Take-Pleasure, and Dick are not written to be likable, even though a traditional reading of *The Convent of Pleasure* would entail these men being the sympathetic characters. Consider this line from Adviser, where he gives his opinion of what the consequences for Lady Happy should be for creating *the Convent of Pleasure*: "Her heretical opinions ought not to be suffered nor her doctrine allowed, and she ought to be examined by a masculine synod, and punished with a severe husband, or tortured with a deboist husband" (*The Convent of Pleasure* 13-14).

This kind of misogynistic call for punishment directed at the protagonist is hardly what would be coming from a character that the reader should consider right, especially considering Cavendish's criticism of patriarchal institutions in her philosophical writing. These characteristics that strongly contrast with the traditional understanding of the play's conflict lend credence to the queer interpretation offered, which further supports the argument that the play's final heterosexual marriage is not a reconciliation of the queer. Instead, the play's conclusion is the sorrowful end to the fancy of same-sex love and female utopia created by Lady Happy and the women of *the Convent of Pleasure*.

Conclusion

Having defended this queer reading of *The Convent of Pleasure*, the Prince's appearance is not then the realization of a romantic fancy, but the death of one. Notably absent from the play is any reaction to the Prince from Lady Happy to her marriage. The Prince declares his intention to marry her, stating that he "will have her by force of arms" (*The Convent of Pleasure* 48) if the councilors of the state do not allow it. This exclamation is a disconcerting expression of intended violence, which frames the marriage between the Prince and Lady Happy as one of possessorship rather than one of mutual affection. This contrasts with the equality found in the romance between Lady Happy and the Princess. Following this, Lady Happy has only four lines of dialogue, contained solely within the final scene, that are mostly irrelevant. Finding herself within a heterosexual marriage, not only has Lady Happy's voice and agency disappeared, but so has the fancy she had constructed of a homosexual romance and a place free of patriarchal oppression. While *The Blazing World* introduces fancy and its potential as a positive endeavor for those whose ambitions are too great for reality, *The Convent of Pleasure* exposes the limit of fancy: its individual focus renders it impotent to meaningfully change oppressive structures in the real world.

References

Bacon, Francis. "New Atlantis." Three Early Modern Utopias, edited by Susan Bruce, Oxford University Press, 1999, p.149-186.

Berlant, Lauren and Michael Warner. "Guest Column: What Does Queer Theory Teach Us about X?". PMLA, Vol. 110, No. 3 (May 1995), pp. 343-349, Modern Language Association, 1995.

Cavendish, Margaret. The Convent of Pleasure. Edited by Liza Blake and Shawn Moore.

Cavendish, Margaret. "The Description of a New World, Called the Blazing World." The Blazing World and Other Writings, Penguin Books, 2004, p.119-225.

Cavendish, Margaret, and Eileen O'Neill. Margaret Cavendish: Observations Upon Experimental Philosophy. Cambridge University Press, 2001. EBSCOhost, search.ebscohost.com/login.aspx?direct=true&db=nlebk&AN=72910&site=eds-live&scope=site.

"Epicene, adj. and n." OED Online, Oxford University Press, December 2021, www.oed.com/view/Entry/63248. Accessed 1 December 2021.

Lascano, Marcy P. "Margaret Cavendish and the New Science." The Routledge Handbook of Feminist Philosophy of Science, edited by Sharon Crasnow and Kristen Intemann, Routledge, 2021, p.28-40.

Muñoz, José Esteban. Cruising Utopia: The Then and There of Queer Futurity. New York University Press, 2009, New York and London.

Prakas, Tessie. "'A World of her own Invention': The Realm of Fancy in Margaret Cavendish's The Description of a New World, Called the Blazing World". The Journal for Early Modern Cultural Studies, Vol. 16, No. 1 (Winter 2016), 2016.

Sidney, Sir Philip. "The Defense of Poesy." The Norton Anthology of English Literature, Volume B: The Sixteenth Century and the Early Seventeenth Century, Edited by Stephen Greenblatt, Tenth Edition, W. W. Norton & Company, Inc., 2018, p.546-585.

Samantha Hall is currently pursuing a B.S. in biomedical engineering with a minor in biology and is expected to graduate in May of 2023. Additionally, she is pursing graduate level coursework through the biomedical engineering Accelerated B.S. to M.S. program. She has worked in Dr. Joel D. Bumgardner's lab since January of 2021 and is primarily involved in studies regarding macrophage polarization. Samantha is involved in the Society of Women Engineers, Tau Beta Pi Honor Society, and Tennessee Louis Stokes Alliance for Minority Participation. In the future, she plans on pursuing a PhD in biomedical engineering as well as a career in biomaterials research.

Samantha Hall, Malika Rad

& Joel D. Bumgardner

Analysis of In-vivo Macrophage Polarization in Response to Raspberry Ketone-Loaded Chitosan Membranes for Guided Bone Regeneration

Faculty Sponsor

Dr. Joel D. Bumgardner

Abstract

Nanofibrous electrospun chitosan membranes (ESCMs) have shown promise for enhanced guided bone regeneration (GBR) in alveolar defects when insufficient bone volume is present. Following GBR, a strategy that can be implemented to facilitate healing is the promotion of macrophage polarization from a pro-inflammatory phenotype (M1) to an anti-inflammatory phenotype (M2). Raspberry ketone (RK) is a natural compound that possesses anti-inflammatory properties. ESCMs were used to locally deliver RK to an in-vivo bone defect site using a rat calvarial model. ESCMs were loaded with 0 or 250 μg RK. Membranes from each treatment were implanted into rat calvarial defects (n=8). Membranes and surrounding tissues were extracted in serial sections and immunohistochemically stained at 1, 2, and 4 weeks using individual markers for M1(iNOS), M2 (CD206), and total macrophages (CD68). Percent-stained area was quantified using NIH ImageJ. Results indicated that ESCMs loaded with 250 μg RK facilitated M1 to M2 macrophage polarization.

Introduction

Alveolar bone loss can occur in patients due to periodontal disease or trauma. In the U.S. alone, more than 50% of adults suffer from periodontal disease (Eke 2012). This condition can become more prevalent as patient age increases. Furthermore, alveolar bone loss directly affects both patient health and patient quality of life. To combat these issues, a procedure called guided bone regeneration is often employed. Due to insufficient bone volume being present, Guided Bone Regeneration (GBR) is a surgical procedure that replaces missing bone with material from a patient's own body or with an artificial, synthetic, or natural substitute (Kumar 2013). As shown in Figure 1, when employing the procedure, a supporting material is placed into the socket where the bone is missing (Rodriguez 2018).

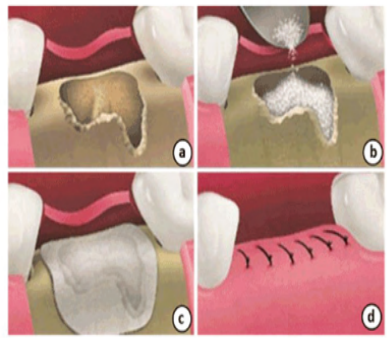

Figure 1. Guided Bone Regeneration procedure used to combat bone loss. (Rodriguez 2018)

A barrier membrane is then used to create a partition between the new bone growth and the soft tissues. However, complications can arise when connective and epithelial tissues invade the defect site, resulting in inadequate bone tissue regeneration. For healing to occur after the barrier membrane has been implanted, the inflammatory phase of the wound healing process must transition to the proliferative phase.

A type of cell that plays a prominent role in all phases of the wound healing process is the macrophage. Macrophages are specialized cells that originate from a type of immune cell called monocytes. Monocytes are attracted to tissues in response to injury, and these cells differentiate into macrophages. Macrophages are involved in the detection, phagocytosis, and destruction of bacteria (Rodriguez 2018). In relation to environmental signals, macrophages can differentiate into distinct populations. Specifically,

macrophages undergo a polarization along a spectrum into their M1 and M2 phenotypes. M1 macrophages are pro-inflammatory and possess antimicrobial properties while M2 macrophages are anti-inflammatory and aid in immune regulation (Fujiwara & Kobayashi 2005). As shown in Figure 2, M1 macrophages are introduced during the inflammatory phase of wound healing, and they polarize to their pro-healing M2 phenotype as tissue formation occurs in the proliferative phase. Moreover, M1 macrophages initiate the tissue repair process while M2 macrophages stabilize the repair process. Therefore, as the wound healing process progresses, M1 macrophages begin to polarize from their M1 phenotype to their M2 phenotype.

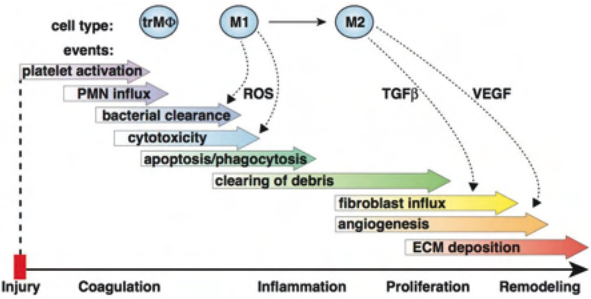

Figure 2. Diagram of macrophage polarization throughout the wound healing process. (Boniakowski et al., 2017)

This polarization was evaluated during an in-vitro study conducted in our lab that examined macrophage polarization from the M1 phenotype to the M2 phenotype in response to different concentrations of raspberry ketone (RK). RK is a natural phenolic compound of red raspberry that is known for its antioxidant and anti-inflammatory properties (Krzyszczyk 2018). Due to its anti-inflammatory properties, RK has shown potential in facilitating macrophage polarization. The in-vitro study found that raspberry ketone increased anti-inflammatory cytokines and decreased proinflammatory cytokines, which are signaling molecules that are specific to macrophage phenotypes and initiate healing properties.

To promote soft tissue healing and bone regeneration in the GBR process through the stimulation of macrophage polarization, the current study uses electrospun chitosan membranes (ESCMs) to locally deliver RK to an in-vivo bone defect site using a rat calvarial model. This will then allow the following questions to be answered:

1- Does RK affect macrophage polarization?

2- Does RK increase the number of anti-inflammatory, M2, macrophages?

Materials and Methods

Nanofibrous electrospun membranes composed of the natural polymer, chitosan, were loaded with RK. Chitosan is a polymer that is synthesized from chitin, a polysaccharide widely distributed in nature (Dodane et al.,1998). Moreover, Chitosan is appropriate for use as a membrane material in guided bone regeneration due to its resorbable nature, biocompatibility, and controlled degradation properties. Additionally, the nanofibrous structure of the membranes provides an increased surface area to volume ratio, allowing for local drug delivery to stimulate healing. This study utilized chitosan membranes that were loaded with a 250 μg dose of RK. These membranes were implanted into the calvarial defects of 8 rats (n=8) for 1, 2, and 4 weeks. Bilaterally separated by the sagittal suture, each rat received one chitosan membrane that was loaded with 250 μg RK and one membrane loaded with 0 μg RK, serving as a control group as shown in Figure 3.

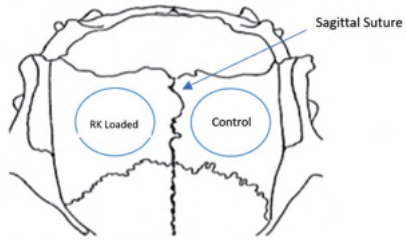

Figure 3. Rat cavlvarial defect model with RK loaded and non RK loaded chitosan membranes.

As rats were euthanized at each time point, three serial sections of tissue were extracted from each animal. The membranes and surrounding tissues were extracted in sagittal sections with a thickness of 5 microns, and an inflammatory score was given by a pathologist. As shown in Figure 4, these sections were immunohistochemically stained with CD68, CD206, and iNOS. These markers stained for the presence of all macrophages, M2 macrophages, or M1 macrophages, respectively. As shown in Figure 5, images of these immunohistochemically stained tissues were taken at 20X magnification using the image stitching function of an Olympus microscope. Images were analyzed by a blind observer using NIH ImageJ.

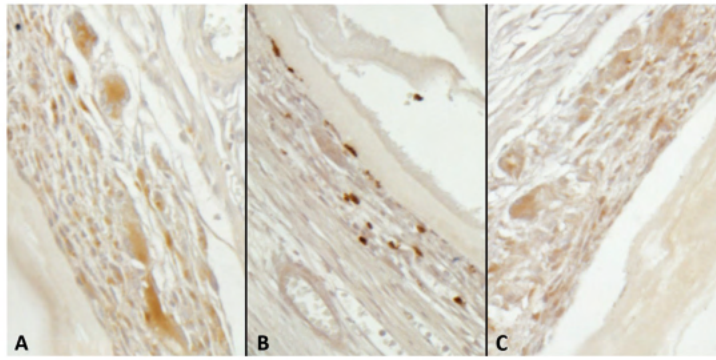

Figure 4. Immunohistochemical staining using CD68 (A), CD206 (B), and iNOS (C) for total, M1, and M2 macrophages, respectively.

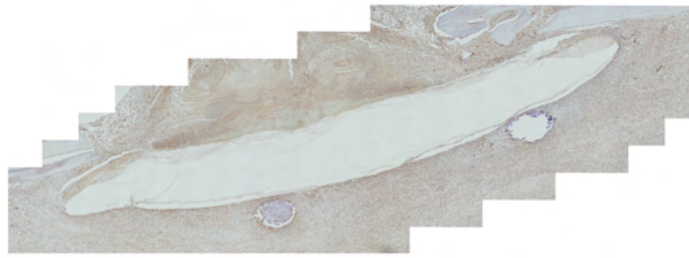

Figure 5. Immunohistochemically stained sample including membrane and surrounding tissue.

Using NIH ImageJ, the macrophages present in the inflammatory area of the membrane's surrounding tissue were quantified autonomously. Specifically, the inflammatory and the membrane areas were identified and isolated. Then, each tissue image was separated into three color channels using color deconvolution. As shown in Figure 6, using the orange color channel, the threshold intensity was manually adjusted to adequately cover the macrophage staining area, which was shown in brown. The size of cell (100-infinity pixel2) and the circularity (0-2) were constant values for all tissue sections. However, the threshold intensity was different for each tissue sample due to differences in staining intensity. The program automatically counted and outlined all macrophages based upon the set parameters, producing a binary image as shown in Figure 7.

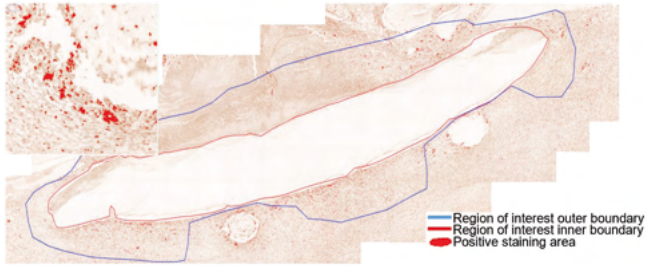

Figure 6. Membrane with isolated inflammatory region and highlighted positive macrophage staining

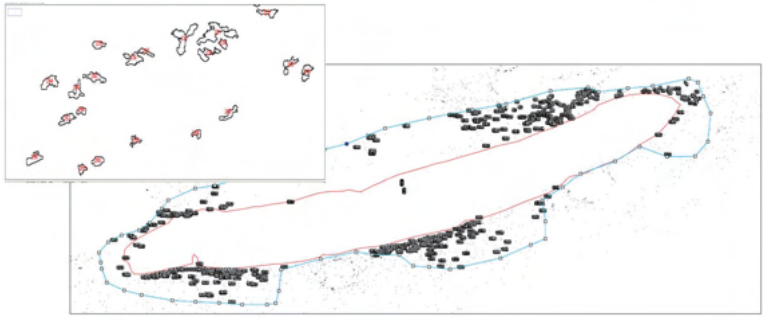

Figure 7. Binary image with individually counted macrophages.

The total area, membrane area, and stained area were also provided. All analysis utilized percent area as calculated in Equation 1.

$$\%\ Area\ (Pixel^2) = \left(\frac{Stained\ Area}{Total\ Area}\right) \times 100 \qquad (1)$$

Percent area was used as opposed to macrophage cell count to combat differences between animals and tissue samples as well as to compare the data to previous studies. At the completion of data compilation, a two-way ANOVA was performed for each of the three markers to identify any statistically significant differences between treatment groups and time.

Results

Figures 8, 9, and 10 display graphs of the average percent area for each treatment group at week 1, week 2, and week 3. Because staining was done on separate serial sections of tissue, total macrophage staining does not

equate the sum of M1 and M2 macrophage staining. As shown in Figure 8, the 250 µg RK treatment group had fewer total macrophages at weeks 2 and 4 and greater total macrophages at week 1. As shown in Figure 9, at the M1 macrophage week 2 timepoint, the control group had a greater number of M1 macrophages present. In Figure 10, at the M2 macrophage week 2 timepoint the 250 µg RK treatment group had a greater amount of M2 macrophages present.

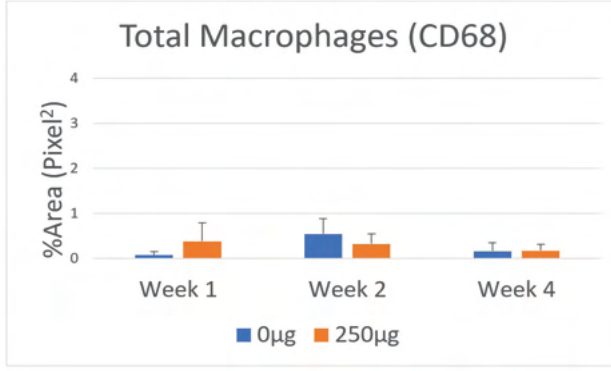

Figure 8. Total macrophage percent area data for 250 µg and 0 µg treatment group at 1, 2, and 4 weeks.

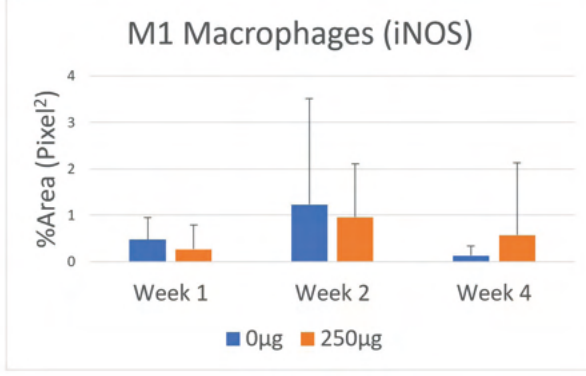

Figure 9. M1 macrophage percent area data for 250 µg and 0 µg treatment group at 1, 2, and 4 weeks.

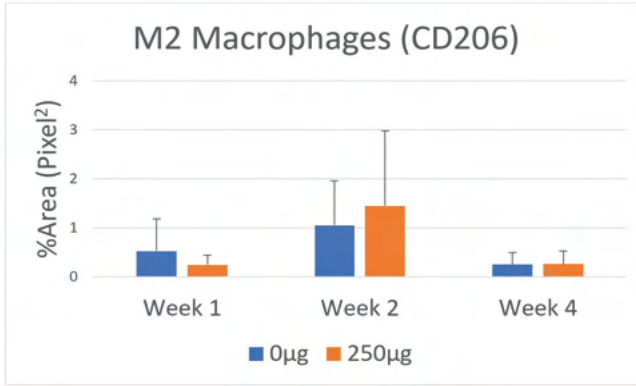

Figure 10. M2 macrophage percent area data for 250 µg and 0 µg treatment group at 1, 2, and 4 weeks.

Outliers based on the 1.5 IQR were also determined using a series of boxplots for both treatment groups for each different macrophage marker as shown in Figures 11, 12, and 13. Outliers were present for the total macrophage and M1 markers.

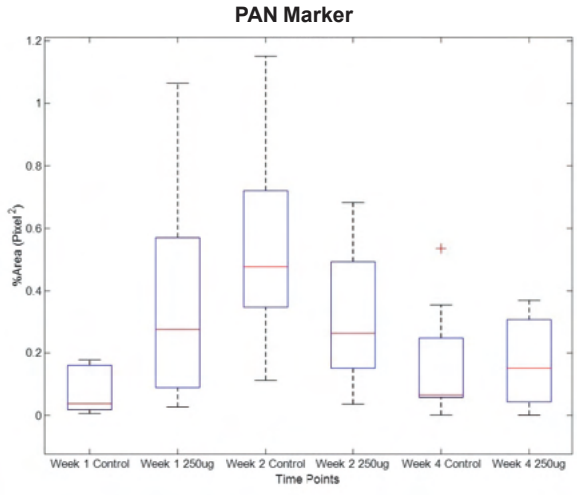

Figure 11. Boxplots of %Area for CD68 for each treatment group and time point (n=8). Red crosses indicate outliers according to upper and lower limits of Q3 + 1.5 IQR and Q1 – 1.5 IQR, respectively.

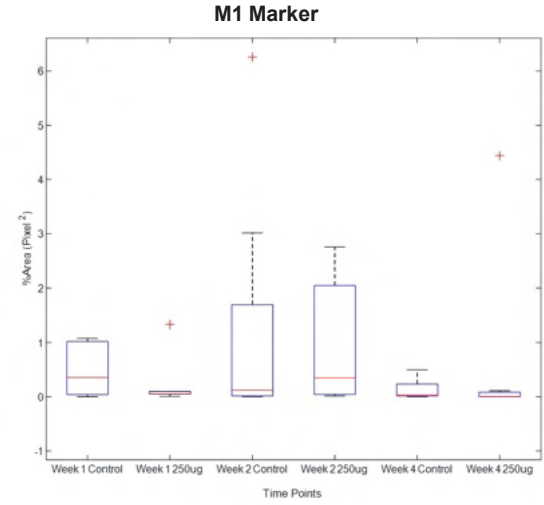

Figure 12. Boxplots of the %Area for iNOS for each treatment group and time point (n=8). Red crosses indicate outliers according to upper and lower limits of Q3 + 1.5 IQR and Q1 – 1.5 IQR, respectively.

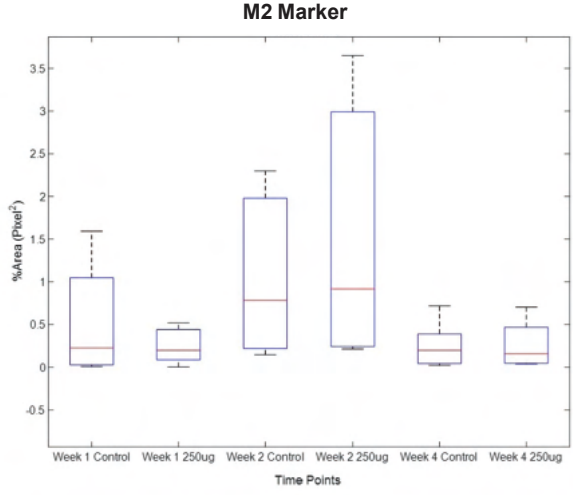

Figure 13. Boxplots of the %Area for CD206 for each treatment group and time point (n=8). Red crosses indicate outliers according to upper and lower limits of Q3 + 1.5 IQR

As shown in the Table 1 two-way ANOVA results, for all three macrophage markers, $p>0.05$ for interactions, indicating that there were no statistically significant interactions. In addition, $p>0.05$ for treatment groups for all three markers. However, $p<0.05$ for time points for CD68 and CD206, and $p>0.05$ for time points for iNOS.

Marker	Interaction	Variable	P-Value
M1 (iNOS)	0.3936	treatment	0.9966
		time	0.0003
M2 (CD206)	0.4157	treatment	0.6634
		time	0.2763
PAN (CD68)	0.1437	treatment	0.9714
		time	0.0062

Table 1. Results of two-way ANOVA

Discussion

The results of the two-way ANOVA show that there was no statistically significant difference between the control group and the 250 μg RK treatment group. However, apart from the M1 marker, which could potentially be due to the presence of outliers, there was a statistically significant difference between time points. The statistical difference between time points is an indicator of macrophage polarization taking place for both treatment groups. This indicates that the wound healing process was able to naturally occur, and the raspberry ketone did not inhibit macrophage polarization.

Although no statistical differences between groups were noted, trends were present throughout the data, indicating that RK did influence macrophage polarization. For total macrophages, on average, the 250 μg RK treatment group had fewer overall macrophages at weeks 2 and 4 and greater overall macrophages at week 1. Early in the wound healing process, macrophage cell counts would be expected to increase as M1 macrophages are introduced, clearing out debris and pathogens. The cell count would then decrease after macrophages transition to their pro-healing M2 phenotype. Macrophages are no longer required as wound healing progresses and tissue formation occurs. Therefore, this total macrophage trend is indicative of the 250 μg RK treatment group being further ahead in the polarization process in comparison to the control group. The M1 macrophage week 2 timepoint shows that the control group had a greater amount of M1 macrophages present, and the M2 macrophage week 2 timepoint shows that the 250 μg RK treatment group had a greater amount of M2 macrophages present. This trend also indicates that the 250 μg RK treatment group had a quicker M1 to M2 polarization in comparison to the control group.

The increased polarization toward the M2 phenotype that these trends exhibit is indicative of the progression of the wound healing process. As previously stated, M2 macrophages are pro-healing. Therefore, increased polarization toward the M2 phenotype indicates increased bone regeneration.

Conclusion

Graphically, it appears that raspberry ketone influences the polarization of macrophages from the M1 to the M2 phenotype in rat calvarial defects. Specifically, the graphed data indicates a lower amount of M1 macrophages and a higher amount of M2 macrophages in the RK treated group, indicating increased polarization and bone regeneration. For future studies, larger sample sizes could be used to increase the statistical significance and to further validate findings. Additionally, due to the presence of large standard deviations, the accuracy of individual markers could be explored. Furthermore, other doses of RK should be analyzed for dose dependent effects.

References

[1] Eke, Paul I., B. A. Dye, Li Wei, G. O. Thornton-Evans, and R. J. Genco. "Prevalence of periodontitis in adults in the United States: 2009 and 2010." Journal of dental research 91, no. 10 (2012): 914-920.

[2] Kumar, Prasanna, Belliappa Vinitha, and Ghousia Fathima. "Bone grafts in dentistry." Journal of pharmacy & bioallied sciences 5, no. Suppl 1 (2013): S125.

[3] Rodriguez, I. A., G. S. Selders, A. E. Fetz, C. J. Gehrmann, S. H. Stein, J. A. Evensky, M. S. Green, and G. L. Bowlin. "Barrier membranes for dental applications: A review and sweet advancement in membrane developments." Mouth Teeth 2, no. 1 (2018): 1-9.

[4] Krzyszczyk, Paulina, Rene Schloss, Andre Palmer, and François Berthiaume. "The role of macrophages in acute and chronic wound healing and interventions to promote pro-wound healing phenotypes." Frontiers in physiology 9 (2018): 419.

[5] Fujiwara, Nagatoshi, and Kazuo Kobayashi. "Macrophages in inflammation." Current Drug Targets-Inflammation & Allergy 4, no. 3 (2005): 281-286.

[6] Boniakowski, Anna E., Andrew S. Kimball, Benjamin N. Jacobs, Steven L. Kunkel, and Katherine A. Gallagher. "Macrophage-mediated inflammation in normal and diabetic wound healing." The Journal of Immunology 199, no. 1 (2017): 17-24.

[7] Dodane, Valérie, and Vinod D. Vilivalam. "Pharmaceutical applications of chitosan." Pharmaceutical Science & Technology Today 1, no. 6 (1998): 246-253.

Coming to the University of Memphis from Pittsburgh, Pennsylvania, Ethan Costello is a double major student in the Department of Electrical and Computer Engineering at the Herff College of Engineering since Fall 2019. In conjunction with his double major, he is a student in the Helen Hardin Honors College. Ethan is expected to graduate in Spring 2023. He has been working as a research assistant in the Optical Imaging Research Laboratory with Dr. Ana Doblas. During his time in the lab, he discovered more about his research interests in imaging and sensing. Ethan is also planning to work with Dr. Eddie Jacobs to become more exposed to complicated sensors and sensor processing. After graduating, Ethan plans to pursue graduate school in electrical engineering.

This paper received a QuaesitUM outstanding paper award.

Ethan Costello & Ana Doblas

Two-Way Pepper Ghost Tunnel: Theory, Design and Analysis

Faculty Sponsor

Dr. Ana Doblas

Abstract

Three-dimensional (3D) displays allow users to experience 2D images/videos in-depth illusions. Among the different 3D displays, we can distinguish the Pepper ghost illusion, which is a common approach to create a 3D hologram without goggles. In this work, we have upgraded the conventional Pepper ghost illusion, named as the two-way Pepper ghost tunnel, to create two simultaneous holograms. Contrary to the conventional Pepper ghost, the Pepper ghost tunnel requires two liquid crystal displays (LCDs), which are controlled by the same Arduino, to illuminate a 45-deg transparency sheet in both directions, allowing two different holograms to be viewed from each side of the tunnel. We have described a practical procedure for building the apparatus and validate its performance. Due to the simplicity of the apparatus, the Pepper Ghost tunnel allows undergraduate students to increase their knowledge in geometrical Optics and its integration with electrical circuits.

Introduction

Holography is an imaging technique that creates an optical illusion to transform two-dimensional (2D) images into 3D perspective. For example, one of the most famous holographic examples within media entertainment is the fictional hologram of Princess Leia from the Star Wars saga. 3D free-standing holograms like Princess Leia's hologram are still costly methods with contemporary's technology, reducing its applicability. The majority of low-cost methods of generating 3D illusions from 2D images used simple concepts of Optics. For example, anaglyph glasses are based on the stereoscopic 3D effect, color encoding two laterally shifted images of the same scene [1, 2]. In other words, anaglyph 3D images are composed of two differently colored images (e.g., red versus cyan) in which each of these images is only perceived by an eye. The 3D images are created by our visual cortex of the brain which realizes that both images are from the same scene and composes them into a 3D scene [3]. The principle of combining two laterally shifted images is also used in the polarizing goggles in which the color filters have been replaced by circular polarizers [4, 5]. Whereas monochrome 3D scenes are created using anaglyph glasses, the polarizing goggles generate full-color 3D scenes.

The use of stereoscopic-based goggles may lead to some user's discomfort such as mild migraines. The Pepper Ghost technique is an approach to create 3D illusions but without using goggles [6], being more user-friendly compared to the polarizing goggles. The Pepper Ghost technique is based on Snell's law [7] in which 2D images are reflected using a transparent sheet set at a 45-deg angle (Figure 1). Only users located in one side of the transparent sheet can observe the hologram. In this work, the traditional Pepper Ghost method has been upgraded to include an extra LCD to illuminate the transparency sheet from above, creating two distinct holograms that can be viewed individually from both sides of the tunnel. This preliminary work will enhance the 3D hologram experiences in media entertainment and gaming venues.

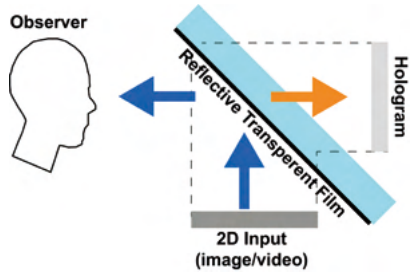

Figure 1. Illustration of the traditional Pepper Ghost method to create holographic images (e.g., hologram) from 2D images based on Snell's law.

Theory of the Two-Way Pepper Ghost Tunnel

The traditional Pepper Ghost hologram (Figure 1) uses the optical principle of Snell's laws [7]. These laws describe the phenomenon of reflection and refraction of light propagating within different uniform media, such as water, glass, or air. In particular, these laws are mathematical formulas to estimate the angles of refraction and reflection based on the angle of incidence. Figure 2 illustrates both phenomena such as refraction and reflection. The Snell's laws are used to ray tracing the optical path knowing the angle of incidence or refraction as well as to estimate the refractive index of a material. It is important to mention that the refraction index of a material is an unitless optical parameter that compares the speed of light traveling through the material and vacuum (e.g., air). These laws state that: (1) the angle of refraction is directly related to the incident angle (see Figure 2a), and (2) the angle of reflection is equal to the incident angle of the light (see Figure 2b). The refraction law states that the ratio of the sines of the angles of incidence (θ1) and refraction (θ2) is equivalent to the reciprocal of the ratio of the indices of refraction. In other words:

$$\frac{\sin\theta_1}{\sin\theta_2} = \frac{n_2}{n_1}.$$

The refraction law is also satisfied in meta-materials, which allow light to be bent backward at a negative angle of refraction with a negative refractive index. The Pepper Ghost effect is related to the backward refraction law, which is the refraction law [7] in the opposite direction. This means that a transparency sheet set at an angle of 45-degree can create a perfect replica of the image displayed on an LCD, creating the illusion of an image floating in the air. Note that, actuality, the image has been only refracted off by the transparency sheet. The use of a 45-deg transparency sheet ensures that the size of the holographic images coincides with the size of the projected imaged onto the LCD. Other angles could lead to an optical magnification or demagnification.

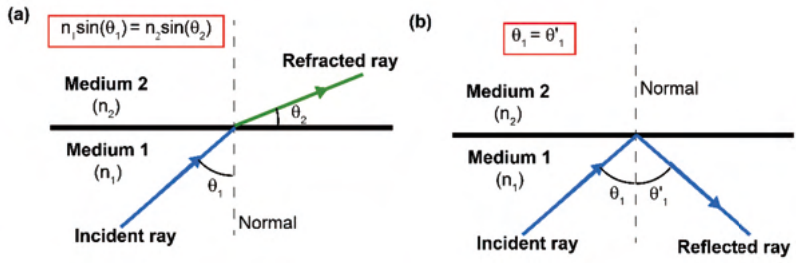

Figure 2. Illustration of the Snell's law: (a) refraction and (b) reflection.

In the design of the tunnel, an additional LCD that is located above the transparency sheet has been added (Figure 3). Since two LCDs are used, the transparency sheet creates two holograms. However, these holograms appear only in one side of the Pepper Ghost device since the transparency sheet refracts the image in different direction depending on which the location of the LCD. In other words, the bottom LCD (named as LCD 1 in Figure 3) refracts the image at a 45-degree angle to the right and reflects it at a 45-degree angle to the left, enabling the observation of the hologram in the left-side of the display. Consequently, the hologram created by the top LCD (e.g., LCD 2 in Figure 3) is only observed from the right-side of the display. Therefore, the use of two opposed LCDs in a traditional Pepper Ghost configuration generates two separate holograms, enabling their distinct observation from the two sides of the device (e.g., creation of a tunnel effect).

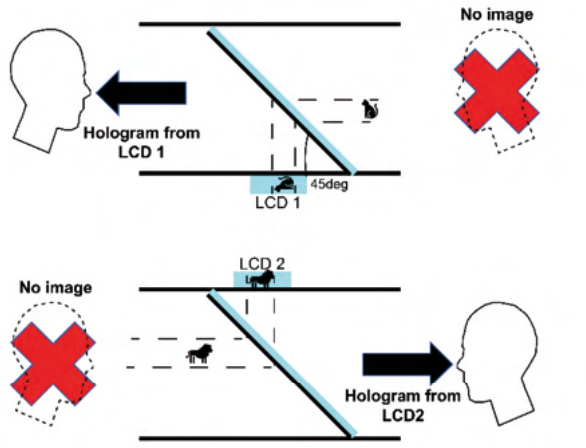

Figure 3. Illustration of the proposed Pepper Ghost tunnel. The observation of each generated hologram occurs in different side of the display (e.g., the hologram displayed by LCD1 and LCD2 is observed from the left-, and right-side of the display, respectively).

Design of the Two-Way Pepper Ghost Tunnel

This section focuses on the description of the design of the prototype of the Pepper Ghost Tunnel (Figure 4). To do this, we have used two liquid crystal displays (LCDs, product item 1480, Adafruit) that are controlled by the same Arduino board (ELEGOO UNO R3). This board is powered by two AA batteries to DC power supplies. The LCDS and the board are connected using a single breadboard and various breadboard jumper wires. Since the Arduino board that we have used for this project does not have enough pins to control more than one LCD at a time, both LCD display the

same sequence of images, generating the same hologram. To create a stable connection to the displays and avoid any loss of images, we have soldered the wires directly to their inputs/outputs. All the electrical components are properly enclosed in blackened cardboard for security reasons.

This experiment could be design as a STEM kit to introduce kids to Optical Engineering, through the hands-on experience of building their first holographic display. The total cost of the material for the Pepper Ghost tunnel sums to approximately $106, the two LCDs being the most expensive parts (2 x $24.95 = $49.90, which is nearly 47% of the total). The transparency sheet used is a regular low-cost transparency film for inkjet printers. This price can be lowered by buying cheaper LCDs, which may lead to worse image quality. Another approach to reduce the cost involves the purchase large volumes of components. For example, the same LCDs could cost 25% if we purchase more than 100 displays. The cost of STEM kits varies from $20-$150. Therefore, a significant reduction in the project cost is necessary to develop a commercial STEM kit.

Figure 4. Experimental prototype of the Pepper Ghost Tunnel using cardboard to enclose the transparency film and the two opposed LCDs. The total size of the prototype is 101.6×241.3×190.5mm (Width×Height×Depth).

Experimental Validation

For the sake of simplicity and to prove the concept, the programming used in our model is the default LCD testing script provided by Adafruit. This script runs through a series of images, text, and video that are created using lines, circles, and triangles to test each pixel of the display. During the design of the prototype, this script has helped us to realize that the displays were disconnecting since they were not displaying the full length of the test images, allowing us to take the decision that soldering of the wires was needed.

This testing script was also used to confirm that the LCDs connected in series could display synchronized video. Therefore, this basic code allowed us to test the electrical components as well as to validate our design concept to upgrade the traditional Pepper Ghost illusion into the proposed Pepper Ghost tunnel. Figure 5 shows the experimental validation of the tunnel effect of the proposed device. This figure illustrates a selected set of displayed images on the LCDs (first column) and the pictures of the generated holograms from each side of the tunnel (second and third column). These images prove that it is possible to view images from both sides of the tunnel without the interference of the other side's hologram.

One can also notice that there is a slight distortion in the hologram images when compared to their originals. In particular, this distortion is more noticeable in the hologram generated by the top LCD. This distortion may be caused by a combination of experimental misalignments between the position of the top LCD and the transparency sheet. Another problem of this prototype is that the holograms are distorted by a severe glaring effect coming from the LCDs, reducing the image contrast of the holograms. A future prototype would involve the design of the device using a 3D-printing house, improving the alignment of the components.

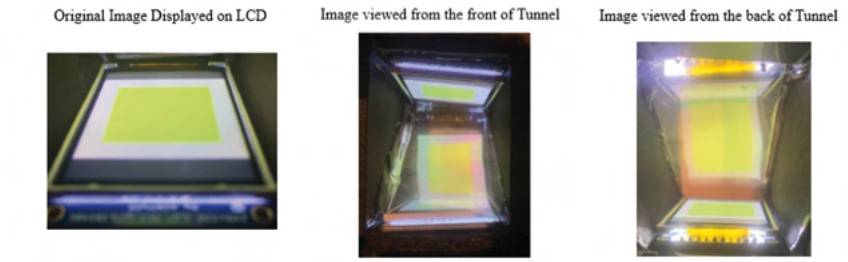

Figure 5. Experimental validation of the proposed Pepper Ghost Tunnel. The first column shows the images displayed on LCDs. The second column illustrates the hologram generated by LCD1 and observed in the left-side of the display. The third column shows the hologram generated by LCD2 and observed in the right-side of the display.

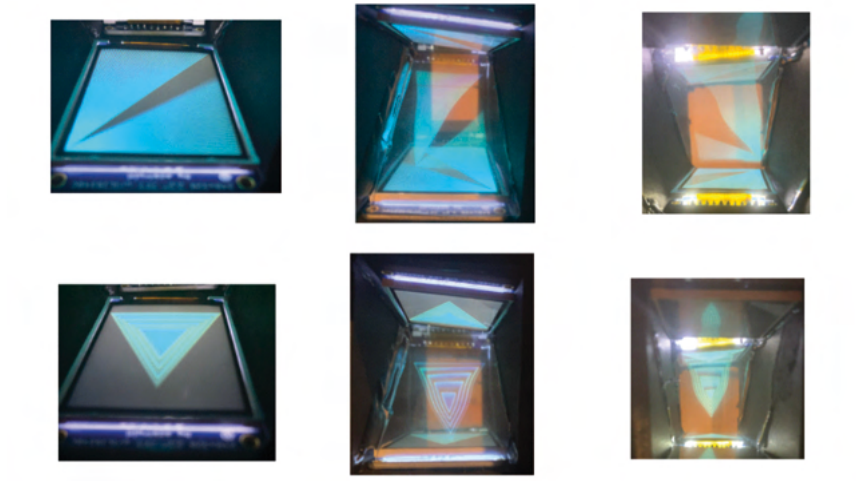

Figure 5. continued.

Discussion and Conclusion

In this work, the traditional Pepper Ghost illusion has been upgraded to create a tunnel effect by introducing an additional LCD. The working principle of the Pepper Ghost tunnel is that both LCDs should illuminate the transparency film in opposed direction, generating distinction holograms in each side of the device. Since we have used a single Arduino to control both LCDs, the two generated holograms display the same image with a reflection along the vertical direction. The performance of the experimental prototype has been evaluated with a sequence of basic images, demonstrating successfully how to expand the idea of the single-view Pepper Ghost illusion to a pair of holograms viewed from each side of a tunnel. The features (size and resolution) of the holographic displays depends on the LCDs used. For example, the size of the holographic image depends on the number of pixels on our LCDs.

The resolution of the holographic images is defined by the minimum separation between two distinguished image features. Experimentally the resolution can be determined by displaying a sinusoidal pattern whose frequency increases and estimating the maximum spatial frequency that we can display. The maximum spatial frequency is the inverse of the minimum spatial period of the sinusoidal pattern. Following the Nyquist sampling theorem, the minimum spatial period of a sinusoid is 3 pixels. Based on the manufacturer's information, the pixel size of our LCDs is 18.67 μm, resulting in a spatial resolution of 56.01 μm. Whereas this is the strict definition of the resolution in the holographic image, it is important to mention that the

perceived resolution also depends on the pixel depth of the LCDs. In other words, a perceived color is related to a given intensity values. Whereas an 8-bit LCD only provides 256 different colors to display an intensity value, an 18-bit LCD enables a more accurate representation of intensity values (up to 2^{18} = 262,144), displaying images with a higher contrast (e.g., difference between the maximum and minimum intensity values). Therefore, the perceived resolution is highly dependent on the based on the pixel depth of the LCDs.

Theoretically, the physical and perceived resolution should not be affected using colored LCDs instead of monochrome ones. One of the major problems of the prototype is the presence of a high intense glare, reducing the contrast of the generated holograms. This glare effect can be reduced by using a better transparency sheet or introducing a single or a combination of linear polarizers set at a specific angle to reduce the amount of glared light. Further improvements of the current prototype also may involve the design of a 3D- printed housing for the electronics, the screens, and the transparency sheets, which would improve the setting of the transparency sheet at 45 degrees by sliding it into a predetermined slot. It would also allow us to replace the sheet in case of breakage or for cleaning purposes. In addition, the design of the 3D-printed cage would allow us to insert the LCDs, hiding them with indentation, reducing the glare problem.

Having a 3D-printed housing would further help us to create a darker environment, improving the contrast of the generated holograms and enhancing the experience of the optical illusion. It may also be possible to enhance the resolution of our system by finding an improved LCD, however we believe that we have found the most cost-efficient option in terms of quality and price of an LCD. Although there are other devices to create holographic displays, only the reflective prism-based Pepper Ghost device [8] and the Pepper Cone [9] provide a similar effect as our Pepper Ghost Tunnel. The reflective prism-based Pepper Ghost device relies on the 2D projection of four images onto the sides of a prism.

The main limitation of such device is the size of the images, since the area of a display must be separated into 4 regions, generating images with reduced size. In contrast, the Pepper Cone only requires a single image. To generate 3D holographic images without any distortion, it is necessary an extensive calibration of the system. Note that such calibration is not required in our device. The main problem of these two versions of the Pepper Ghost is that they do not generate 3D images with real parallax. Parallax is the perceived effect when the distance between two 3D objects changes when we move our heads. The proposed Pepper Ghost Tunnel can potentially be improved by inserting additional transparency sheets in tandem with their

corresponding pair of LCDS, leading to the first 3D parallax Pepper Ghost Tunnel.

This project is under development and has been submitted to the upcoming Imaging and Applied Optics Congress host by OSA. We envision that such Pepper Ghost Tunnel could be widely use in museums to display simultaneous 3D holograms. In addition, the integration of such system with audio and interactive screens would enhance the 3D experience for visitors. Another potential application of such system is in gaming venues as potential gaming monitors.

Acknowledgements

Doblas acknowledges the support from the National Science Foundation (NSF, # 2042563), the University of Memphis, UMRF Ventures, and the Herff College of Engineering.

References

[1] D'Almeida, Joseph Charles (1858). "Nouvel appareil stéréoscopique" [A New Stereoscopic Device] (image). Gallica (Lecture) (in French). p. 61.

[2] Picard, Emile (December 14, 1931). "La Vie et L'œuvre de Gabriel Lippmann (membre de la section de physique générale)" [The Life and Work of Gabriel Lippmann] (PDF). academie-sciences.fr (Public Lecture) (in French). Institut de France. Académie des Sciences. p. 3.

[3] Finlayson, Nonie J., Zhang, Xiaoli, Golomb Julie (February 2017). "Differential patterns of 2D location versus depth decoding along the visual hierarchy." NeuroImage. 147: 507. doi: 10.1016/j.neuroimage.2016.12.039

[4] Make Your own Stereo Pictures Julius B. Kaiser The Macmillan Company 1955 page 271 Archived 2011-02-26 at the Wayback Machine

[5] Cowan, Matt (5 December 2007). "REAL D 3D Theatrical System" (PDF). European Digital Cinema Forum. Archived from the original (PDF) on 10 September 2016. Retrieved 5 April 2017.

[6] Shein, Esther (July 2014). "Holographic Projection Systems Provide Eternal Life". Communications of the ACM. 57 (7): 19–21. doi:10.1145/2617664. S2CID 483782.

[7] Hecht, E. Optics 4th. ed (Addison Wesley, 2002)

[8] Doyle, Christopher. (2017, January 1) Reflective Prism using Pepper Ghost [Video]. YouTube https://youtu.be/NYrcLK9NYZI

[9] Luo, Xuan, Lawrence, Jason & Seitz, Steven M. (2017). Pepper's Cone: An Inexpensive Do-It-Yourself 3D Display. In Proceedings of the 30th Annual ACM Symposium on User Interface Software and Technology (UIST '17). Association for Computing Machinery, New York, NY, USA, 623–633. DOI:https://doi.org/10.1145/3126594.3126602

Justin L. Brutger graduated from Drake University in the spring of 2022, obtaining a Bachelor's of Science with a major in Physics and Mathenatics, and a minor in Computer Science. His main interests are theoretical phyics and computational physics. He was awarded the Drake Physics Prize scholarship in 2018 and conducted undergraduate research at the University of Memphis in 2021. Currently his future plans involve pursuing higher education in the form of a Ph.D.

Justin Brutger

Si2Te3 Dimer Orientation Structure

Faculty Sponsor

Dr. Xiao Shen

Abstract

Experimental material data can often be lacking; reasons include lack of interest, as well as lack of feasibility. This lacking can be made up for through computational modeling, which is less costly and time consuming than experimental testing. The aim of this study was to examine the unique structure of Si2Te3 and to determine possible phase transitions that result from the orientation behavior of the silicon dimers that comprise the compound. Results showed the continuation of near absolute zero behavior up to a sudden phase transition occurring around 50° K. This was followed by a more gradual phase transition starting at 200° K that continued until the sudden transition at 623° K noted by prior research that renders the study's implemented model physically irrelevant. A degree of dimer organization was maintained at all temperatures up to the model limit of 623° K.

Introduction

There is a near limitless amount of possibilities when it comes to the design of material research experiments. However, due to the finite resources and time available to researchers, experiments must be chosen pragmatically; the costs and projected benefits of experimental research into a given material must be weighed in order to make a proper choice of study. For this purpose computational physics proves invaluable. Simulating physical phenomena in material provides a resource light alternative to experimental research that can provide insight into potential discovery. It effectively produces strong hypotheses to motivate experimental research. This study was founded on a similar motive. The behavior of silicon dimer orientations in Si2Te3 is poorly studied in experimental research. This dissatisfaction is further compounded by a disagreement between experimental and computational studies concerning the composition of dimer orientations [1-3]. The perceived lacking in experimental research and the disagreement with recent computational research provides the basis for this study is motivated.

Si2Te3 naturally forms in a unique configuration consisting of a hexagonal lattice of tellurium atoms, with two out of every three hexagons being filled with a pair of bonded silicon atoms [2,3]. This silicon pair, called a dimer, can occupy one of four different orientations as shown in Figure 1. These lattices then stack to form multilayered structures. This structure is fairly unique, making research lack commonality with other materials.

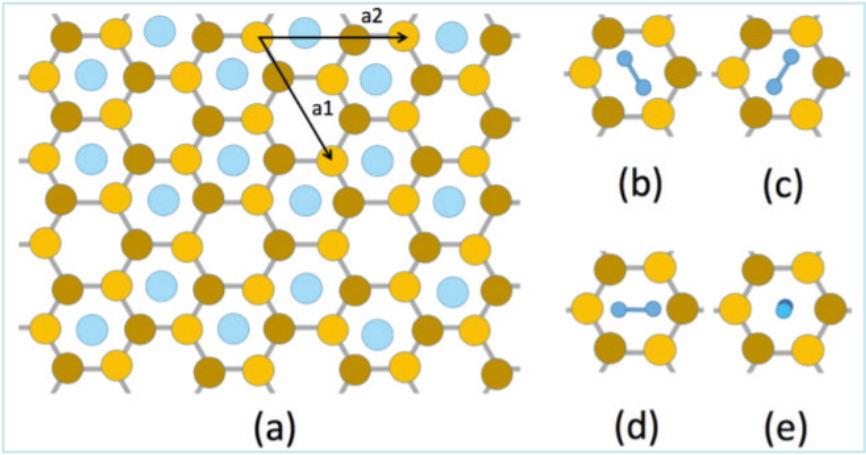

Figure 1: (a) A diagram of a Si2Te3 lattice. (b-d) The three in-plane dimer orientations. (e) The out-of-plane dimer orientation. [1]

X-Ray and electron diffraction experiments indicate an equal distribution of the four orientations among all dimers [3]. However, recent computational research has indicated a temperature dependence of the orientation distribution that doesn't align with the diffraction experiments [1]. It is most likely that the highly perturbative nature of the experimental methods excites the dimers and leads to this discrepancy. It is this discrepancy and computational research that this study is based upon. The goal is exploratory; to study the distribution of dimer orientations at various temperatures up to the phase transition temperature of 623° K where the dimers disassociate, and the silicon atoms cease to pair.

Methods

Application of Monte Carlo

The dimer orientation behavior of a single sheet of Si2Te3 was determined through the Metropolis Monte Carlo method. It is a statistical method used to find the average behavior of a system through a statistical sampling of system states. The set of all system states is treated as a Markov chain, with the probability of transitioning from one state to a neighboring perturbation being equal to the ratio of the weights of the two states. The sampled states were chosen by attempting random perturbations of the state and accepting the new perturbed state based on the transition probability in the Markov chain. The weighting function for the states was chosen in the study by treating the Si2Te3 system as a canonical ensemble. Due to this choice, any measurable calculated using this method is an approximation of the expectation value of the measurable. [4]

Choice of measurables

Two aspects of the dimer layout were chosen for examination. The first was the total system energy or Hamiltonian. Since the stored energy in the system comes exclusively from the interaction of neighboring mismatched dimer orientations, this serves as a rough benchmark for the disorder present in a given state. The second aspect was the layout of connected regions of like orientations. The ability of the dimer orientations to organize into distinct regions is a significant indicator of order and contains information the Hamiltonian does not detail, thus warranting observation. The specific observables measured for the simulation were the Hamiltonian, the number of major connected regions, the average region size by orientation, and the average centers for connected regions. Major regions were chosen to be those large enough to not be considered minor chance fluctuations, and thus required to contain at least 5% of the total number of dimers.

There were three metric scenarios considered for comparison. The first was the completely ordered scenario; here all dimers are aligned in parallel. This is the simplest scenario that occurs at 0° K and similar low temperatures. The second is the completely disordered scenario where all dimers are equally likely to be in any state. The last scenario is the disordered scenario where all dimers are equally likely to be in any in-plane orientation. This last scenario was included for comparison due to the much larger energy contribution the out-of-plane (OOP) orientation caused when interacting with in-plane orientations [1].

Results

For the simulation a ten-by-ten Si2Te3 lattice was used. Larger lattices showed identical behavior but ran at exponentially higher times to produce similar quantities of data. The measurables of the metric scenarios are shown in Table 1 and were used to benchmark the system behavior at various temperatures.

	Hamiltonian (meV)	Major regions	Average region size of present orientations (% of all dimers)
Ordered	0	1	100%
Disorded	1674	2.17	2.2%
Mostly Disordered	350	3.7	2.65%

Table 1. Measurable values of the three metric scenarios.

The Hamiltonian was determined over the range of relevant temperatures and experienced a sudden rise between 30° K and 70° K, followed by a period of constant growth before accelerating again gradually starting at 200° K. This is shown in Figure 2.

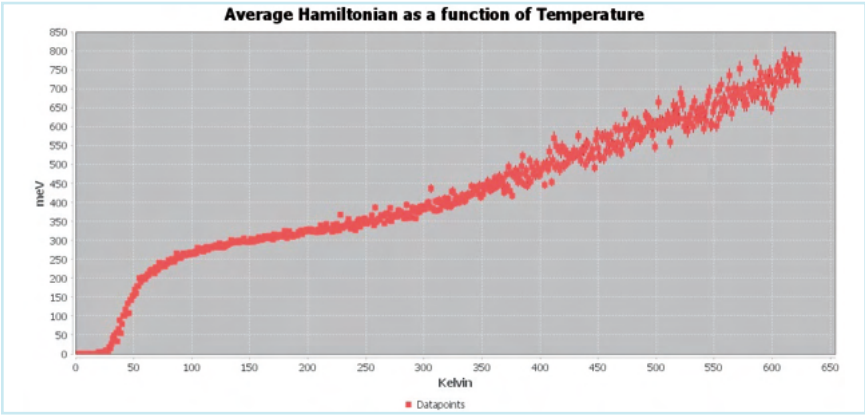

Figure 2. System Hamiltonian behavior over temperature

The number of major regions showed a similar sudden transition in behavior between 30° K and 70° K, but no additional behavior past 200° K. This is shown in Figure 3.

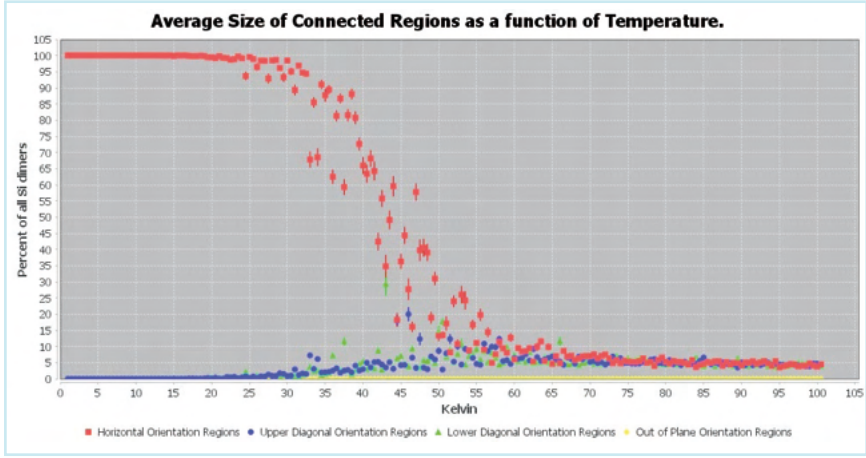

Figure 3: System major region count over temperature

The sudden behavior change between 30° K and 70° K is continued in the average region size behavior; during this temperature range misaligned orientations begin to be prevalent. Similarly at 200° K the out of plane orientation starts to become prevalent, but not prior. Two graphs of the behavior are shown in Figures 4 and 5; 5 contains a higher temperature resolution calculation of the 30° K to 70° K range.

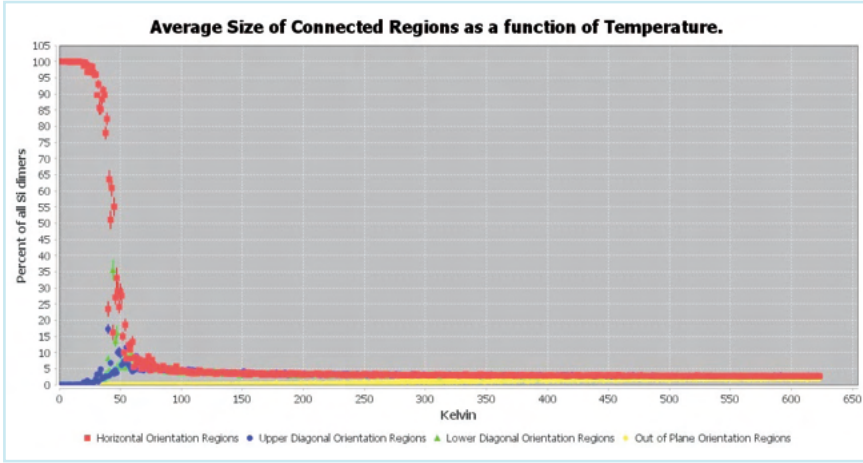

Figure 4: System region size behavior over temperature

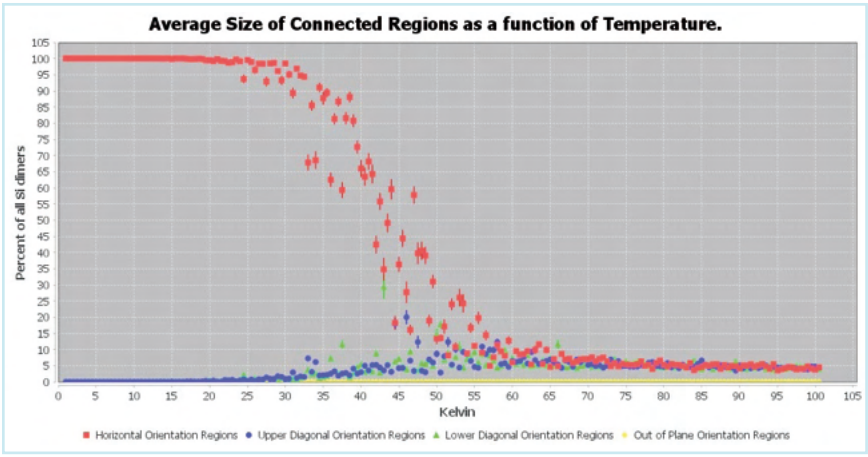

Figure 5: System region size behavior over temperature

Additional unexpected behavior was found when measuring the average connected region centers. When perturbations in the ordered metric scenario begin to be prevalent, they usually are clustered around the sides of the lattice. This similarly occurs for the OOP orientation when it becomes prevalent at around 200° K. After each of these initial periods of growth from the side perturbations become more prevalent in the middle of the lattice. This first insulting effect is shown in Figure 6, and second one in Figure 7.

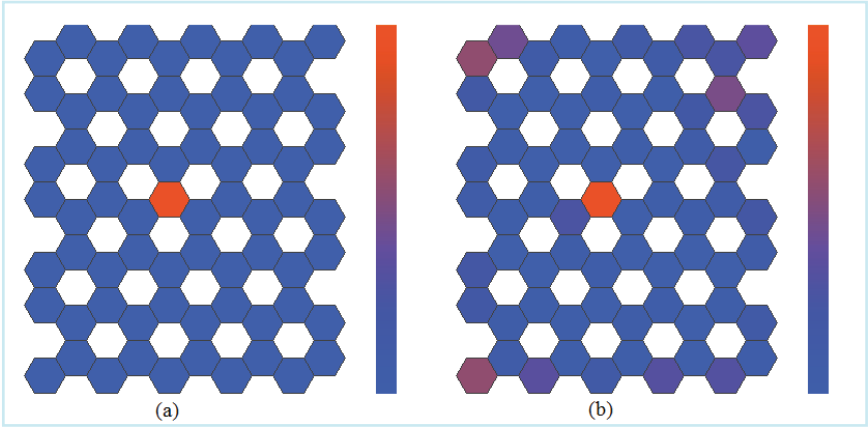

Figure 6: Heatmaps of region centers over the course of Monte Carlo sampling at various temperatures. (a) 10° K, 100 counts (b) 35° K, 55 counts.

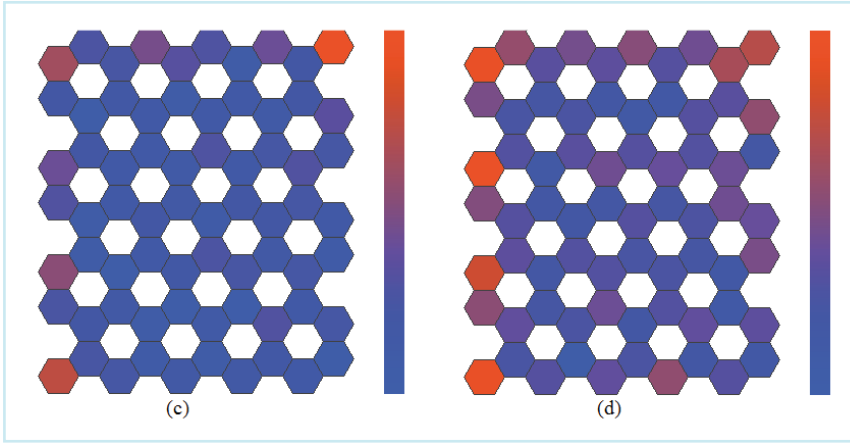

Figure 6 (continued): Heatmaps of region centers over the course of Monte Carlo sampling at various temperatures. (c) 50° K, 65 counts (d) 60° K, 55 counts. (c) 50° K, 65 counts (d) 60° K, 55 counts

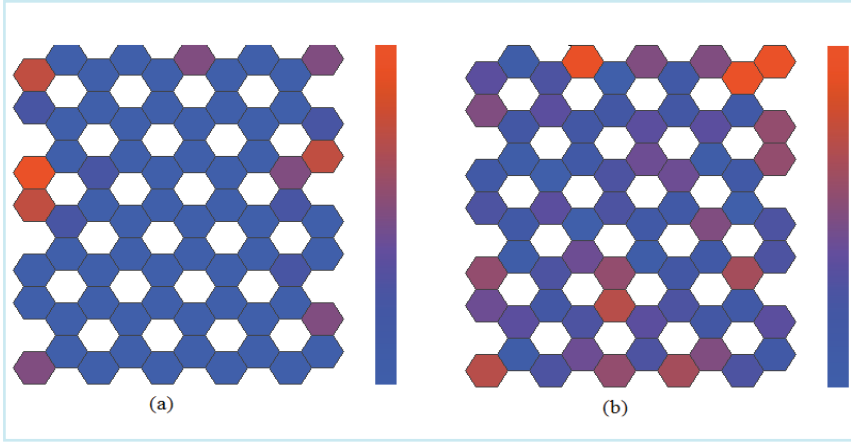

Figure 7. Heatmaps of out of plane (O.O.P.) orientation region centers over the course of Monte Carlo sampling at various temperatures. (a) 225° K, 4 counts (b) 585° K, 14 counts

Discussion

Two phase transitions can be observed: one centered at 50° K and another gradual transition starting at 200° K. The ordered, or 0° K, scenario is maintained closely up to the sudden first transition. This first transition occurs due to the temperature being high enough to allow misalignments to become commonplace. Additionally, the second transition occurs when the temperature is high enough that the OOP dimer orientation, which requires the most energy, can occur, although not frequently. Both the

completely disordered and in-plane disordered scenarios are not reached at any temperature. Some measurables are reached, such as the Hamiltonian, but never all. This implies that at all temperatures up to the known dimer dissociation transition at 623° K the dimer orientations never truly randomize. Additionally, these phase transitions are accompanied by an insulating effect where in the early stages of each transition perturbations in the status quo mostly appear on the edges of the lattice.

Two primary sources of error can be identified as part of the Monte Carlo method. The first is the standard deviation in the measurable that is averaged from the sampled states. This was dealt with by increasing the sampling size, but the downside of increased calculation time made large lattice calculations time consuming. The second error source is from domain boundaries. Since the sampled states are more likely to perturb towards the lower energy states of their neighbor perturbations, it is possible for sampled points to become trapped in a local minimum. This can cause multiple identical Metropolis Monte Carlo simulations to return measurables with very small standard deviations, despite having large differences between them. This is the error source causing the large spread observed in the later temperatures of Figure 2 and 3, as well as the phase transition shown in Figure 5. In this case the only solution would be to increase the lattice size in order to make local minimum trapping less likely. Since the spread caused by this was not enough to obscure the overall behavior, this was not an issue of concern in the study. In future work comparing the results to experimental data, quantitative fits of these curves will be necessary, and thus greater precision that was not needed here will be required.

Conclusion

Two proposed phase transitions for Si2Te3 in the low temperature range have been calculated using statistical methods. Since the orientation of a dimer causes a perturbation in the surrounding tellurium lattice, and thus affects the expansion of the material, it is possible that these transitions can be observed on the macro level by a varying coefficient of thermal expansion due to the varying prevalence of orientations and a non-uniform expansion throughout the material due to the insulating effect [1]. Since the results are concerning a single layer of Si2Te3, additional study is required to determine similar behavior in multilayer samples.

There were three metric scenarios considered for comparison. The first was the completely ordered scenario; here all dimers aligned in parallel. This is the simplest scenario that occurs at 0° K and similar low temperatures. The second is the completely disordered scenario where all dimers equally

likely to be in any state. The last scenario is the disordered scenario where all dimers was equally likely to be in any in-plane orientation. This last scenario was included for comparison due to the much larger energy contribution the out-of-plane (OOP) orientation caused when interacting with in-plane orientations [1].

Funding

This research was supported by the NSF Graduate Research Fellowship Program.

References

[1] X. Shen, Y. S. Puzyrev, C. Combs, and S. T. Pantelides. "Variability of structural and electronic properties of bulk and monolayer Si2Te3", Applied Physics Letters 109, 113104 (2016)

[2] K. Ploog, W. Stetter, A. Nowitzki, and E. Schönherr. Mater. Res. Bull. 11, 1147 (1976).

[3] P. E. Gregoriades, G. L. Bleris, and J. Stoemenos, Acta Crystallogr., Sect. B 39, 421 (1983)

[4] Pang, Tao. “Monte Carlo Simulations.” An Introduction to Computational Physics, 2nd ed., Cambridge University Press, pp. 285–297.

Julian Lopez is a first-generation Latino student and OUS Scholar at Colgate University, a current junior, and will graduate in the spring of 2023. He is planning on obtaining a bachelor's degree in physics from Colgate University and participating in a Pre-Engineering program that will allow him to obtain a bachelor's degree in engineering at Washington University. Julian's future goal is to become a Mechanical Engineer and help his community through. The research for this paper was done through a Research Experience for Undergraduates (REU) program in association with the University of Memphis. Activities that Julian enjoys are playing volleyball, attending Physics Club, and leading the student population at his university through outdoor activities including mountain biking, ice-climbing, and kayaking.

Julian I Lopez

High-quality Few-layered MoS2 Thin Films through Plasma-enhanced CVD

Faculty Sponsor

Dr. Shawn Pollard

Abstract

As a 2D material, Molybdenum disulfide (MoS2) has been attracting attention due to its electrical, optical, mechanical, and possible magnetic properties that can be used in a wide variety of applications. However, precise control of monolayer thickness and high-quality growth is still a huge challenge with multiple methods. In this paper, we have successfully grown predominately few-layered MoS2 on nearly lattice-matching muscovite mica by using a plasma-enhanced low-pressure chemical vapor deposition (PELPCVD) method. The approach presented here synthesizes films in 15 minutes using sulfur powder (S) and molybdenum trioxide powders (MoO3) as precursors. Deposition utilizes a nonthermal plasma reactor and temperatures ranging from 500 °C to 600°C. Thin film growth characteristics and nucleation are studied as a function of argon flow rate, plasma, and temperature using SEM, AFM, XRD and Raman spectroscopy.

Introduction

Recently, ultrathin two-dimensional (2D) layered materials have captivated the nanoelectronic, spintronic, and valleytronic scene because of their availability to a wide variety of applications. The electrical, mechanical, optical, and magnetic characteristics of these materials are the epicenter of the attracted attention because of their dependence on overall structure and thickness [1]. This dependence on structure and thickness also constitutes them to be transition-metal dichalcogenides (TMDCs). With respect to structure, these atomically thin materials have adjacent layers that are subject to van der Waals (vdW) forces that hold them together [2].

Aligning with this research, molybdenum disulfide (MoS2) has extraordinary properties including a tunable bandgap, high tensile strength, thermal stability, and extreme flexibility that would make them the perfect candidate for devices such as photodetectors, solar cells, and light-emitting diodes [3]. The flexibility aspect of this material is mirrored with mica that not only has continuous flexibility itself but also has a lattice structure well-suited for the growth of few-layer MoS2 growth on the surface. Specifically, muscovite mica, which is used in this research, has a lattice constant in the (001) plane of 0.5199 nm. In comparison to MoS2, the lattice constant, a, is 0.3161 nm. The lattice constant of mica closely approximates $\sqrt{3}$ a, which equals to 0.5475 nm, with an approximate -5% lattice mismatch with MoS2 [4]. This means that an approximately 30-degree rotation of the MoS2 2 lattice leads to a commensurate structure with the mica substrate and promotes epitaxial growth. There are various other forms of mica that would provide a high-quality match; however, the cost outweighs the more favorable comparability which could limit their use in applications. For example, fluorophlogopite mica has a lattice constant of 0.5309 nm, a 2% better match than muscovite mica, but has a market price of 4-5 times higher. Apart from the previously mentioned devices, MoS2 on mica could also be used for technology where flexibility is key.

The electronic sphere continues to grow and the ultimate desire to create smaller, faster technology exponentially increases. This continual process of betterment is the primary rationale as to why these 2D materials are so important for the advancement of technology. The successful growth and creation of these materials with fascinating characteristics can lead to new generational multifunctional electronic and spintronic devices. A crucial progression in digital-analog applications is advancing the functional integration of electronics and logic circuits, which could easily be solved using ultrathin 2D materials [1].

Most of the materials that are already being used as 2D semiconductors and other devices were produced with the mechanical exfoliation method. This method results in poor control of thickness and domain size, which leads to restrictions in fundamental characteristic examination [1]. The size and quality of the materials produced in this manner are a cause of concern for the applications that they may be used for. Regarding this issue, chemical vapor deposition (CVD) is the perfect substitution because it provides a controllable way to grow high-quality and large-area 2D materials [5]. Specifically, low-pressure CVD (LPCVD) produces a dramatic increase in uniform growth rate and reduces overall auto-doping, which is the introduction of volatile impurities into the epitaxial layer that originate from the substrate [6]. In addition to LPCVD, the introduction of a plasma-enhanced variation (PELPCVD) is used to decrease the required growth temperature and time period of these 2D few-layered materials. The use of PELPCVD has the advantage of a higher deposition rate, which stated before, decreases the growth time of these materials, thereby saving time and decreasing the amount of resources used and wasted.

Qingqing Ji, Yanfeng Zhang, Teng Gao, and others took in account some of the methods described above to research thin films of MoS2 in Epitaxial Monolayer MoS2 on Mica with Novel Photoluminescence [4]. With a procedure very similar to the one discussed in this paper, the researchers were able to grow monolayered MoS2. Two of the major differences between theirs and our methods is the use of fluorophlogopite mica in the paper mentioned above and the implementation of enhanced plasma in this paper. Ji et al. grew these monolayered MoS2 on mica through LPCVD with typical growth conditions being "pressure of 30 Pa, carrier gas flow rate of 50 sccm, growth temperature of 530 °C and growth time of 30-60 min" [4]. The result was full coverage of monolayer MoS2 on mica with distinct triangles that correspond to monolayer MoS2. This research team experienced full monolayer growth around the center of their substrate and sub monolayer growth as the edge was reached, i.e., distinct triangles. These results were very similar to the ones achieved in this paper. However, I was able to improve upon the methods described by including the implementation of plasma and the use of lower-cost mica.

To understand the influence of growth conditions on the quality and uniformity of MoS2 grown on Muscovite mica using PELPCVD, various parameters, i.e., growth temperature, carrier gas flow rate, and plasma power, were systematically modified and the quality of the grown films was evaluated utilizing a variety of materials characterization techniques. The purpose of this research is to understand the dependence of MoS2 growth on the given

parameters and the impact they have on the consistent geometric shape and size configurations grown on the surface that indicate high-quality growth, i.e., triangular, and hexagonal formations.

Methods

Experimental Section

The molybdenum disulfide (MoS2) thin films were synthesized via an PELPCVD process. The thin films grown within this experiment consisted of molybdenum trioxide powders (MoO3) (99.5% Sigma Aldrich) as the molybdenum source, and sulfur powders (S) (99.5% Alfa Aesar). To initiate the growing process, MoO3 and S powders were loaded into two separate alumina combustion boats positioned at the center of the left section of a dual-temperature-zone tube furnace and the edge of the hot zone upstream, respectively. A freshly cleaved piece of muscovite mica (Grade V2 Ted Pella Inc.) was loaded directly above the MoO3 boat face down. Before the film grows, the inside of the tube furnace would be put into a vacuum by turning on a pump downstream from the precursors. In addition, the tube furnace would be purged with nitrogen to replace impurities that could influence growth. Then, the temperature of the MoO3 was increased to a series of temperatures ranging from 500° C to 600° C while the sulfur was placed just outside of the hot zone at 180° - 200° C. The argon gas flowing downstream varied from 30 to 150 sccm and was maintained for 15 minutes of growth time with the plasma turned on at 100 W. There were some samples that did not have the implementation of the plasma to establish a baseline for comparison. Finally, the furnace was naturally cooled down to room temperature. Figure 1 shows a schematic of the process used in this work.

Characterization Section

The as-prepared MoS2 thin films were analyzed by SEM (Hitachi, S-4700) with a range of magnification from 10x to 20x, XRD (Bruker, D8 Advance), Raman spectroscopy (Thermo Scientific, DXR, excitation wavelength of 532 nm) with a collection time ranging from 1 to 5 minutes, and AFM (Nanosurf CoreAFM) under ambient conditions. The thin films were also coated with 1-2 nm of Gold (Au) to prevent major drifting in instruments mentioned above.

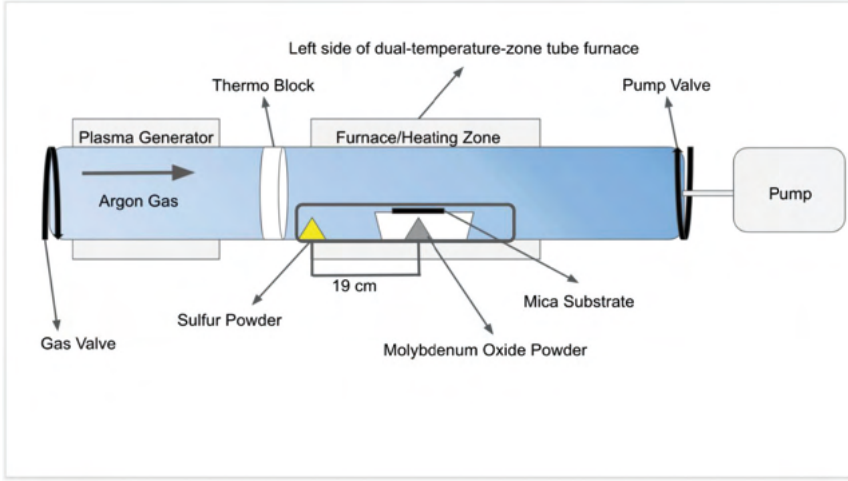

Figure 1. Schematic illustration of a CVD setup for the synthesis of ultrathin MoS2 flakes on mica on S powder and MoO3 powder as the co-evaporation sources.

Results and Discussion

van der Waal's Structure of Gexagonal MoS2

The typical process of creating Hexagonal MoS_2 through this form of CVD method is that MoO_3 is partially reduced by sulfur vapor, creating a volatile MoO_{3-x} series which is carried downstream by Ar carrier gas. It is then absorbed on mica, slowly diffuses on the surface, and reacts with sulfur to rearrange into MoS_2 layers [4].

$$S_2 + MoO_{3-x} \rightarrow MoS_2 + SO_2 \text{ [4]}$$

Figure 2 below illustrates the typical crystal structure of 2H-MoS2 through various frames of reference including a top view, a perspective view, and side views. MoS2's crystal structure consists of a hexagonal plane of S atoms on either side of a hexagonal plane of Mo atoms. These triple planes stack on top of each other, with weak van der Waal forces holding the Mo and S layers together, which is a commonality within TMDC's. These three planes form a monolayer of MoS2, which can be found in three different phases but mainly the 2H-MoS2 and 3R-MoS2 phases, where the "H" and the "R" indicate hexagonal and rhombohedral symmetry, respectively [7].

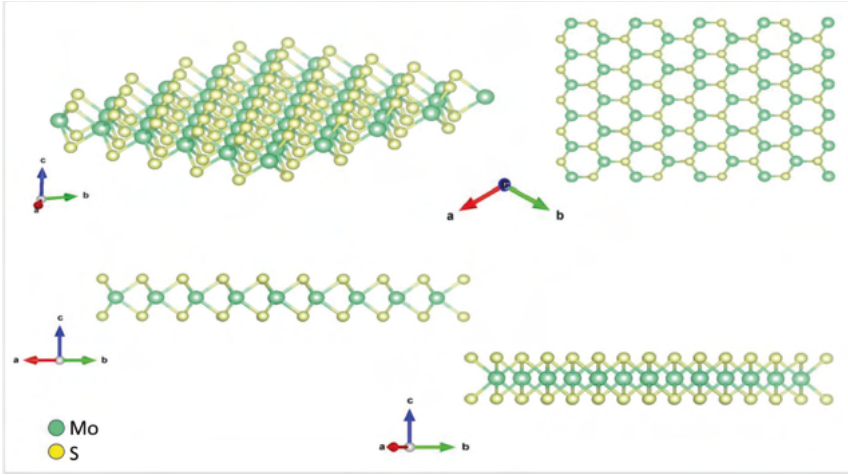

Figure 2. Structural models: perspective view, top view, and side views of the crystal structure of MoS_2.

Identification of Gexagonal MoS2

X-ray diffraction (XRD) analysis was carried out to determine the overall crystal structure of the synthesized material on the mica substrate and validate that the growth was what I desired to create: MoS2. As shown in Figure 3, the two prominent peaks of (002) and (105) were indexed to the crystal plane of 2H-MoS2, confirming that the desired growth was completed. Of the various samples that were created and examined, the position of the scattering angles rarely varied from MoS2, but frequently showed signs of other peaks as well including some MoO3 growth. As I was able to better synthesize high-quality thin-layered MoS2, the signs of MoO3 decreased but still never disappeared. The larger repeated peaks that can be seen throughout the Figure 3 are typical peaks related to the substrate mica. These repeated peaks of mica and two prominent peaks of MoO3 are highlighted in Figure 4.

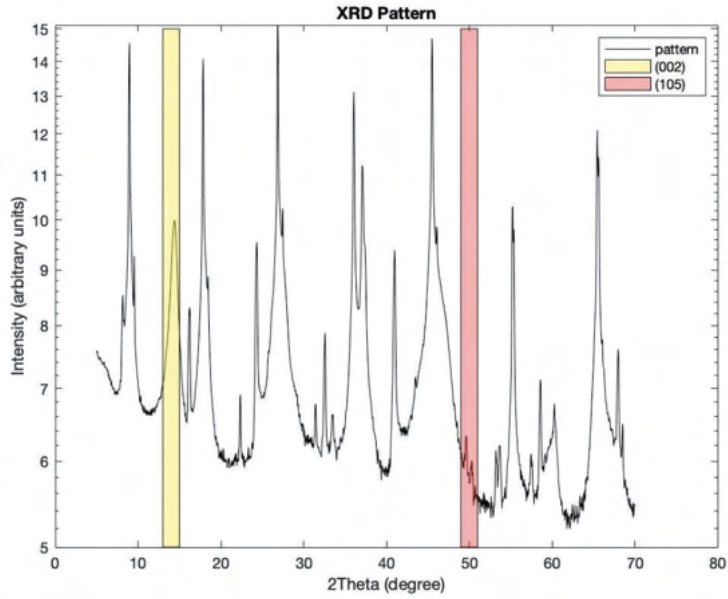

Figure 3. XRD pattern for MoS2 sample and highlighting of prominent diffraction peaks: (002) and (105).

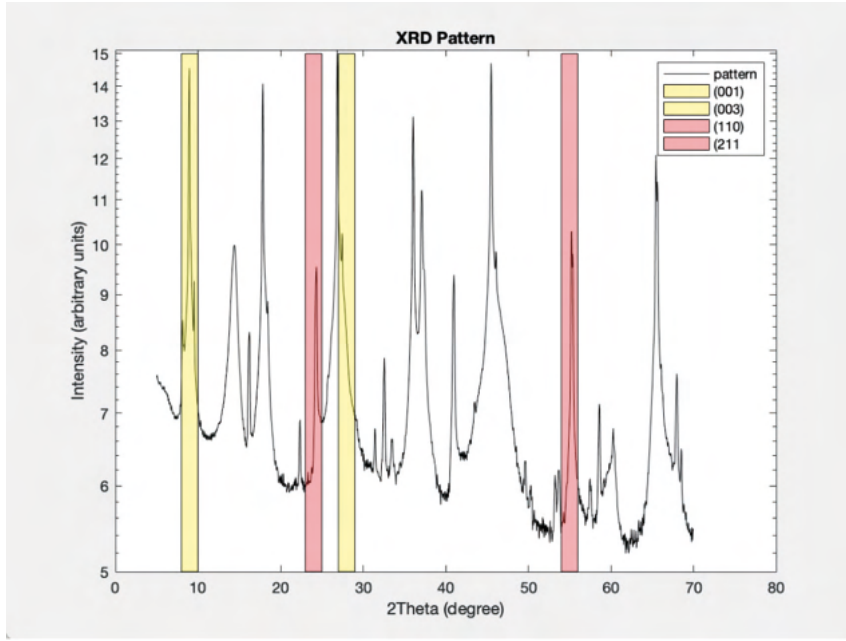

Figure 4. Same sample of MoS2 but highlighting the XRD pattern of MoO3 (red) and muscovite mica (yellow)

In addition to the use of XRD, Raman spectroscopy was also utilized to characterize the synthesized material. The ~384.0 cm-1 peak corresponding to the in-plane E2g mode and the peak at ~408.0 cm-1 in line with the out-of-plane A1g mode that characterizes MoS2 can clearly be seen in the Raman spectral mapping in Figure 5. As I was able to better synthesize high-quality MoS2, the Raman intensities associated with these two peaks increased. In addition to the location of these two peaks, the frequency difference of ~24 cm-1 between the E2g and A1g modes is also consistent with a two-dimensional MoS2 thin film [8]. A Raman spectral mapping of mica was also included within the graph to contrast the MoS2 shift from the mica shift within the examined sample.

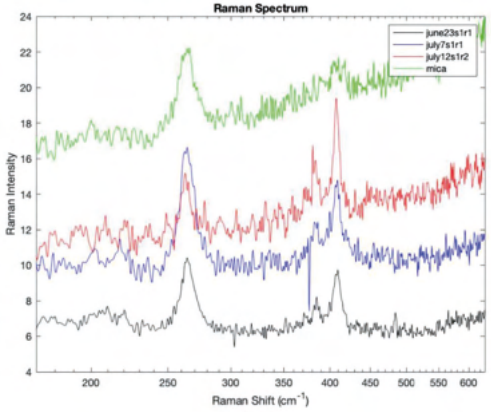

Growth Conditions of samples

1. June23s1r1
   a. 650°C, 50 SCCM, Sulfur (60 mg) & MoO3 (5 mg)
2. July7s1r1
   a. 550°C, 30 SCCM, Sulfur (120 mg) & MoO3 (5 mg)
3. July12s1r2
   a. 525°C, 30 SCCM Sulfur (120 mg) & MoO3 (5 mg)

Figure 5. Raman spectra of MoS2 thin films and Raman spectrum of mica substrate.

Atomic Resolution Study of Hexagonal MoS2

The scanning electron microscope (SEM) was implemented to produce images and examine the surface topography and composition of the synthesized MoS2 on mica substrates. To verify that the growth of MoS2 was high-quality, I searched for epitaxial and uniform growth of triangular and hexagonal geometric shapes. Within the search for these geometric shapes, I was able to identify three different areas that constitute the samples, i.e., Thick Region, Center Region, and Thin Region. The Thick Region was directly above the MoO3 precursor and comprised numerous layers of thick MoS2 that were in various shapes such as nanosheets and tubes. Within this region it was difficult to clearly identify the individual shapes, and as a result, this region was not considered further in this study. The Center Region varied from the various series of temperatures that were conducted.

Some samples were very similar to the Thick Region, while others had clear geometric shapes. Geometric shapes were consistently found in the Thin Region. However, these shapes decreased in size as the edge reached. Figure 6 shows representative images of the various regions.

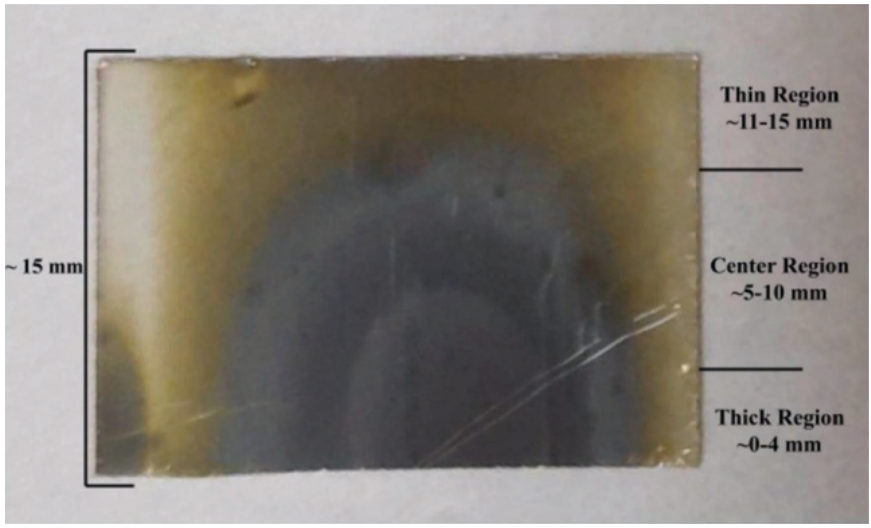

Figure 6. Illustration showing the three separate regions and their ranges within a sample that exhibit different growths.mica substrate.

After gathering images and data from the various series ranging from 500° to 600° and 30 to 150 sccm, I was able to determine the relationship between edge length, temperature, and the use of plasma. The edge length of MoS2 has an inverse proportion to the growth temperature, and gradually decreases with the increase of growth temperature. Figure 7 clearly shows that the longer edge lengths are associated with lower temperature and decrease in size as the temperature increases to 600°. In addition, it can clearly be seen in Figure 6 that the use of plasma significantly increases the edge length growth. The green, red, and blue plots are MoS2 samples that were synthesized with the use of plasma. The black plot is a MoS2 sample that was synthesized without the use of plasma. The 500° series grown utilizing plasma have an approximate magnitude of five times larger than those that did not.

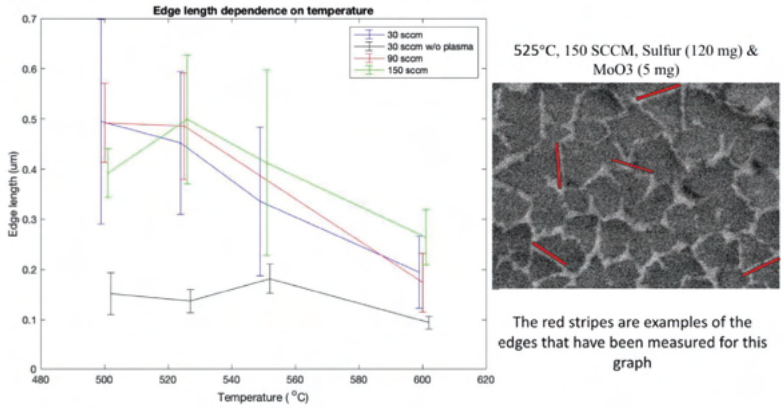

Figure 7. Edge length dependence on temperature and flow rate with standard deviation error bars. Examples of edge length measurements

To illustrate the dependence of high-quality growth on temperature, I held a constant flow rate and varied temperature in Figure 8. As seen in the previous figure, the edge length of these geometric shapes decreases as temperature increases. The 500°C image shows bigger semi-triangular shapes with a low density in the frame. As I increase to 550°C, the size of the geometric shapes decreases, and the density of them increase within the frame. The 600°C image does not have a dramatic decrease in size, but it does contain a huge variety of multilayered growth. While it may have some larger geometric shapes, however, the average size in this frame is smaller than the previous two.

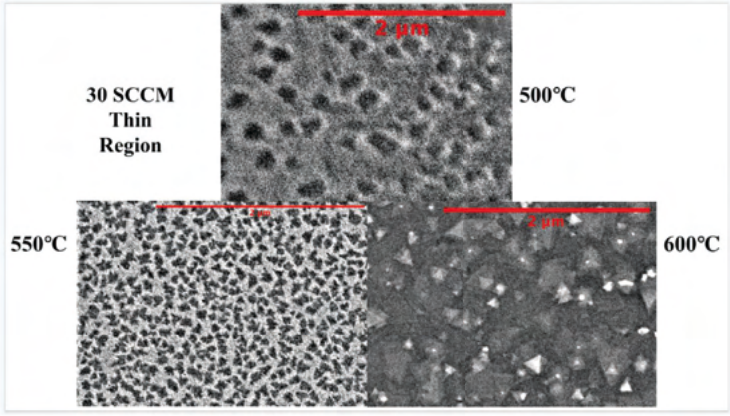

Figure 8 Illustration that presents the thin region of samples grown at ranging temperatures and held at a constant flow rate.

In similarity with growth being dependent on temperature, it is also dependent on the distance from the precursor. As stated before, I noticed that there was a discontinuity of growth within an individual sample. Each sample could be split into three different regions: thick, center and thin. To try and find a relationship between distance from precursor and epitaxial high-quality growth, I imaged the structures found in each region, as shown in Figure 9, at different flow rates but at a constant temperature. Although no clear relationship between the conditions is present, I found a decrease of the thick growth in the Thick Region as the flow rate increased, indicating a more uniform growth process. The triangular structures found within the Thin Region were consistent and almost independent of flow rate, but the center varied too much to find a correlation. In relation to finding geometric shapes that indicate high-quality growth, it seems as if 90 sccm is the more favorable of the three different flow rates.

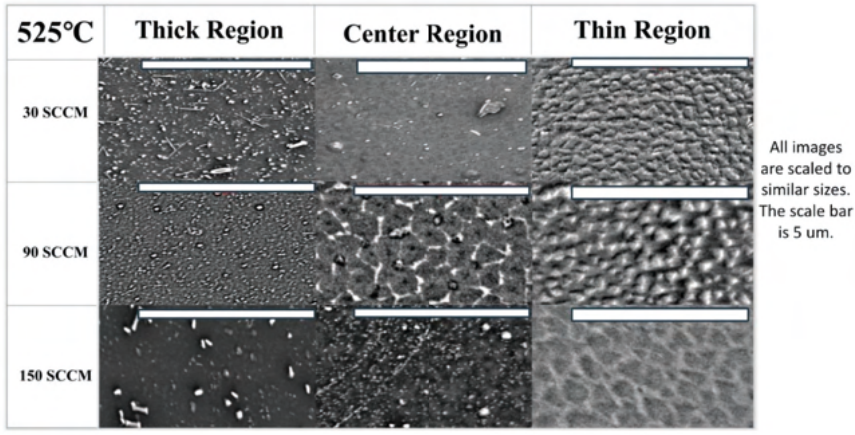

Figure 9. Illustration that presents the three different regions within a sample that were grown at 525° C with various flow rates.

In addition to the use of the SEM, the atomic force microscope (AFM) helped us produce images and examine the surface topography and composition of the synthesized MoS2. Figure 10 is a 5um x 5um AFM image that helped indicate around and sub-nm growth. Growth below a few nanometers is consistent with monolayer growth but can also be associated with few-layer growth. Due to instrument limitations, I was unable to confirm single layer growth.

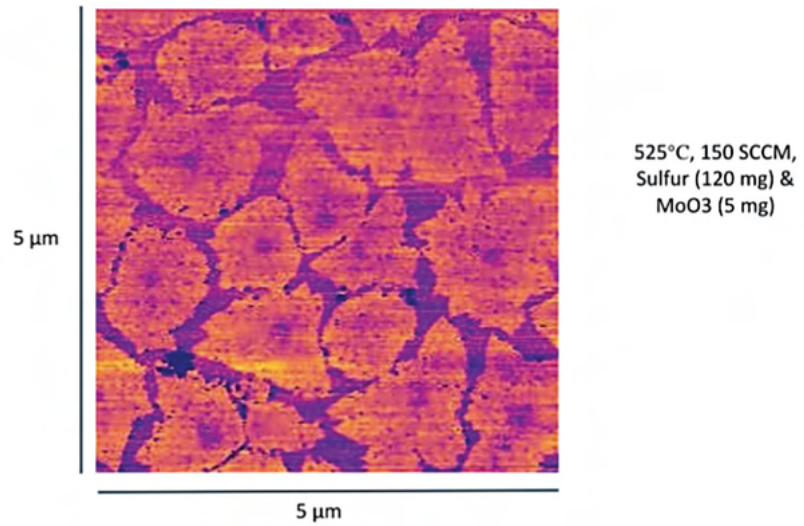

Figure 10. AFM image that shows triangular geometric shapes that indicate high-quality growth

Conclusion

In conclusion, I was able to synthesize high-quality few-layered MoS2 at various conditions. This study has found evidence of high-quality growth in both of my series relating to temperature and flow rate. The temperature series were 500° C, 525° C, 550° C, and 600° C, while the flow rate series was 30 sccm, 90 sccm, and 150 sccm. Through this extensive research, it can be inferred that MoS2 growth is highly sensitive to both temperature and flow rate and that the presence of an argon plasma significantly increased the size of triangular MoS2 domains. The maximum size measured within the samples was approximately 1.69 um. The use of the AFM also helped indicate there was growth below a few nanometers. However, due to instrument limitations, single-layer growth could not be confirmed.

In the future, the space confined method, or more colloquially known as the sandwich method, will most likely be employed. The space confined method was used near the end of this research and also be desirable to determine the lower temperature limit which still yields high-quality growth. Concerning applications, this work may pave the way towards growth of MoS2 on cheap, available flexible substrates, making it a candidate for flexible optoelectronics, LEDs, Photodetectors, Solar Cells, Sensors, and Wearable devices.

Acknowledgements

I thank Dr. Shawn Pollard for advising me through this project, and also thanks go to the University of Memphis for hosting the REU program. Finally, I would like to share my gratitude to the NSF for funding this research program.

References

[1] F. Cui et al., “Controlled Growth and Thickness-Dependent Conduction-Type Transition of 2D Ferrimagnetic Cr2S3 Semiconductors,” Advanced Materials, vol. 32, no. 4, p. 1905896, 2019.

[2] The Editors of Encyclopaedia, “van der Waals forces,” Encyclopædia Britannica, 16-Mar-2016. [Online]. Available: https://www.britannica.com/science/van-der-Waals-forces. [Accessed: 23-Jun-2021].

[3] M. S. Ullah, A. H. Yousuf, A. D. Es-Sakhi, and M. H. Chowdhury, “Analysis of optical and electronic properties of MoS2 for optoelectronics and FET applications,” Applied Physics Letters, pp. 020001–1-020001–7, 2018.

[4] Q. Ji, Y. Zhang, D. Ma, M. Liu, Y. Chen and et.al., "Epitaxial Monolayer MoS2 on Mica with Novel Photoluminescence," NANO Letters, vol. 13, no. 8, pp. 3870-3877, 2013.

[5] Z. Cai, B. Liu, X. Zou, and H.-M. Cheng, “Chemical Vapor Deposition growth and applications of two-dimensional materials and their heterostructures,” Chemical Reviews, vol. 118, no. 13, pp. 6091–6133, Jan. 2018.

[6] S. D. Hersee and J. P. Duchemin, “Low-Pressure Chemical Vapor Deposition,” Annual Review of Material Science, vol. 12, pp. 65–81, Aug. 1982.

[7] "Wikipedia, the free encyclopedia," Wikipedia, 29 June 2021. [Online]. Available: https://en.wikipedia.org/wiki/Molybdenum_disulfide#Structure_and_physical_properties. [Accessed 11 July 2021].

[8] J. Held, C. Beaudette, K. Mkhoyan and U. Kortshagen, "NonThermal Plasma-Enhanced chemical vapor deposition of Two Dimensional molybdenum disulfide," ACS Omega, vol. 5, no. 34, pp. 21853-21861, 2020.

Andy Johnson is a physics and mathematics dual major at the University of Idaho graduating in the Spring of 2022. He hopes to attend gradschool in Fall 2022 semester to pursue a doctorate in Physics. Born and raised in north Idaho, Andy had shown a fascination for all things science from a young age. He conducted research in multiple fields of physics. At the University of Memphis in the summer of 2021, he participated in an NSF funded research internship resulting in 2 papers being published.Andy is very thankful for the time he spent in Memphis meeting many new professionals in the field and making connections he hopes to maintain in the coming years.

Andrew Johnson

Remotely Controlled Curvature on Liquid Crystal Elastomer Networks Using Light

Faculty Sponsor

Dr. Chenhui Peng

Abstract

Liquid crystal polymer networks are a new and revolutionary field of soft matter physics with a strong application in soft robotics. However, this new genre of soft robotics is not well understood and thus calls for research to be conducted to learn more about its material properties. In this paper we discuss a method of "programming" the movement of macroscopic liquid crystal polymer networks by using photopatterning techniques and inducing the movement of said polymer films by optical means produced by an intense blue (400nm) light. The induced curvature from this light produces results consistent with the Gauss-Bonet theorem of curvature and can be analyzed using the corresponding Euler Characteristic for each handlebody created.

Introduction

Using liquid crystal elastomers for soft robotics is a method that has been used previously to analyze different forms of motion, such as reproducing that of a caterpillar [1]. studies, this caterpillar-like motion was able to be produced in samples that mimic the actual scale of a real-world caterpillar, thus showing that this locomotion also can be reproduced in macroscopic samples [1]. This caterpillar was made from a liquid crystal elastomer which was then controlled by light [1]. This motion opens the way to many new developments in the fields of soft robotics.

Although the creation of this caterpillar is very important for the field of soft robotics, the method used to "program" the motion of the caterpillar can be difficult to reproduce. There have been recent developments in the methods used to create this programmable pattern, namely photopatterning. This new form of programming allows for many different types of motion to be produced. In this paper, we use a form of photopatterning using SD1 as detailed in a paper by Chenhui Peng [2]. The method of photopatterning using SD1 is the primary method of producing samples in this paper.

While the method of SD1 photopatterning has been studied there is still a need to understand which photopatterns produce which result and how each photopattern can potentially be used in the future. There are many types of photopatterns that have been identified and experimentally produced using focusing a beam of light through a rotating polarizer to produce samples with various alignments [3]. One special feature of using this method is that it converts topology (the differential geometry of an object) into topography (the physical surface of the sample) [3]. This allows us to connect the mathematical theory to the experimental result.

In this paper we use SD1 photopatterns to produce samples with unique topologies, topographies and induced curvatures. Every sample we produced has a unique curvature and all curvatures follow the Gauss-Bonet theorem. Thus, we plan to show that our experimental findings are consistent with the theory guiding them.

Methods and Materials

The experimental process began by preparing the sample for testing. This consisted of a 2.5cmx7.5cm glass substrate being cut into 3 equal pieces (2.5cmx2.5cm). Before the substrate was cut it was inspected for any scratches on the surface that would alter the result. Glass substrate found to have no significant amount of damage or dirt was placed in an ultrasonic cleaner for 8 minutes in order to remove minor dust particles on the surface.

The samples were removed and washed thoroughly (on both sides) with tap water to remove any detergent that might still be attached to the substrate. The substrate was then given a thorough rinse on both sides with acetone and then isopropanol. After most of the isopropanol had dripped off the substrate it was placed in an oven at 100° C for a minimum of 20 minutes to evaporate any remaining fluid that present on it. After this time in the oven the substrate was placed in a UV-Ozone cleaner for 5 minutes.

After the substrate was taken out of the UV-Ozone cleaner it coated with photosensitive dye solution. A pipet was used to apply 5-10 drops of the photosensitive solution onto the glass substrate which was then equally spread around the rest of the substrate in a spin coater leaving behind an imperceptibly thin film. At this point, the substrate was photosensitive be handled in a low-light environment while experimenting.

The experimental setup for the study is depicted in Figure 1. It consisted of one laser projector with its beam focused through two lenses to concentrate and maximize the intensity of light produced into a small area for photopatterning purposes. To photopattern the sample, the light beam traveled through a linear polarized film attached to a rotating stage, allowing change in the angle of polarization on the sample. Finally, we had attached two-sided scotch tape to a vertical mount such that the incidence of light was perpendicular to the sample's surface. The amount of exposure per sample depended on criteria such as the pattern desired, and temperature/humidity, and production environment. The common range for photopattern exposure time was 30-120 seconds.

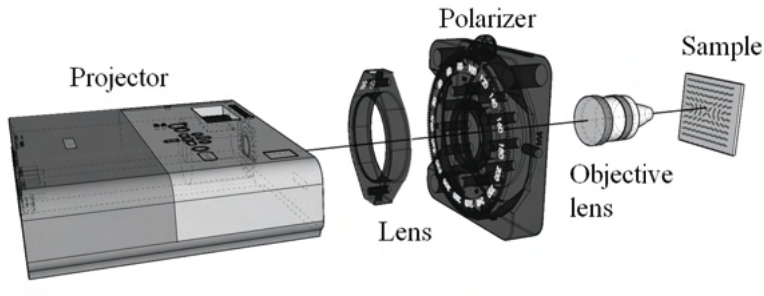

Figure 1. Depiction of our photopatterning setup.

After photopatterning had occurred, the sample was tested to confirm a pattern imprinted. To do this we applied 2-3 drops of RM257 liquid crystal solution before it became an elastomer and spun the substrate at 6000RPM in the spin coater to get an even coating. Applying and spin-coating the sample with RM257 is a time sensitive endeavor, needing to be completed in under 10 seconds. This is due to the fact that the RM257 will react with the SD1 film and make the solution thick and viscous, thus unable to produce a uniform film of RM257 on the sample. After successful coating has occurred, we held the substrate up to a background light (such as a ceiling light, desk lamp, etc.) to observe dark regions on the substrate in the shape of the photopattern used. If the observable region was clear, then photopatterning is successful. At this time the sample was placed under a UV-light for 20 minutes to polymerize the RM257 solution that was applied to it.

The sample was then prepared for the addition of the liquid crystal elastomer solution. The solution in question contained RM257, RM105 (both chemicals being the makeup of our LCE), Irgacure-31 photoinitator (allow the solution to be sensitive to light) and DR1-A (red dye) all thoroughly dissolved in DCME (Solvent). After each chemical has dissolved in solution, the vial containing said solution was placed on a hot plate at 105° C for 1 hour and 30 minutes to evaporate the remaining DCME. The remaining syrup-like liquid is our liquid crystal elastomer solution (LCE solution). When preparing the sample for addition of the LCE solution a very small drop of 20 micrometer UV-activated epoxy spacer was placed in all 4 corners of the sample and then topped with a homeotropically aligned glass substrate (with the aligned face of the original substrate and homeotropically aligned substrate facing each other). At this point the glass "sandwich" was cured under UV-light for 30s-1 min.

The sample was then placed onto a heat-controlled hotplate at 80° C. After reaching 80° C the LCE solution was carefully injected between the two plates until all available space was covered due to capillary action. Once all available space had been filled the sample was brought down to 45° C at a rate of 5° C/min. Once the entire sample had reached this temperature it was then polymerized underneath a UV-light for 30 minutes. The two glass substrates were then carefully separated via razor blade. The three stages of the process can be seen in Figure 2.

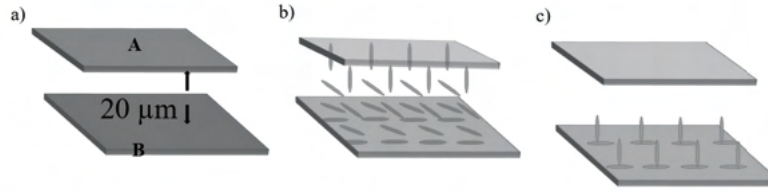

Figure 2. Three stages of sample preperation.

In Figure 2, it can be seen that the homeotropically aligned layer was attached to the photopatterned layer (B) using 20-micron spaced epoxy. The LCE solution was then injected between the two plates where the polymer began to align perpendicularly with the homeotropically aligned layer on the top and parallel with the photopatterned layer on the bottom. In the final phase, once polymerization had occurred, the two layers were separated leaving the solid polymer film attached to the photopatterned layer with a homeotropically aligned layer and a photopatterned aligned layer.

The hardened LCE was then attached to the original substrate instead of the homeotropically aligned substrate. At this point a laser cutter was used to separate the photo patterned LCE film from the film that did not contain any photopattern. The sample was once again placed in the sonicator, for 1-2 minutes to aid in the removal of the sample from the glass substrate. Once removed from the sonicator, tweezers were used to remove the sample from the glass substrate, and placed under a 400nm blue light for analysis.

Results and Discussion

In total, many different LCE films were created each with a unique patterning and a unique curvature. The first samples were created in the shape of letters that spelled "physics world". Each letter had its own unique motion and thus created with its own unique curvature. Before creating every letter with a unique movement, we first made every letter having uniform horizontal alignment, as seen in Figure 3. Unfortunately, due to time constrictions, we were unable to complete the entirety of "physics world" but we were able create most of the letters, as seen in Figures 3 and 4. Curvature was successfully induced due to the intense blue light used. The energy of the 400nm blue light was transferred into thermal energy upon interaction with our LCE material and thus induced a phase change, causing the material to expand on one side and contract on the other. Based on this curling motion, and how the photopattern was used to control this curling, we were able to use the 400 nm blue light to remotely control the programmed motion of the soft robots produced.

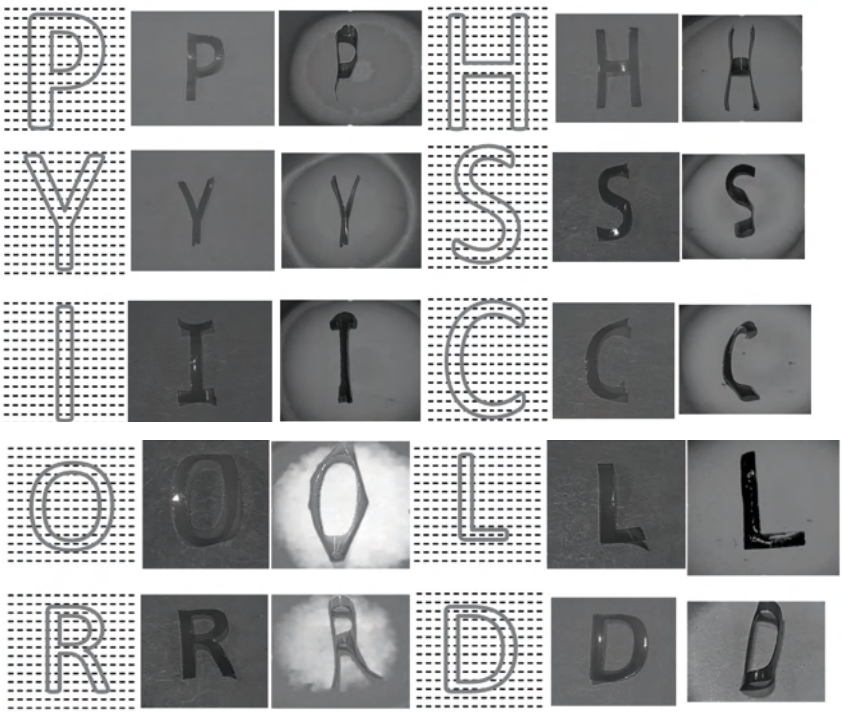

Figure 3. It can be seen that most of the letters in "physics world" with their director field, relaxed form and excited form while underneath the blue light (λ=460nm).

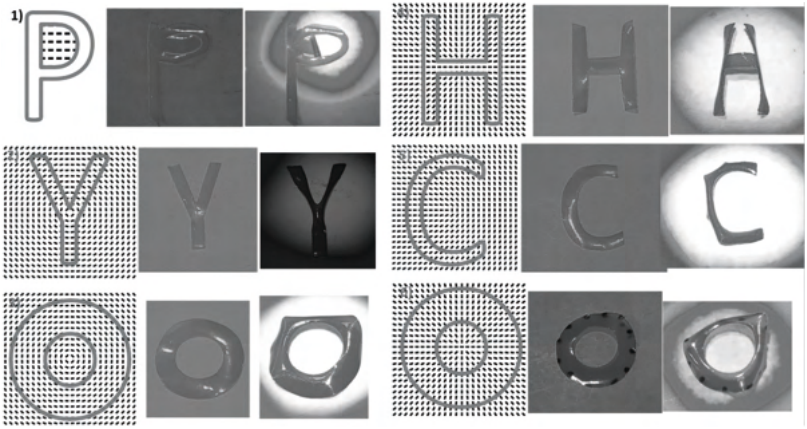

Figure 4. On the first sample, letter "P" with uniform alignment only on the space inside the ring in the center. Next, letter "Y" with circular+1 alignment. The third sample, letter "O" (ring) with circular alignment. The fourth sample, Letter "H" with radial+1 alignment. The fifth sample, Letter "C" with +half alignment. Finally, the last sample, Letter "O" (ring) with radial+1 alignment.

After the creation of these letters the focus was shifted to curvature in n-hole handlebodies. Namely, we started with one ring of a certain alignment and analyzed it under the 460nm light and then created a ring of the same dimensions but different alignments to see how the motion would vary between samples. This led to the creation of "ring arrays" containing anywhere from 1 to 5 rings all placed in different patterns to see how each unique curvature would total into the entire curvature of the sample. These were the samples used to create a link between the experimental results and the Gauss-Bonet theorem. Equation 1 below.

$$\iint_M K\,dA + \oint_{\partial M} K_g\,ds = 2\pi\chi$$

Equation 1. The Gauss-Bonnet Theorem

The theorem in Equation. 1 cites the Gauss-Bonnet Theorem. Let us dissect this equation term by term. The double integral term is the total curvature of a surface, or the sum of each individual curvature on a surface. The middle term, or the term with the line integral, represents the total turning round boundary. For us, this term is equal to 0 since the integral only applies if there are sharp angles in the boundary of a surface. Since we are only working with rings, our integral becomes zero. On the right side of the equal sign, we see $2\pi\chi$, where χ is called the Euler characteristic and $\chi=2-2g$ where g is the number of holes in the surface. Analyzing four different ring configurations gives us the data shown in Figure 5:

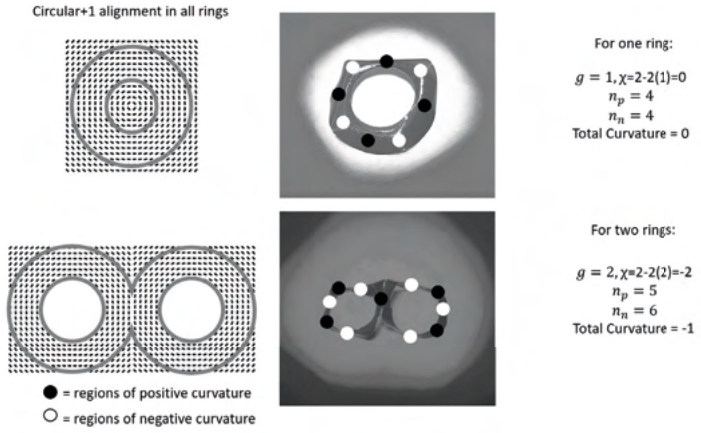

Figure 5. Ring Configurations

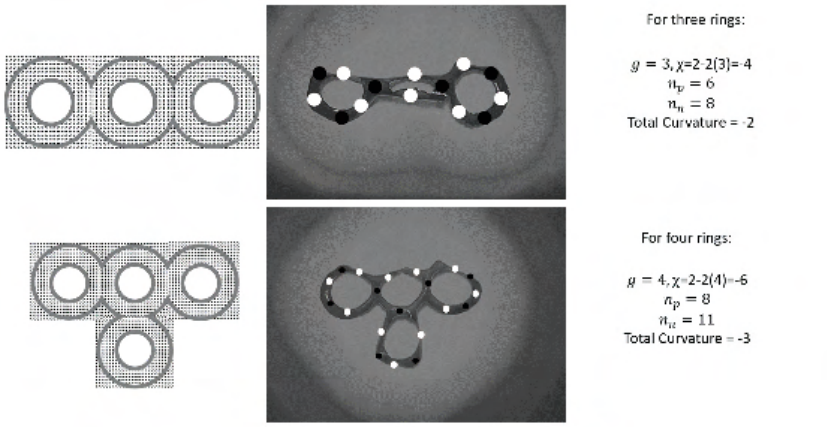

Figure 5. Continued.

Figure 5 depicits 4 different circular+1 ring configurations while they are in their "excited" state under intense light (λ=460nm). We can notice through the Total Curvature (tot. curv . = n_p-n_n, where n_p is the number of positive curves and n_n are the number of negative curves) that as the number of holes in a sample (g) increase, the total curvature in the sample begins to decrease. The analytical pattern we can see forming is that the total curvature is equal to (1-g)4π. The 4π comes from the fact that we are dealing with circles which gives us a circumferential constant we need to include. We can split this equation into 2(1-g)2π=(2-2g)2π=2πχ. Since we have shown that the total curvature of each ring array is equal to 2πχ, we have successfully shown that our experiments are consistent with the Gauss-Bonnet theorem.

Conclusion

In conclusion, this new form of programming soft robots is reproducible and follows the Gauss-Bonet theorem indicating that theoretical consistency is intact. The results shown that we can program LCE films, based on photopatterns, and can thus create soft robots with abilities from basic folding to more complex motions such as locomotion. We have also demonstrated that by using the SD1 photopatterning method, we are able to create samples that are capable of different forms of motion. We also have demonstrated that our findings are consistent with the Gauss-Bonnet theorem and thus do not deviate from theory.

Acknowledgements

I would like to acknowledge the Peng laboratory at University of Memphis for advising and guiding this research project. I would also like to thank Juan Chen who taught the material and helped guide the experimental procedures laid out in this paper. Lastly, I would like to give my deepest thanks to the NSF for funding projects for undergraduate students and giving me the ability to explore different fields of physics while at the same time contribute to physics and other disciplines.

References

[1] Rogóż, Mikołaj, et al. "Soft Robotics: Light-Driven Soft Robot Mimics Caterpillar Locomotion in Natural Scale (Advanced Optical Materials 11/2016)." Advanced Optical Materials, vol. 4, no. 11, 2016, pp. 1902–1902., doi:10.1002/adom.201670064.

[2] Peng, Chenhui, et al. "Patterning of Lyotropic Chromonic Liquid Crystals by Photoalignment with Photonic Metamasks." Advanced Materials, vol. 29, no. 21, 2017, p. 1606112., doi:10.1002/adma.201606112.

[3] McConney, Michael E., et al. "Liquid-Crystal Polymers: Topography FROM Topology: Photoinduced Surface Features Generated in Liquid Crystal Polymer Networks (Adv. Mater. 41/2013)." Advanced Materials, vol. 25, no. 41, 2013, pp. 5830–5830., doi:10.1002/adma.201370258.

Jacob Mims is on track to graduate from the University of Memphis in the spring of 2023. He plans on continuing studying Physics in graduate school, and while there, Jacob hopes to conduct research that is a blend of computational and theoretical physics. During his time at the University of Memphis, Jacob has worked on a variety of projects in a computational biophysics group that is under the direction of Dr. Mohamed Laradji. These research projects have ranged from molecular dynamics to polymer field theory. In the summer of 2021, Jacob was honored to receive an internship for the National Science Foundation funded Research Experience for Undergraduates program at the University of Memphis.

Jacob Mims & Mohamed Laradji

Self-Induced Spatial Organization of Nanoparticles in a Polymer Brush: A Molecular Dynamics Study

Faculty Sponsor

Dr. Mohamed Laradji

Abstract

The interactions of spherical nanoparticles absorbed into a polymer brush was investigated using molecular dynamics simulations of a coarse-grained implicit solvent model. Our simulations indicate a few phenomenon including self-assembly into superstructures that contain HCP and FCC symmetries.

Introduction

Understanding the way nanoparticles (NPs) interact with various media can lead the way to the development of advanced materials. One such important media would be a polymer brush. This understanding is important for the development of lightweight nanomaterials for use in the automobile and aerospace industries. It would also give further insight into biomedical applications, which can help deter potential toxic effects on living organisms. One such important phenomenon would be self-assembly of the nanoparticles.

Interactions between NPs and polymer brushes have been studied both theoretically and experimentally for differing applications. Kim *et al.* performed self-consistent field theory calculations to study the repulsive effect of polymer brushes cushioning a single NP.[1] Kesal *et al.* used an experimental set-up to study the attractive interactions between gold NPs and a polyelectrolyte brush.[2] The varying attempts to characterize such interactions shows the interest in these types of problems.

Recently in our group, studies have been conducted on NPs at the interface of a lipid membrane.[3, 4] In these studies, certain self-assembled structures were found, and their stability was characterized. There have also been Molecular Dynamics simulations in the case of spatial organization in polymer brushes. Cheng *et al.* investigated a system in which NPs are placed randomly above a brush in an evaporating solvent.[5] After evaporation, a neatly organized layer could be seen.

Some experimental studies have shown that the interactions between NPs and various polymer medias can lead to spatial organization. Bockstaller *et al.* used diblock copolymers to induce spatial organization in the NPs in their system.[6] In order to further probe interactions between NPs and polymer brushes, a series of systematic Molecular Dynamics simulations were conducted.

Model and Computational Method

In this study, we used a coarse-grained implicit-solvent model that was developed to study self-assembled lipid membranes.[7, 8] This model has been adapted to describe fully flexible linear homopolymer chains for use in these simulations, coarse-graining the chain into many monomers. The potential energy of the polymer chains is comprises two contributions:

$$U(\{\vec{r_i}\}) = \sum_{i,j} U_0^{\alpha_i \beta_j}(r_{ij}) + \sum_{<i,j>} U_{\text{bond}}(r_{ij}) \qquad (1)$$

where $\vec{r}_i$ describes the coordinates for the center of mass for particle *i* in the simulation, $r_{ij} = |\vec{r}_i - \vec{r}_j|$, and α_i indicates the type of particle that *i* is, i.e. $\alpha_i = m$ for a monomer or $\alpha_i = s$ for an NP. In the second contribution of Eq. 1, the angled brackets indicate that *i* and *j* are constituents of the same polymer chain. $U_0^{\alpha\beta}$ is a soft two-body potential between two particles of types α and β that are separated by some distance *r*, given by a piece-wise function:

$$U_0^{\alpha\beta}(r) = \begin{cases} \left(U_{\max}^{\alpha\beta} - U_{\min}^{\alpha\beta}\right)\dfrac{(r_m - r)^2}{r_m^2} + U_{\min}^{\alpha\beta} & \text{if } r \le r_m, \\ 0 & \text{if } r > r_m, \end{cases} \tag{2}$$

where $U_{\max}^{\alpha\beta} > 0$ and $U_{\min}^{\alpha\beta} \le 0$ for any pairing of (α, β). For monomers, this piecewise potential implies a repulsive force up to r_m, which is half of the radial cutoff, r_c.

In Eq. 1, the second term, $U_{\text{bond}}(r_{ij})$, is a harmonic potential used to ensure the connectivity of monomers along the same polymer chain. Explicitly:

$$U_{\text{bond}}(r) = \frac{k_{\text{bond}}}{2}(r - a_b)^2 \tag{3}$$

Wherein, k_{bond} is the bond stiffness coefficient and a_b is the preferred bond length. It is also important to note that bonded monomers interact with each other with Eq. 2 along with Eq. 3.

In our model, NPs are assumed to be a sphere of radius R and a homogenous surface. Under this assumption, NPs are sufficiently described with only three degrees of freedom, each of which correspond to the center of mass of the NP. This is due to the spherical symmetry of the NP. This is in stark contrast to the numerous degrees of freedom that are implied by a model that constructs NPs by beads connected by fluctuating bonds.[9] The interaction that occurs among a monomer and an element of the NP's surface area, δ*a*, separated by some distance ρ is assumed to have the same form as Eq. 2, but has an added condition that allows for an attractive force between a monomer and the NP. Explicitly stated,

$$\delta U^{s\alpha}(r) = \begin{cases} \left[(u_{\max}^{s\alpha} - u_{\min}^{s\alpha})\dfrac{(r_m - \rho)^2}{r_m^2} + u_{\min}^{s\alpha}\right]\delta a & \text{if } \rho \le r_m, \\ \left[-2u_{\min}^{s\alpha}\dfrac{(r_c - \rho)^3}{(r_c - r_m)^3} + 3u_{\max}^{s\alpha}\dfrac{(r_c - \rho)^2}{(r_c - r_m)^2}\right]\delta a & \text{if } r_m < \rho \le r_c, \\ 0 & \text{if } \rho > r_c, \end{cases} \tag{4}$$

where $u_{\min}^{s\alpha}$ is the value of the potential, per unit of area, that is separated some distance r_m from the surface of the NP. Due to the fact that this is a soft potential, the inequality $u_{\max}^{s\alpha} > 0$ is required and the value of the parameter must be strong enough to prevent monomers from penetrating into the NP. $u_{\min}^{s\alpha} = 0$ implies a fully repulsive interaction between a NP and another particle of type α, and $u_{\min}^{s\alpha} < 0$ implies a short-range attractive interaction. The total interaction between an NP and some particle of type α, $U^{sa}(r)$, is given by integrating Eq. 4 over the surface of the NP and explicitly given by

$$U^{s\alpha}(r) = \begin{cases} 2\pi r_m^2 \frac{R}{r}\left[\frac{A^{s\alpha}(R+r_m-r)^4}{4r_m^4} - \frac{A^{s\alpha}(R+r_m-r)^3}{3r_m^3} - \frac{u_{\min}^{s\alpha}(R+r_m-r)^2}{2r_m^2} + \frac{u_{\min}^{s\alpha}(R+r_m-r)}{r_m} + \frac{13u_{\min}^{s\alpha}}{20}\right] & \text{if } r \le R + r_m \\ 2\pi r_m^2 \frac{R}{r}\left[\frac{2u_{\min}^{s\alpha}(R+r_c-r)^5}{5r_m^5} - \frac{7u_{\min}^{s\alpha}(R+r_c-r)^4}{4r_m^4} + \frac{2u_{\min}^{s\alpha}(R+r_c-r)^3}{r_m^3}\right] & \text{if } R + r_m < r \le R + r_c \\ 0 & \text{if } r > R + r_c \end{cases} \quad (5)$$

where $A^{s\alpha} = u_{\min}^{s\alpha} - u_{\max}^{s\alpha}$.

All monomers and NPs' center of mass are moved using a molecular dynamics scheme with a Langevin thermostat, i.e.

$$\dot{r}_i(t) = v_i(t), \quad (6)$$

$$m_i \dot{v}_i(t) = -\nabla U(\{r_i\}) - \Gamma v_i(t) + \sigma \Xi_i(t) \quad (7)$$

where m_i is the mass of particle i and Γ is a particle's drag coefficient. $\sigma\Xi_i(t)$ is a random force with zero that is uncorrelated for differing particles and times. Γ and σ are inter-related through the fluctuation–dissipation theorem, leading to the equality $\Gamma = \sigma^2 / 2k_b T$.

For our simulations, the model's parameters are given by the following:

$$\begin{gathered} U_{\min}^{mm} = 0 \\ U_{\max}^{mm} = 100\epsilon \\ u_{\min}^{sm} = 0 \\ u_{\max}^{sm} = 235.2\epsilon / r_m^2 \\ u_{\max}^{ss} = 235.2\epsilon / r_m^2 \\ k_{\text{bond}} = 100\epsilon / r_m^2 \\ a_b = 0.7 r_m \end{gathered} \quad (8)$$

For all the simulations in this study, they were performed at $k_b T = 3.0$ with a time step of $\Delta t = 0.02\ \tau$. Eqs. 1 and 2 are integrated using a standard velocity-Verlet method where $\Gamma = \sqrt{6m/\tau}$[10].

For this study, we consider a case where varying numbers of NPs with diameter $D_{np} = 4R$ are placed randomly above a polymer brush. This polymer brush is consisted of a set number of chains $N_{chains} = 800$ and each chain consists of 100 monomers. The chains have been grafted randomly onto a static substrate using a metropolis Monte-Carlo Method. The area

of the xy-plane of the simulation box is determined with the parameters of this grafting, being $\text{Area}_{xy} = N_{chains}$ /σ where σ is the grafting density of polymers.σ The polymer chains remain grafted throughout the simulation by not time-evolving the monomers that are used to graft the chains. The simulation box extends into the z axis to give enough room for the NPs to be placed without overlapping.

Results and Discussion

Fig. 1 contains snapshots of various systems at an equilibrated state with the corresponding value of $|U_{min}|$ labeled providing a nice qualitative overview of the study. As shown in the figure, NPs begin penetrating the brush at low values of $|U_{min}|$ and the fraction absorbed increases along with said parameter. For the case of this system, the NPs are fully absorbed into the brush at $|U_{min}| = 0.3$. These absorbed NPs then find their way deeper into the brush with increasing $|U_{min}|$. Saliently, the snapshot at $|U_{min}| = 0.3$ showcases the NPs ability to self-assemble into a well-ordered superstructure with next to no diffusivity. At lower values, the NPs penetrate the brush and are dispersed into a liquid-type state with no order. The NPs in this liquid-type state retain some value of diffusivity. As the value of $|U_{min}|$ increases from the form that needed for a superstructure, the NPs form an amorphous glass with almost no diffusivity.

In Figs. 2 and 3, there is a clear dependence of the average height of the

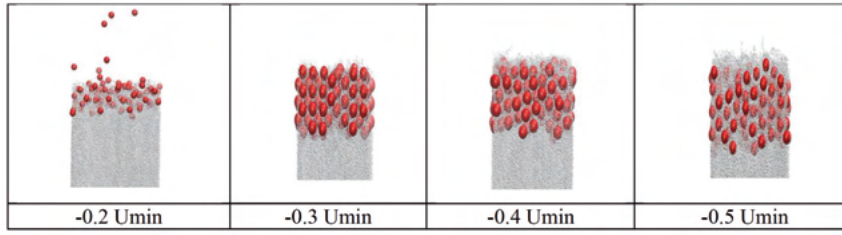

Figure 1. Side-view snapshots taken from different systems of 800 Chains 224 NPs and 0.5 grafting density.

NPs on the value of $|U_{min}|$ In both graphs, there is an initial stark downwards trend that begins to saturate and level off. This saturation is prescribed by the polymer brush. As the NPs continually dive deeper into the brush, they eventually reach a point at which the value of the monomer density is too high to permit them to reach further into it. The monomer density is proportional to the grafting density of the polymer brush. This would explain how the NPs at a lower value of grafting density would have a lower minimum height.

In Fig. 3, the average height of the NPs inhabiting the less-dense brush begins to level off at $|U_{min}|$= 0.2, while their higher density counterparts start at $|U_{min}|$= 0.3. This implies that, as the grafting density of the polymer brush is lowered, the threshold value of $|U_{min}|$ for the NPs to be penetrative is decreased.

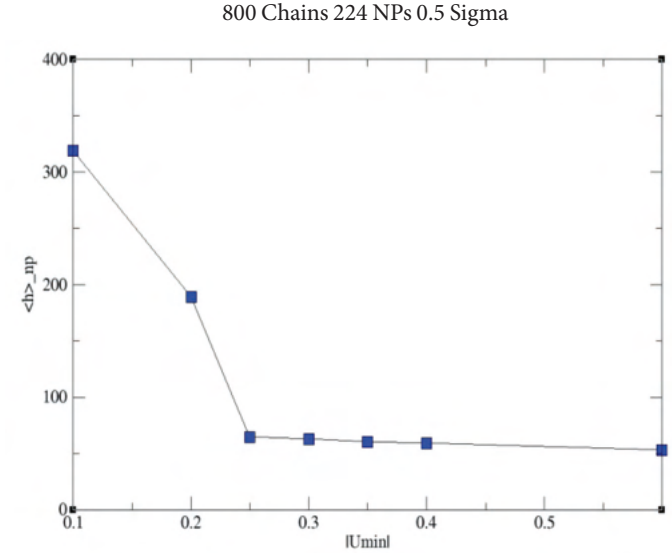

Figure 2. Average height of the NPs as a function of $|U_{min}|$. This data was taken from a system of 800 chains, 224 NPs, and grafting density of

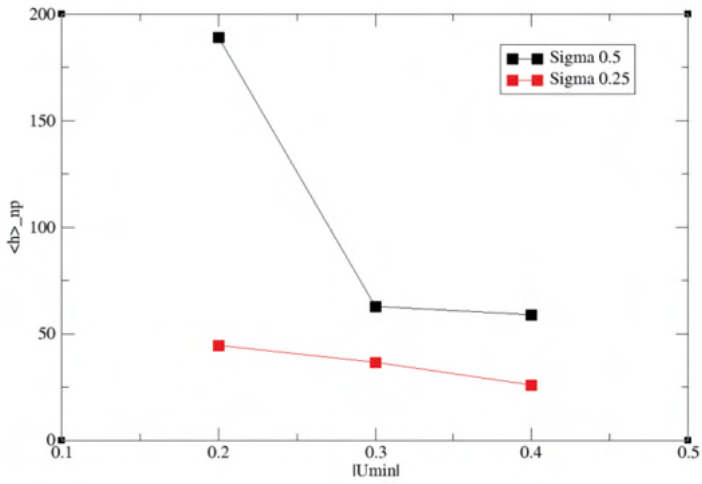

Figure 3. Average height of the NPs as a function of $|U_{min}|$. This data was taken from systems with 800 chains, 224 NPs, and variable grafting densities. his data was taken from a system of 800 chains, 224 NPs, and grafting density of 0.5

In Figs. 4, 5 and 6 the lefthand column shows of density profiles along the z-axis for three varying systems at an equilibrated state, while the right hand column is shows a corresponding snapshot. These snapshots showcase the three different states penetrative NPs. The upper-most row (Figure 6) showcases the liquid-type state, in which the NPs still show some manner of diffusivity. The NPs in this state showcase no order and inhabit a shallow location. The next row (Figure 5) showcases a system of great crystalline order, with the oscillatory NP and polymer profiles being characteristic of this order. Although these oscillatory profiles greatly characterize order, they fail to define a specific orientation. As of now, it appears as though the crystalline structures can take any number of preferred orientations inside of the brush. The bottom-most row (Figure 4) provides an example of an amorphous solid formed by the NPs. In terms of $|U_{min}|$, penetrative NPs enter and take a liquid-type configuration and with increasing $|U_{min}|$ the NPs will find a range of great order and then melt into an amorphous solid.

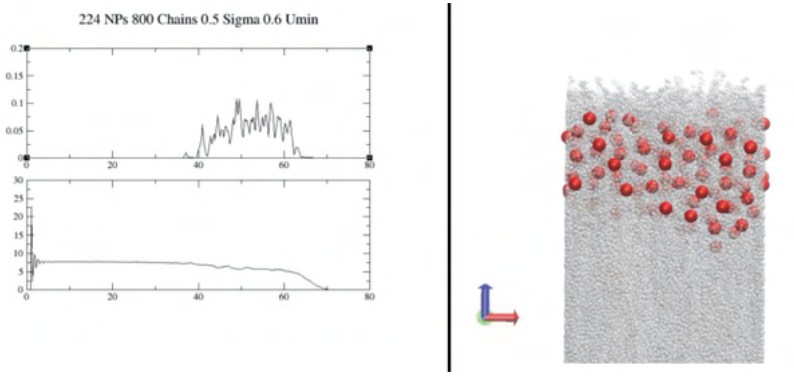

Figure 4. $|U_{min}|$ 0.6 Density profile of NPs & monomers (left) and snapshot of system (right)

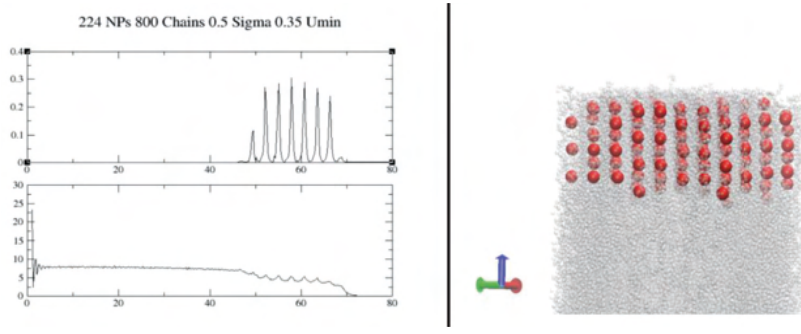

Figure 5. $|U_{min}|$ 0.35 Density profile of NPs & monomers (left) and snapshot of system (right)

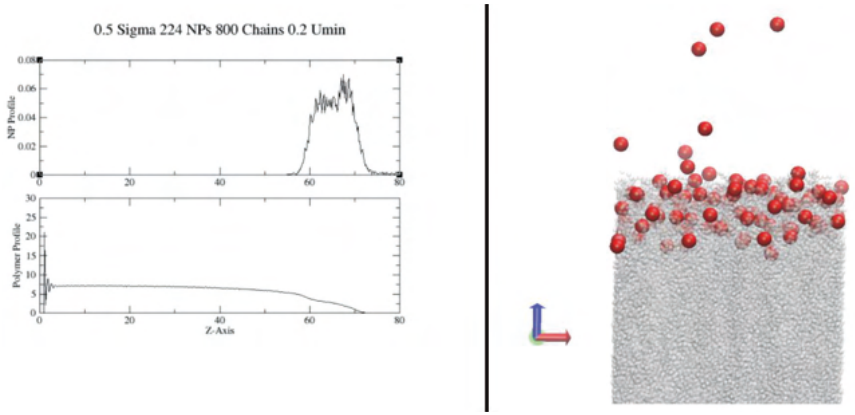

Figure 6. $|U_{min}|$ 0.2 Density profile of NPs & monomers (left) and snapshot of system (right)

The radial distribution function (rdf) of NPs in a crystalline configuration is plotted in Fig. 7. This rdf has peaks that are characteristic of both HCP and FCC crystals. HCP and FCC unit cells were observed in said simulation and snapshots are provided in Fig. 8. Both unit cells are commonly found inside naturally formed lattices; a FCC unit cell can be made into a HCP by rotating the third layer (the most transparent layer) of the snapshot in Fig. 8 (top left) by 60 degrees.

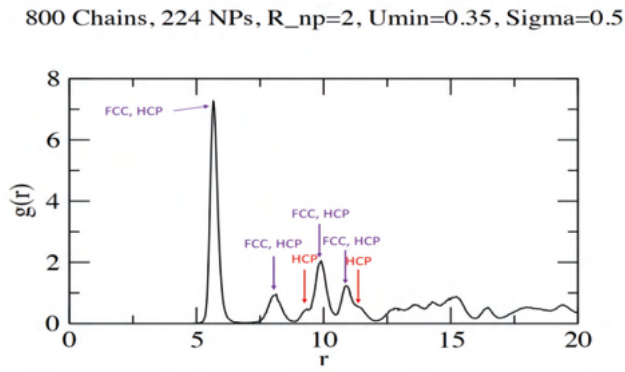

Figure 7. A graph that provides the pair-pair correlation function of NPs in a system of 800 Chains, 224 NPs, 0.35 Umin, and a grafting density of 0.5. Peaks that are characteristic of face-centered cubic (FCC) and hexagonal close packed (HCP) structures are notated.

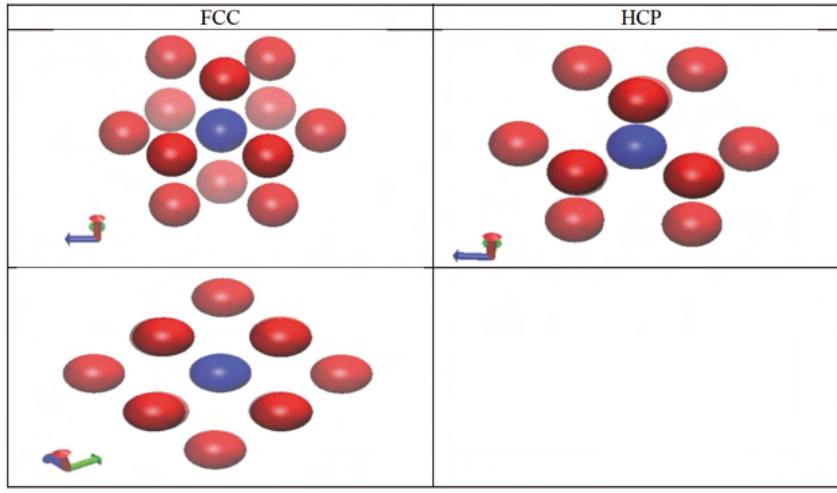

Figure 8. Snapshots taken from a system of 800 chains, 224 NPs, 0.35 $|U_{min}|$, and a grafting density of 0.5

The fact that order was observed is highly surprising. This is a preliminary study into such systems, and not many arguments exist as to why this occurs. One that can be made is due to the conformational entropy of the polymer chains. As the NPs are absorbed, some chains are compressed quite a bit as shown in Fig. 9. This reduction of entropy is not preferred by the chains, therefore there could be some counter-active force upward along the z-axis. This force is in competition with the attractive potential which is orientated downwards. There appears to be some optimal balance between these two forces that leads to the surprising order that we have observed.

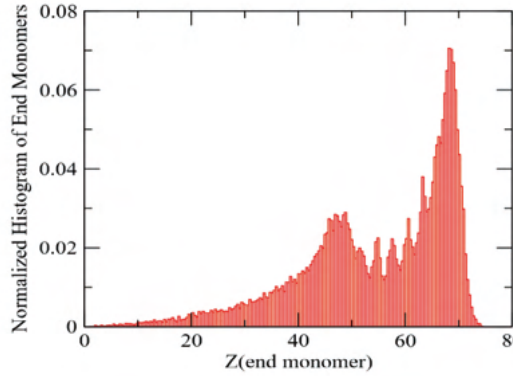

Figure 9. Normalized histogram of end-to-end distances of the polymer chains NPs in a system of 800 Chains, 224 NPs, 0.35 Umin, and a grafting density of 0.5.

Conclusions

This paper presents a course-grained implicit-solvent model of many NPs at the interface of a polymer brush. A systematic study of such model was then preformed. In this study, the fraction of NPs absorbed into the brush was highly correlated with $|U_{min}|$; as $|U_{min}|$ was increased, so was the fraction absorbed. This fraction begins to receive a non-trivial increase at values of $|U_{min}|$ as low as 0.1. There also exists a strong dependence between $|U_{min}|$ and the preferred location of the NPs in the polymer brush. As $|U_{min}|$is increased, the average height of the NPs begins to decrease. The average height can only be decreased until it saturates at a minimum value prescribed by the polymer brush. The NPs cannot penetrate further than this minimum value regardless of the value of $|U_{min}|$. The minimum value is directly related to the grafting density of the brush.

One striking phenomenon noted in this study was the formation of superstructures. For the case of a polymer brush with grafting density of 0.5 and 800 chains, a range of superstructures were visible for values of $|U_{min}| \approx 0.3$. These superstructures were formed in an undefined orientation and consisted of both FCC and HCP unit cells. Due to the aggregation of NPs into one portion of the brush, there is a clear compression of the polymer chains leading to a reduction in conformational entropy. This reduction could be a leading factor in the advent of these superstructures.

This was a computational preliminary study into such a system; as such it is meant to be a starting point for other studies into this interesting phenomenon. Our systematic numerical study showcases the self-assembly of superstructures for a range of NP-polymer interactions. It is with great hope that other researchers will be able to use the qualitative and quantitative information of this study to probe into such systems experimentally.

Acknowledgements

This research would not be possible without the REU program at the University of Memphis funded by the NSF. I extend my greatest thanks to the NSF for this opportunity. All simulations were done on the HPC at the University of Memphis. I would like to thank Eric Spangler for his continued help with computing, and my supervisor Dr. Mohamed Laradji for helping me and allowing me to work through such a project. Thanks also go to the staff of *Quaesitum* for their continued work on this journal, as they provide a much-needed platform for the research conducted by undergraduate students here at the University of Memphis.

References

1. Jaeup U. Kim and Mark W. Matsen, "Repulsion Exerted on a Spherical Particle by a Polymer Brush", Macromolecules, 41, 1, 246–252, (2007). doi: https://doi.org/10.1021/ma071906t

2. Dikran Kesal, Stephanie Christau, Patrick Krause, Tim Möller, and Regine Von Klitzing, "Uptake of pH-Sensitive Gold. Nanoparticles in Strong Polyelectrolyte Brushes", Polymers (Basel). (2016) doi: 10.3390/polym8040134.

3. Eric J. Spangler, P. B. Sunil Kumar, and Mohamed Laradji, "Stability of membrane-induced self-assemblies of spherical nanoparticles". Soft Matter. doi: https://doi.org/10.1039/C8SM00537K

4. Eric J. Spangler and Mohamed Laradji, "Spatial arrangements of spherical nanoparticles on lipid vesicles", J. Chem. Phys. 154, 244902 (2021). doi: https://doi.org/10.1063/5.0054875

5. Shengfeng Cheng, Mark J. Stevens, and Gary S. Grest, "Ordering nanoparticles with polymer brushes", J. Chem. Phys. 147, 224901 (2017) doi: https://doi.org/10.1063/1.5006048

6. Michael R. Bockstaller, Yonit Lapetnikov, Shlomo Margel, and Edwin L. Thomas, "Size-Selective Organization of Enthalpic Compatibilized Nanocrystals in Ternary Block Copolymer/Particle Mixtures". doi: https://doi.org/10.1021/ja034523t

7. Joel D. Revalee, Mohamed Laradji, and P. B. Sunil Kumar, "Implicit-solvent mesoscale model based on soft-core potentials for self-assembled lipid membranes", J. Chem. Phys. 128, 035102 (2008) doi: https://doi.org/10.1063/1.2825300

8. Mohamed Laradji et al 2016 J. Phys. D: Appl. Phys. 49 293001

9. Eric J. Spangler, Alexander D. Olinger, P. B. Sunil Kumar, and Mohamed Laradji, "Binding, unbinding and aggregation of crescent-shaped nanoparticles on nanoscale tubular membranes", Soft Matter, 2021,17, 1016-1027, doi: https://doi.org/10.1039/D0SM01642J

10. William C. Swope, Hans C. Andersen, Peter H. Berens, and Kent R. Wilson, "A computer simulation method for the calculation of equilibrium constants for the formation of physical clusters of molecules: Application to small water clusters", J. Chem. Phys. 76, 637-649 (1982) doi: https://doi.org/10.1063/1.442716

Rohith Narra was a REU student at the University of Memphis, Department of Physics and Materials Science during Summer 2021. A junior from the University of Texas at Dallas, Rohith is pursing degrees in physics and chemistry. Upon finishing undergraduate studies, he seeks to pursue a Ph.D. in Applied Physics or Electrical Engineering specializing in Nanophotonics, and then become an industrial research associate.

Rohith Narra

Utilizing Silver Nanocubes to Promote Förster Resonance Energy Transfer (FRET) Between Cadmium Selenide and Perovskite Quantum Dots Embedded in a Polymer Layer Upon Optical Excitation

Faculty Sponsor

Dr. Thang B. Hoang

Abstract

In this work, we investigate the physical consequences of integrating a metal optical cavity into a mixed quantum dot donor-acceptor embedded in a polymer layer. The metal optical cavity is composed of silver nanocubes and the positively charged polymer PAH, and the quantum dots used are perovskite quantum dots emitting at 530 nm and CdSe/ZnS quantum dots emitting at 635 nm which are embedded in a PMMA layer. The system is optically excited with a 475 nm beam of varying power, and we seek to investigate whether the metal optical cavity is successful in promoting Forster Resonance Energy Transfer (FRET) between the quantum dots and if so with what efficiency. Based on the results, we will further improve the engineering of the system's electromagnetic environment. The implications of this research extend to nanophotonic devices and next generation opto-electronics through the conversion of incident infrared or UV photons into visible light.

Introduction

Quantum dots are semiconductor particles that are 1-10 nm in diameter, and they exhibit distinctive optical and electronic properties. Consequently, they hold applications in a variety of areas including in the context of quantum dot-based light-emitting diodes in photonics, replacing organic dyes for fluorescence-based sensing in biomedical science, and increasing the efficiency of photovoltaic cells when incorporated into their design. In order to understand how quantum dots are able to enjoy such unique characteristics, their electronic structure and the effect of quantum confinement must be examined.

The highest energy electrons within the quantum dot exist in the outermost electronic orbital which is known as the valence band. These electrons become conductive once supplied with enough energy to exit the valence band and enter the conduction band, and this energy difference is known as the "bandgap". When an electron in the valence band is promoted into the conduction band, it leaves behind a mobile positively charged vacancy in the valence band known as a "hole" and forms an electron-hole pair. The electron and its hole are bound by coulombic interactions to form a quasiparticle known as an "exciton" and will thus recombine once the electron drops back down into the valence band which results in photon emission [5]. This entire process is known as photoluminescence (PL).

The wavelength of the light emitted upon exciton recombination is dependent upon the bandgap which is related to the size of the quantum dot due to quantum confinement. Specifically, as the size of the quantum dot decreases, the distance between the electron-hole pair decreases which results in more energy being required to separate the exciton pair for photoluminescence and results in a "blue shift" (lower wavelength) in emission [5]. To accurately measure the wavelength of peak emission of a particular type of quantum dot, one would perform PL spectroscopy on a sample that generates a PL spectrum – a plot of intensity (counts) as a function of wavelength (nm). When two different types of quantum dots are in close proximity together, the type which emits at a lower wavelength and the type which emits at a higher wavelength may serve as an energy donor and energy acceptor respectively upon optical excitation of the donor in certain energy transfer processes such as FÖrster Resonance Energy Transfer (FRET).

FRET is a non-radiative energy transfer from an excited fluorescent donor to a lower energy acceptor, and the driving force for this energy transfer is long range dipole-dipole interactions [1]. The chief requirement for FRET to occur between a donor-acceptor pair is spectral overlap between the emission spectrum of the donor with the absorbance spectrum of the

acceptor, and it must be noted that FRET is a highly distance-dependent phenomenon as the efficiency of the FRET process is directly proportional to $1/r^6$ where r is the distance between the acceptor and donor. The first step of FRET is excitation of the donor which forms a dipole that oscillates and dissipates energy during "vibrational relaxation" which occurs in the course of picoseconds [4]. The donor is then oscillating at an energy equivalent to the electronic energy gap of its excited state. In order for the resonance energy transfer to occur, the excited donor must be oscillating at a frequency resonant with the ground state electronic energy gap of the acceptor [4]. Once the energy transfers to the acceptor, vibrational relaxation followed by emission from the acceptor take place [4]. This can be observed from the PL spectrum following FRET where a spectral shift occurs – The height of the donor's peak decreases and the height of the acceptor's peak increases [4]. Another expected observation is from Time-Correlated Single Photon Counting (TCSPC) measurements where the decay times of the emitted photons are measured – the lifetimes of the photons emitted by the donor should decrease due to the nonradiative energy transfer process.

Suppose there is insufficient overlap between donor's emission and acceptor's absorbance spectrum for FRET to take place, the FRET effect will be negligible. To enhance the FRET effect, one would need to improve the spectral overlap between the appropriate spectra for the donor and acceptor. Furthermore, the donor's spontaneous emission can also be enhanced with an additional component in the system by the Purcell effect – the rate at which a quantum system spontaneously emits increases following modifications to its photonic environment as it increases the photonic density of states [2]. For example, researchers from Henan University demonstrated that metal-optical nanocavities (composed of silver nanocubes and PVP layer) when coupled to perovskite quantum dots (PQD) were able to enhance the spontaneous emission of the PQDs by nearly 3.5-fold [3]. Thus, incorporating metal-optical cavities into a donor-acceptor system with little spectral overlap should, in principle, increase the likelihood of FRET taking place between the two by bridging the gap.

Experimental Methods

In our setup, we incorporated silver nanocubes that act as plasmonic nanoparticles. They are meant to bridge the gap between donor and acceptor. All four of our samples consist of the donor-acceptor system consisting of PQDs (donor) and CdSe QDs (acceptor) embedded in a poly (methyl methacrylate) (PMMA) monolayer bound to a glass substrate. Of those four, two included, the silver nanocubes as well, and one of those two include

a poly (allylamine hydrochloride) (PAH) monolayer bound to the silver nanocubes forming a complete metal-optical cavity. We then checked for the presence of the FRET effect along with its strength in each sample upon optical excitation with a 475 nm beam with varying power.

The quantum dots used were supplied by Sigma Aldrich with the CdSe/ZnS quantum dots emitting at 635 nm (731870) and the Perovskite quantum dots emitting at 530 nm (905062). Additionally, the 100 nm Ag nanocubes were supplied by Nanocomposix (NCXSCPH100) and the PMMA solution was supplied by Kayaku Advanced Materials. The PAH solution was prepared by dissolving 132 mg of PAH powder and 29 g of NaCl in 500 mL of DI H2O. Other materials involved in sample assembly included glass slides, plastic strips, microcentrifuge conical tubes, and 20-200 uL pipette with the corresponding tips. The instruments and apparatuses used in sample assembly were a glass cutter, forceps, double-sided tape, sample containers, spin coater, sonicator, and vortex machine. After assembly, the samples were put in "dark" storage until we optically excited them with a Ti: Sapphire laser. The PL spectra were collected by our Horiba spectrometer. The TCSPC data was collected with our Pico quant Time-Correlated Single Photon Counting apparatus, and the data is then analyzed with the Easy Tau software.

With regards to sample assembly, first four sample containers were gathered, labeled by sample number, and a strip of double-sided tape was placed inside each container. Then, four square-shaped glass slides were cut, and three different quantum dot-polymer mixtures were prepared via quantitative transfers and stored in separate microcentrifuge conical tubes. Solution 1 was used in preparing sample 1, and it consists of 200 μL of colloidal perovskite quantum dots (PQD) solution diluted with the 200 μL of PMMA solution. Solution 2 was used in preparing sample 2, and it consists of 200 μL of colloidal CdSe quantum dots (CdSe QD) solution diluted with 200 μL of the PMMA solution. Solution 3 was used in preparing samples #3 and #4, and it consists of 150 μL of solution 1 mixed with 150 μL of solution 2. All three solutions were blended via vortexing and sonication.

To prepare sample 1, 100 μL of solution 1 was pipetted unto one of the glass pieces. Then, the glass piece with the solution was placed on the spin-coater's rotating drum and then spun at 1,000 rpm for one minute to create the monolayer. Finally, the glass slide was placed on the tape in the sample container with forceps. The same process was repeated for samples 2, 3, and 4 except with solutions 2 and 3 respectively. Prior to taking optical measurements, 75 μL of Ag nanocubes are pipetted unto a plastic piece and touched against the sample 4 slide for fifteen minutes to allow the nanocubes to bind. Then, the slide was submerged in the PAH solution for five minutes

to form another monolayer above the nanocubes, sandwiching them with the PMMA monolayer.

Sample #	Constituents
1	Perovskite Quantum Dots (PQD), and PMMA
2	Cadmium Selenide Quantum Dots (CdSe), and PMMA
3	PQD, CdSe, PMMA, and PAH
4	PQD, CdSe, PMMA, PAH, and Ag Cubes

Table 1. Sample Components

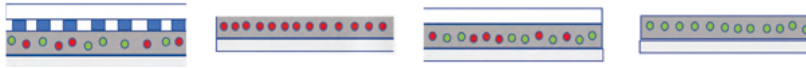

Sample 1 Sample 2 Sample 3 Sample 4

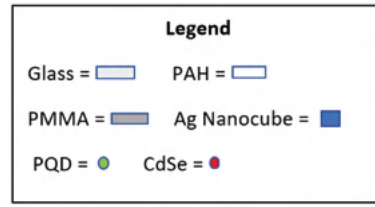

With regards to optical measurements, the sample was first placed on the sample holder which was set up on top of the light microscope's stage. Then, the sample was viewed under the microscope to ensure that the correct side will interact with the beam. The Ti: Sapphire laser was tuned to emit a light beam with a wavelength of 970 nm that passes through a second harmonic generation apparatus to reduce the beam's wavelength to 485 nm. An optical path (system of mirrors and lenses was set up) on the optics table such that the incoming beam hit the sample at the desired position with reasonable intensity. Next, a PL spectrum was recorded to verify that each emitter is active in the sample and then upon verification, TCPSC measurements were taken scanning between 502 nm and 690 nm with a scan taken every five nanometers. The collection time for PL spectroscopy was ninety seconds and fifteen seconds per scan for TCSPC. This procedure was repeated for each laser power tested per sample. In addition to taking TCSPC measurements for all four samples, a scan of the laser hitting a gold piece on the sample stage was taken to obtain the instrument response function (IRF) which was used later when performing curve fitting of the decay curves.

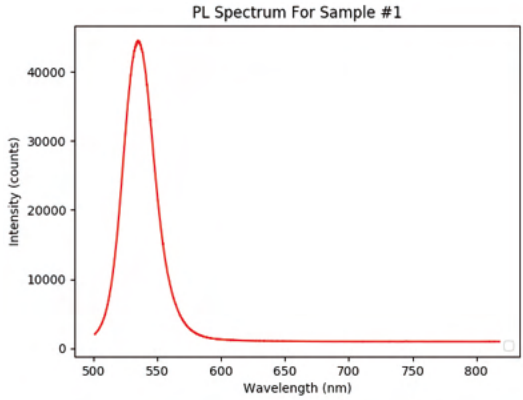

Figure 1. Sample 1's PL spectrum (537 nm max)

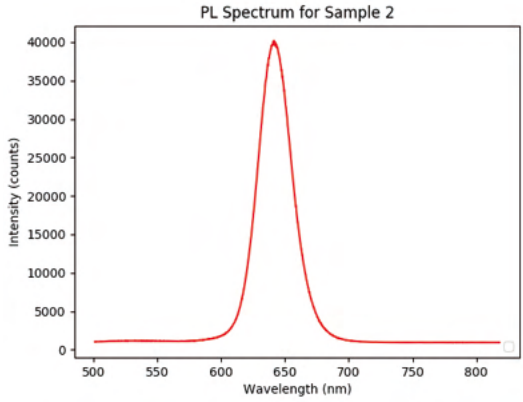

Figure 2. Sample 2's PL spectrum (632 nm max)

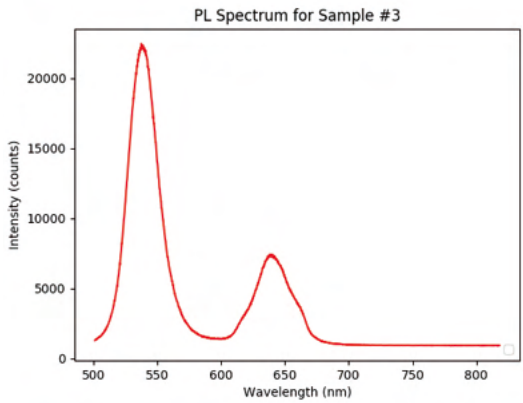

Figure 3. Sample 3's PL spectrum

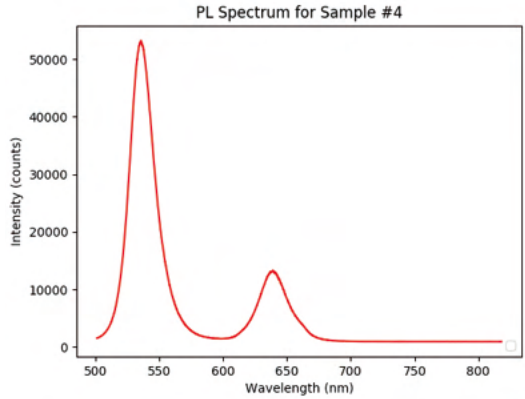

Figure 4. Sample 4's PL spectrum

Results

Even though decay spectra were collected between wavelengths containing each peak, the decay times were measured for the photons of wavelengths in a 20 nm range where the middle of that range is the peak wavelength. For samples 1, 3, and 4, we measured the decay times for the PQD emission photons in the range between 527 nm and 547 nm. For samples 2, 3, and 4, we measured the decay times for the CdSe QD emission photons in the range between 622 nm and 642 nm. To obtain the decay times for the relevant wavelengths, we performed nonlinear curve fitting of the respective decay spectra using the Easy Tau software. The fit we performed was an "exponential reconvolution" fit where the IRF is deconvoluted from the decay curve and fitted to one term which is $I_1 e^{-t}/T$ where I_1 is the peak intensity, *t* is time, and T is the decay time. Upon obtaining the desired decay times, we then calculated the mean decay times in each range with standard error of the mean per sample.

Sample #	PQD Wavelengths Mean Decay Time (ns)	Standard Error of Mean (ns)
1	95.06	11.68
3	69.77	3.29
4	108.64	10.86

Table 2. Mean decay times for PQD emission photons for samples containing PQDs at lower powers (2 uW or 10 uW)

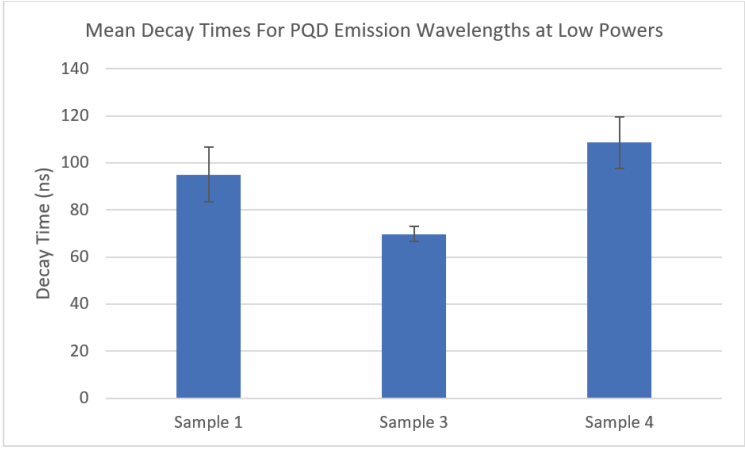

Figure 5. Mean decay times for PQD at lower powers (2 uW or 10 uW)

Sample #	PQD Wavelengths Mean Decay Time (ns)	Standard Error of Mean (ns)
1	47.72	5.33
3	55.68	2.78
4	73.95	1.50

Table 3. Mean decay times for PQD emission photons for samples containing PQDs at higher powers (5 uW or 20 uW)

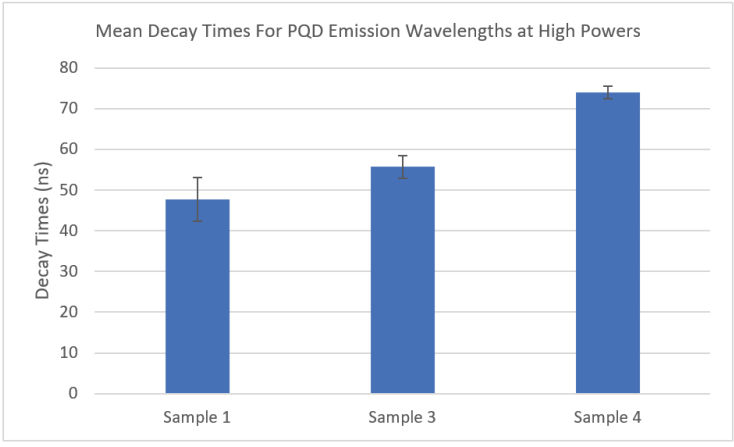

Figure 6. Mean decay times for PQD at higher powers (5 uW or 20 uW)

Sample #	CdSe Wavelengths Mean Decay Time (ns)	Standard Error of Mean (ns)
2	23.43	0.79
3	29.17	0.80
4	27.10	0.41

Table 4. Mean decay times for CdSe emission photons for samples containing CdSe QDs at 10 uW power

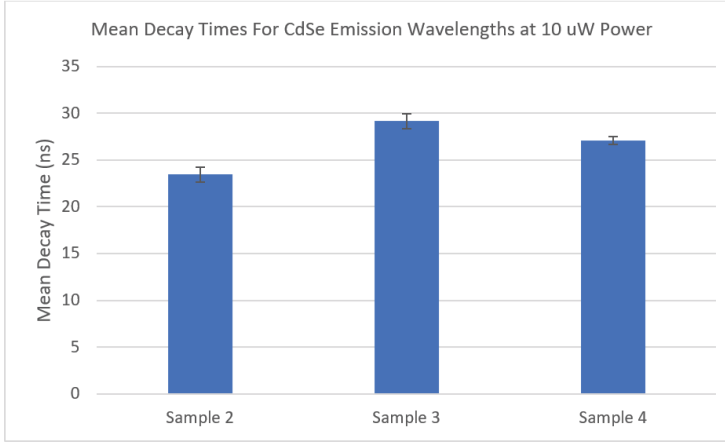

Figure 7. Mean decay times for CdSe QDs at 10 uW power

Sample #	CdSe Wavelengths Mean Decay Time (ns)	Standard Error of Mean (ns)
2	23.10	1.10
3	21.09	0.86
4	24.44	0.61

Table 5. Mean decay times for CdSe emission photons for samples containing CdSe QDs at 20 uW power

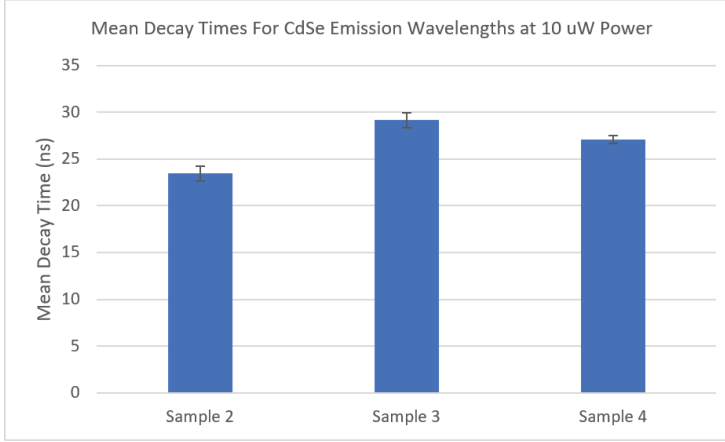

Figure 8. Mean decay times for CdSe QDs at 20 uW

One sample was prepared for each sample number, but multiple data points were acquired for statistical analysis by testing each sample at different laser powers. The PL spectra were taken once for each sample, and the data points were the mean decay time for the relevant photons at each power. The degrees of freedom per test varied between four to six degrees depending on the quality of the TCSPC data acquired for a sample at a given power. As the silver nanocubes were meant to enhance the emission of the perovskite quantum dots and promote FRET between the donor-acceptor pair, two sample t-tests assuming unequal variances were performed using Microsoft Excel's Data Analysis package on the decay time data comparing:

Sample 1 vs Sample 4 for PQD emission for both lower and higher powers

Sample 3 vs Sample 4 for PQD emission for both lower and higher powers

Below are the results of the t-tests including the statistical conclusions to be drawn:

Null Hypothesis (H_0)	$T_{sample\ 1} = T_{sample\ 4}$
Alternative Hypothesis (H_A)	$T_{sample\ 1} < T_{sample\ 4}$
Test Statistic	-0.851936
P-Value	0.2095103
Statistical Conclusion	Accept H_0 at significance of 0.05

Table 6. Two sample one-sided t-test results for comparison of Samples 1 and 4's PQD decay times at lower powers

Null Hypothesis (H_0)	$T_{sample\ 1} = T_{sample\ 4}$
Alternative Hypothesis (H_A)	$T_{sample\ 1} < T_{sample\ 4}$
Test Statistic	-4.735716
P-Value	0.0025849
Statistical Conclusion	Reject H_0 and accept H_A at significance of 0.05

Table 7. Two sample one-sided t-test results for comparison of Samples 1's and 4's PQD decay times at higher powers

Null Hypothesis (H_0)	$T_{sample\ 3} = T_{sample\ 4}$
Alternative Hypothesis (H_A)	$T_{sample\ 3} < T_{sample\ 4}$
Test Statistic	-3.426882
P-Value	0.0093492
Statistical Conclusion	Reject H_0 and accept H_A at significance of 0.05

Table 8. Two sample one-sided t-test results for comparison of Samples 3's and 4's PQD decay times at 10 uW power

Null Hypothesis (H_0)	$T_{sample\ 3} = T_{sample\ 4}$
Alternative Hypothesis (H_A)	$T_{sample\ 3} < T_{sample\ 4}$
Test Statistic	-5.7879297
P-Value	0.000582
Statistical Conclusion	Reject H_0 and accept H_A at significance of 0.05

Table 9. Two sample one-sided t-test results for comparison of Samples 3's and 4's PQD decay times at 20 uW power

Two sample t tests assuming unequal variances were also performed on the decay time data comparing:

Sample 2 vs Sample 4 for CdSe QD emission for 10 uW and 20 uW

Sample 3 vs Sample 4 for CdSe QD emission for 10 uW and 20 uW

Null Hypothesis (H_0)	$T_{sample\ 2} = T_{sample\ 4}$
Alternative Hypothesis (H_A)	$T_{sample\ 2} < T_{sample\ 4}$
Test Statistic	-4.10654
P-Value	0.003155
Statistical Conclusion	Reject H_0 and accept H_A at significance of 0.05

Table 10. Two sample one-sided t-test results for comparison of Samples 2's and 4's CdSe QD decay times at 10 uW power

Null Hypothesis (H_0)	$T_{sample\ 2} = T_{sample\ 4}$
Alternative Hypothesis (H_A)	$T_{sample\ 2} < T_{sample\ 4}$
Test Statistic	-1.06847
P-Value	0.163201
Statistical Conclusion	Accept H_0 at significance of 0.05

Table 11. Two sample one-sided t-test results for comparison of Samples 2's and 4's CdSe QD decay times at 20 uW power

Null Hypothesis (H_0)	$T_{sample\ 3} = T_{sample\ 4}$
Alternative Hypothesis (H_A)	$T_{sample\ 3} > T_{sample\ 4}$
Test Statistic	2.300064
P-Value	0.030548
Statistical Conclusion	Reject H_0 and accept H_A at significance of 0.05

Table 12. Two sample one-sided t-test results for comparison of Samples 3's and 4's CdSe QD decay times at 10 uW power

Null Hypothesis (H_0)	$T_{sample\ 3} = T_{sample\ 4}$
Alternative Hypothesis (H_A)	$T_{sample\ 3} < T_{sample\ 4}$
Test Statistic	-3.19702
P-Value	0.007564
Statistical Conclusion	Reject H_0 and accept H_A at significance of 0.05

Table 13. Two sample one-sided t-test results for comparison of Samples 3's and 4's CdSe QD decay times at 20 uW power

Discussion and Conclusion

Based on the observations stated above, we can conclude that the silver nanocubes did not succeed in promoting FRET between the donor-acceptor system as the Purcell effect dominated the FRET effect in our setups. If FRET had occurred, an acceptor peak taller than the donor peak on the PL spectrum for sample #4 would have been observed. Also, the mean decay times of both PQD and CdSe QD emissions should have decreased. Regardless of these results, future experiments could be performed in which one alters the amount of each constituent and assess how successful they would be at promoting FRET.

Specifically, we could perhaps observe what occurs when we reduce the spatial density of the silver nanocubes on the QD-PMMA monolayer in order to obtain the desired Purcell enhancement without it dominating the overall FRET effect or we could prepare different samples where we vary the donor to acceptor ratios. Another avenue which could be explored is integrating another plasmonic structure into our sample designs such as a gold or silver sheet to increase the likelihood of the dipole-dipole coupling needed for FRET due to enhanced dielectric effects upon optical excitation

From the PL spectrum for sample #4, there was no decreasing of the donor peak and increasing of the acceptor peak which is the first indication that FRET may not have occurred between the PQDs and CdSe QDs. Still, the decay data must be examined to draw any definite conclusions. At higher powers, there was statistically significant Purcell enhancement of the PQD's for sample #4 when compared to sample #1 but not at lower powers. At both lower and higher powers, there was statistically significant Purcell enhancement of the PQD's for sample #4 when compared to sample #3. From this, we can state that the silver nanocubes did indeed succeed in promoting increased spontaneous emission from the donor. With regards to CdSe emission, no consistent trends could be observed because all outcomes were represented roughly equal in the data.

Acknowledgements

I would like to first thank the National Science Foundation for funding me, and I would like to extend my gratitude to Dr. Hoang, Bryson Krause, and Jolaikha Sultana for impeccable mentorships. Finally, thanks also go to Dr. Firouzeh Sabri for making the arrangements for us students to get the most out of the University of Memphis Physics REU program.

References

[1] Chou, K., & Dennis, A. (2015). Förster resonance energy transfer between quantum DOT donors and quantum DOT ACCEPTORS. Sensors, 15(6), 13288–13325. https://doi.org/10.3390/s150613288

[2] Hoang, T. B., Akselrod, G. M., Argyropoulos, C., Huang, J., Smith, D. R., & Mikkelsen, M. H. (2015). Ultrafast spontaneous emission source using plasmonic nanoantennas. Nature Communications, 6(1). https://doi.org/10.1038/ncomms8788

[3] Li, H., He, F., Ji, C., Zhu, W., Xu, Y., Zhang, W., Meng, X., Fang, X., & Ding, T. (2019). Purcell-Enhanced spontaneous emission From PEROVSKITE quantum Dots coupled to Plasmonic Crystal. The Journal of Physical Chemistry C, 123(41), 25359–25365. https://doi.org/10.1021/acs.jpcc.9b06919

[4] Libretexts. (2020, August 15). Fluorescence. Chemistry LibreTexts. https://chem.libretexts.org/Bookshelves/Physical_and_Theoretical_Chemistry_Textbook_Maps/Supplemental_Modules_(Physical_and_Theoretical_Chemistry)/Spectroscopy/Electronic_Spectroscopy/Radiative_Decay/Fluorescence.

[5] Parak, W. J., Manna, L., & Nann, T. (2010). Fundamental principles of quantum dots. Nanotechnology. https://doi.org/10.1002/9783527628155.nanotech004

Faculty Review Board

Dr. Gustav Borstad
Instructor Coordinator
Department of Physics and Materials Science

Dr. Dean Clement
Instructor
Department of English

Dr. Judith Cole
Associate Professor
Department of Biological Sciences

Dr. David H. Dye
Professor
Department of Archaeology

Dr. Mohamed Laradji
Professor
Department of Physics and Materials Science

Dr. Sanjay Mishra
Professor
Department of Physics and Materials Science

Dr. Felio Perez
Materials Science Lab Manager
Integrated Microscopy Center

Dr. Caroline Peyton
Instructor
Department of History

Dr. Helen J.K. Sable
Associate Professor
Department of Psychology

Dr. Aaryani Sajja
Assistant Professor
Department of Biomedical Engineering

Dr. Charlie Santo
Associate Professor
Department of City and Regional Planning

Ms. Amanda Lee Savage
Instructor
Department of History

Dr. Ali Shiri Sichani
Instructor
Department of Electrical and Computer Engineering

Dr. Nicholas Simon
Assistant Professor
Department of Psychology

Mr. Halil Andaç Yiğit
Ph.D. Candidate, Graduate Assistant
Department of Electrical Engineering
École Polytechnique Fédérale de Lausanne

Submission Guidelines

Eligibility

QuaesitUM considers submissions from any current University of Memphis undergraduate student; eligibility also extends to those who have graduated within the last two semesters. Research must reflect University of Memphis student projects. Manuscripts may be single or co-authored, but the primary author must have been a University of Memphis undergraduate student during the time the research was conducted. Faculty members and graduate students are not eligible.

Content

Papers should present analytical research performed by the author(s). Submissions should include a section in which data and research methodology are described in detail.

All submitted text is to be the sole creation of the author(s) with the exception of correctly cited paraphrases and properly indicated quotations. In the case of collaborative research with faculty, papers should represent the student's contribution to the larger project.

Any research involving human subjects must have approval from the appropriate Institutional Review Board. Submitting authors are responsible for adhering to IRB guidelines. Check with your faculty advisor for further information.

While there is no minimum or maximum length for articles, 8,000 words or less is preferred. We understand academic disciplines have different norms, and we take this into account.

Copyright

Submissions may not be under review for publication elsewhere.

Authors retain copyright of their work. Authors may publish their papers elsewhere later so long as the requirements of all involved parties are satisfied. Given the hard work that our editorial team puts into each paper prior to publication, we ask that if you publish the work elsewhere, you include an acknowledgement of Quaesitum and its editorial staff.

Formatting

1. Remove all occurrences of author(s) names from the manuscript.

2. Include a cover sheet as a separate document that contains author name(s), title, faculty sponsor*, date, citation style, and one of the following categories:

    - Life and Health Sciences
    - Physical and Applied Sciences
    - Math/Computer Science/Engineering
    - Social and Behavioral Sciences
    - Humanities
    - Professional

    *The faculty sponsor is someone who gave feedback on your paper, taught the class for which you conducted the research, or provided some form of guidance for the paper.

3. Include an abstract of 150 words or less.

4. Upload your manuscript as a .docx or .doc file (Let us know if your academic discipline uses a different format). The manuscript should be formatted as follows:

    - Single-space the body of the text.
    - Use 12 point Times New Roman.
    - Number pages.
    - Properly cite all referenced works.

5. Figures and Tables

    - Use greyscale when possible.
    - Tables in Word/Excel should be no more than 5 inches wide according to the Word/Excel ruler.
    - Avoid extremely small letters/details whenever possible. These can become too small to read if we have to shrink the figure/table to fit within the 5" page width.
    - Place figures and tables in your manuscript.
    - Number and title all figures and tables in your manuscript.
    - Upload a seperate, high quality file for each table and figure.

6. Carefully check that each item in your references section follows the punctuation, capitalization, and italicization conventions of your citation style (APA, MLA, etc.).

Review Process

Submissions are uploaded to the Quaesitum submission manager, Scholastica (see the link on the next page). After submission, articles are screened by the Quaesitum editorial staff. Manuscripts meeting and exceeding the panel's criteria are then forwarded to volunteer faculty reviewers who have expertise in a field of research relevant to the manuscript. This is a double-blind process: both authors and faculty reviewers remain anonymous. Final selection decisions are left to the editorial staff.

Revision Process

After the review process is complete (usually mid-March), authors will be notified of the review board's decision. Authors whose papers are selected for publication will receive suggestions for revision from the faculty reviewers and editorial board. Authors are required to revise their manuscript before final publication.

Deadline for Submissions

For publication in Issue 8, papers should be submitted by January 19, 2021.

Submit Your Research Paper

Upload your manuscript to our Scholastica page:

https://submissions.scholasticahq.com/sites/quaesitum/for-authors

Questions

Contact us at quaesitum@memphis.edu with any questions.